

ATLANTIC ZONE MONITORING PROGRAM

AZMP Bulletin PMZA

PROGRAMME DE MONITORAGE DE LA ZONE ATLANTIQUE

ISSN 1916-6362

http://www.meds-sdmm.dfo-mpo.gc.ca/zmp/main_zmp_e.html**Contents / Table des matières**

The Atlantic Zone Monitoring Program / Le Programme de monitorage de la zone Atlantique	p.2
AZMP Personnel / Personnel du PMZA	p.2
Environmental Review / Revue environnementale	p.3
Physical, Chemical, and Biological Status of the Labrador Sea	p.11
Using the Long-Term Bottom-Trawl Survey of the Southern Gulf of St. Lawrence to Understand Marine Fish Populations and Community Change	p.19
Macrozooplankton Diel Migration in the Estuary and Gulf of St. Lawrence: Links to Abiotic Factors	p.28
An Evaluation of Operational Sea-Surface Temperature Analyses Using AZMP Data Over the Eastern Canadian Shelves.....	p.35
A Preliminary Investigation of Two Potential Stability Data Products for AZMP	p.40
Currents and Temperature Variability from Moored Measurements on the Outer Halifax Line in 2000–2004.....	p.44
La station de monitorage de Rimouski : plus de 400 visites et 18 ans de monitorage et de recherche	p.51
Publications	p.55

Edited by / Rédigé par

Patrick Ouellet¹, Laure Devine¹, & Brian Petrie²
Layout by / Mis en page par Claude Nozères¹¹Institut Maurice-Lamontagne
850, route de la Mer, Mont-Joli, QC, G5H 3Z4²Bedford Institute of Oceanography
Box 1006, Dartmouth, NS, B2Y 4A2

BulletinPMZA-AZMP@dfo-mpo.gc.ca

Le Bulletin du PMZA

Le bulletin annuel du PMZA publie des articles anglais, français ou bilingues afin de fournir aux océanographes et aux chercheurs des pêches, aux gestionnaires de l'habitat et de l'environnement, ainsi qu'au public en général les plus récentes informations concernant le Programme de monitorage de la zone Atlantique (PMZA). Le bulletin présente une revue annuelle des conditions océanographiques générales pour la région nord-ouest de l'Atlantique, incluant le golfe du Saint-Laurent, ainsi que de l'information reliée au PMZA concernant des événements particuliers, des études ou des activités qui ont eu lieu au cours de l'année précédente.

The AZMP Bulletin

The AZMP annual bulletin publishes English, French, and bilingual articles to provide oceanographers and fisheries scientists, habitat and environment managers, and the general public with the latest information concerning the Atlantic Zone Monitoring Program (AZMP). The bulletin presents an annual review of the general oceanographic conditions in the Northwest Atlantic region, including the Gulf of St. Lawrence, as well as AZMP-related information concerning particular events, studies, or activities that took place during the previous year.

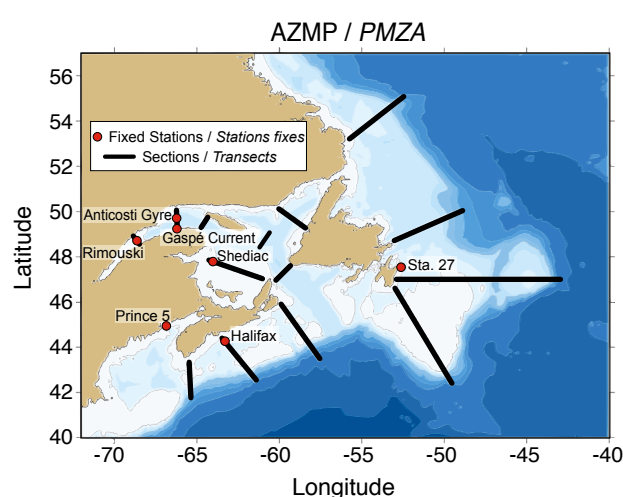


Fig. 1 Locations of sections and fixed stations.

Localisation des transects et des stations fixes.

The Atlantic Zone Monitoring Program

The AZMP was implemented in 1998 with the aim of collecting and analyzing the biological, chemical, and physical data to detect and monitor seasonal and interannual variability in eastern Canadian waters. A full description of the program can be found in Therriault et al. 1998. Proposal for a northwest Atlantic zonal monitoring program. Can. Tech. Rep. Hydrogr. Ocean Sci. 194: vii+57pp. (available online at <http://www.dfo-mpo.gc.ca/Library/224076.pdf>). Additional information is available at the AZMP website <http://www.meds-sdmm.dfo-mpo.gc.ca/isdm-gdsi/azmp-pmza/index-eng.html>.

The key element of the AZMP sampling strategy is the oceanographic sampling at fixed stations (every two weeks, conditions permitting) and along sections (1–3 times per year) (Fig. 1). Field sampling and laboratory analyses are carried out following well-established common protocols (Mitchell et al. 2002. Atlantic Zonal Monitoring Program sampling protocol. Can. Tech. Rep. Hydrogr. Ocean Sci. 223: iv + 23 pp.).

The editorial team strives to assure the quality of the information presented in each issue of the bulletin; however, we remind our readers that it is still essential to obtain the authors' permission before using or citing information or specific contents from their articles. We welcome comments and suggestions from our readers; these may be sent to BulletinPMZA-AZMP@dfo-mpo.gc.ca.

Le Programme de monitorage de la zone Atlantique

Le PMZA a été institué en 1998 dans le but de récolter et d'analyser des données biologiques, chimiques et physiques afin de détecter et de suivre la variabilité saisonnière et interannuelle dans les eaux de l'est canadien. Une présentation complète du programme se trouve dans Therriault et al. 1998. Proposition pour un programme zonal de monitorage de la région nord-ouest de l'Atlantique. Rapp. tech. can. hydrogr. sci. océan. 194F: vii+69p. (on-line: <http://www.dfo-mpo.gc.ca/Library/232003.pdf>), informations additionnelles à <http://www.meds-sdmm.dfo-mpo.gc.ca/isdm-gdsi/azmp-pmza/index-fra.html>.

L'élément principal de la stratégie d'échantillonnage du PMZA est l'échantillonnage à des stations fixes (aux deux semaines si les conditions le permettent) et le long de transects (1 à 3 fois par année) (Fig. 1). Le travail de terrain et les analyses en laboratoires se font selon des protocoles communs bien reconnus (Mitchell et al. 2002. Atlantic Zonal Monitoring Program sampling protocol. Can. Tech. Rep. Hydrogr. Ocean Sci. 223: iv + 23 pp.).

Bien que l'équipe de rédaction s'efforce d'assurer la qualité de l'information présentée dans chaque numéro, nous tenons à rappeler qu'il demeure essentiel de rechercher la permission des auteurs avant d'utiliser ou de citer l'information ou des faits spécifiques contenus dans leurs articles. Les commentaires et suggestions des lecteurs sont bienvenus et peuvent être transmis à BulletinPMZA-AZMP@dfo-mpo.gc.ca.

AZMP Personnel / Personnel du PMZA

Chairman / Président:

Michel Mitchel (BIO)

Steering committee / Comité de direction:

Glen Harrison (BIO), Patrick Ouellet (IML),
Pierre Pepin (NAFC), Brian Petrie (BIO)

Each year, the successful achievement of AZMP objectives would not be possible without the dedication of the people from each region who are listed below. In addition, thanks are extended to Martin Castonguay for linguistic revision of the French texts.

Maritime Region / Région des maritimes

Kumiko Azetsu-Scott², Glen Harrison², Erica Head², Ross Hendry¹, Catherine Johnson², Mary Kennedy³, Bill Li², Heidi Maass⁴, Michel Mitchell¹, Kevin Pauley^{5,6}, Tim Perry^{5,6}, Brian Petrie¹, Liam Petrie⁸, Roger Pettipas⁸, Cathy Porter⁴, Victor Soukhovtsev⁸, Jeff Spry^{5,6}, Igor Yashayaev¹, Phil Yeats²

Newfoundland and Labrador Region / Région de Terre-Neuve et du Labrador

Wade Bailey¹, Robert Chafe^{5,6}, Eugene Colbourne¹, Joe Craig¹, Frank Dawson^{5,6}, Dwight Drover⁵, Charles Fitzpatrick¹, Sandy Fraser², Paula Hawkins⁵, Trevor Maddigan^{5,6}, Gary Maillet², Pierre Pepin², Scott Quilty^{5,6}, Greg Redmond², Dave Senciali³, Tim Shears², Paul Stead¹, Dave Sears^{5,6}, Maitland Samson^{5,6}, Marty Snooks^{5,6}, Keith Tipple^{5,6}

Chaque année la réalisation des activités du PMZA ne serait pas possible sans le travail formidable des équipes suivantes impliquées au niveau de chacune des régions. De plus, nous tenons à remercier le Dr. Martin Castonguay pour sa révision des textes français.

Québec Region / Région du Québec

Marie-France Beaulieu⁵, Laure Devine³, Marie-Lyne Dubé⁵, Alain Gagné⁵, Yves Gagnon⁵, Peter Galbraith¹, Denis Gilbert¹, Michel Harvey², Pierre Joly⁵, Caroline Lafleur^{1,3}, Pierre Larouche⁴, Caroline Lebel⁵, Sylvie Lessard^{2,5}, Patrick Ouellet², Bernard Pelchat³, Bernard Pettigrew⁵, Stéphane Plourde², Pierre Rivard⁵, Liliane St-Amand^{2,5}, Isabelle St-Pierre³, Jean-François St-Pierre^{2,5}, Michel Starr²

Integrated Science Data Management / Gestion des données scientifiques intégrée

Bob Keeley³, Mathieu Ouellet^{3,7,8}, Anh Tran³

Gulf Region / Région du Golfe

Joël Chasse¹, Doug Swain⁶

¹Physical Oceanography / Océanographie physique; ²Biological/Chemical Oceanography / Océanographie biologique/chimique; ³Data Management / Gestion des données; ⁴Remote Sensing / Télédétection; ⁵Sampling & Laboratory Analyses / Échantillonnage & analyses en laboratoire; ⁶Fish Surveys / Missions d'évaluation de poissons; ⁷Webmaster / Webmestre; ⁸Graphic & Data Analyst / Graphiste et analyste de données.

Physical, Chemical, and Biological Status of the Environment¹

État de l'environnement physique, chimique et biologique¹

AZMP Monitoring Group

Northwest Atlantic Fisheries Centre, Box 5667, St. John's, NL, A1C 5X1

Institut Maurice-Lamontagne, B.P. 1000, Mont-Joli, QC, G5H 3Z4

Bedford Institute of Oceanography, Box 1006, Dartmouth, NS, B2Y 4A2

Integrated Science Data Management, 200 Kent St., Ottawa, ON, K1A 0E6

michel.mitchell@mar.dfo-mpo.gc.ca (AZMP Chairman / Président PMZA)

Physical Environment

Ice cover dominated the Labrador and NE Newfoundland shelves as well as the Gulf of St. Lawrence in late winter 2008 in contrast to the lesser coverage in 2007 (Fig. 1A). The offshore branch of the Labrador Current on the eastern edge of the Grand Banks, clearly indicated as a stream of cold water,

Environnement physique

La surface de glace était importante sur les plateaux du Labrador et du nord-est de Terre-Neuve et dans le golfe du Saint-Laurent à la fin de l'hiver 2008 en comparaison avec la plus faible couverture de 2007 (Fig. 1A). La branche hauturière du courant du Labrador sur le bord est des Grands Bancs, clairement identifiée comme un écoulement d'eau froide, est interrompue au sud de la passe Flamande. Cependant, il y a des indications que le courant s'étire plus au sud près de la queue du Grand Banc. La branche côtière est observée au niveau du chenal d'Avalon et au sud et à l'ouest de la péninsule d'Avalon. De l'eau froide et un peu de glace provenant du golfe du Saint-Laurent indiquent le courant de la Nouvelle-Écosse du détroit de Cabot à la côte est de la Nouvelle-Écosse.

De plus, il y a une extension de ce courant vers l'ouverture du chenal Laurentien et l'ouest des Grands Bancs. Des températures chaudes en surface, approchant 20 °C, ont été observées dans le sud du golfe du Saint-Laurent en août (Fig. 1B), ainsi que les eaux plus fraîches du courant du Labrador au large du bord est du Grand Banc et vers le nord au large de la côte du Labrador. Dans l'ensemble, les températures de la surface de la mer étaient plus froides en août 2008 relativement à 2007.

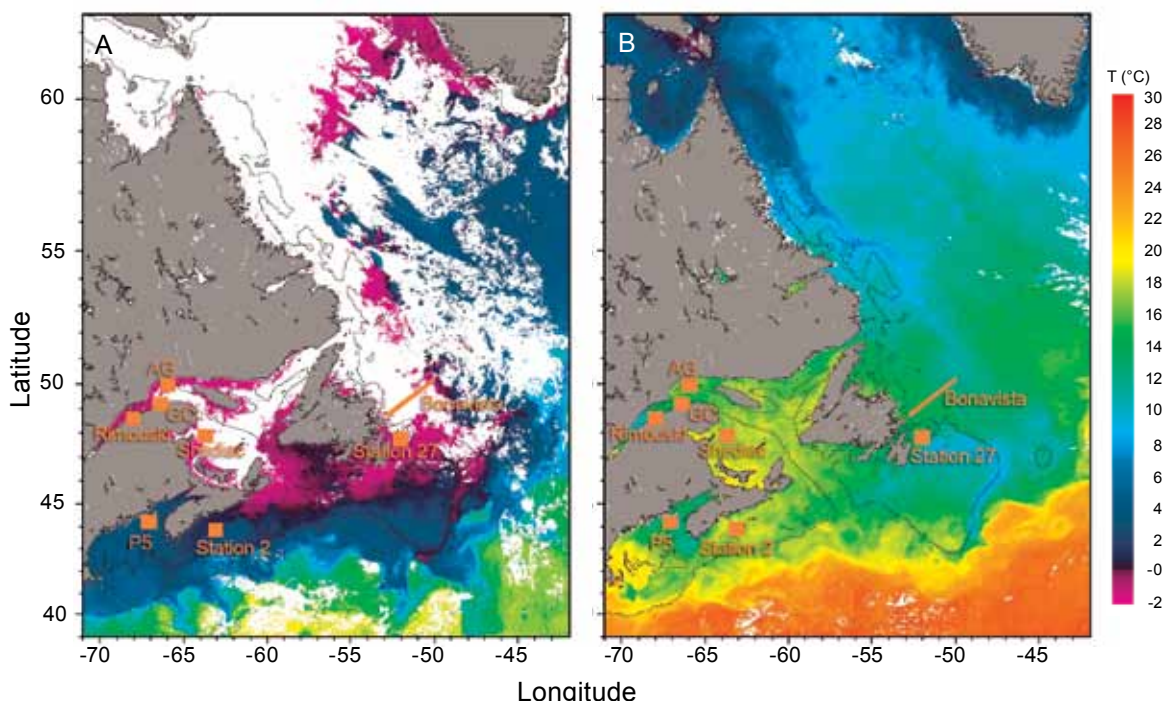


Fig. 1 Sea-surface temperature in the AZMP region during (A) March and (B) August 2008. The locations of fixed stations (squares; Rimouski, Anticosti Gyre [AG], Gaspé Current [GC], Shediac Valley [Shediac], Station 27, Halifax [Station 2], Prince 5 [P5]) and the Bonavista section (line) are shown. White areas indicate sea ice or clouds.

Températures de la surface de la mer dans la région du PMZA au cours de (A) mars et (B) août 2008. Les carrés montrent la localisation des stations fixes (Rimouski, gyre d'Anticosti [AG], courant de Gaspé [GC], vallée de Shediac [Shediac], Station 27, Halifax 2 [Station 2], Prince 5 [P5]) et la ligne indique le transect de Bonavista. Les espaces blancs indiquent la présence de glace ou de nuages.

is truncated south of Flemish Pass; however, there is evidence of a more southward extension of the flow near the Tail of the Bank. The inshore branch is seen in Avalon Channel and south and west of the Avalon Peninsula. Cold water and some ice from the Gulf of St. Lawrence mark the Nova Scotia Current from Cabot Strait to the eastern shore of Nova Scotia;

20 °C, ont été observées dans le sud du golfe du Saint-Laurent en août (Fig. 1B), ainsi que les eaux plus fraîches du courant du Labrador au large du bord est du Grand Banc et vers le nord au large de la côte du Labrador. Dans l'ensemble, les températures de la surface de la mer étaient plus froides en août 2008 relativement à 2007.

¹ The environmental overviews are presented in greater detail as research documents and science advisory reports available at http://www.dfo-mpo.gc.ca/csas/csas/Publications/Pub_Index_e.htm

¹ Les revues environnementales sont présentées plus en détail dans les documents de recherche et les avis scientifiques disponibles sur le site http://www.dfo-mpo.gc.ca/csas/csas/Publications/Pub_Index_f.htm

moreover, there is an extension of this outflow towards the mouth of the Laurentian Channel and onto the western Grand Banks. Warm surface temperatures approaching 20°C are seen in the southern Gulf of St. Lawrence in August (Fig. 1B) as are the cooler waters of the Labrador Current off the eastern edge of Grand Bank and northward off the coast of Labrador. Overall, sea-surface temperatures in August 2008 appear cooler than in 2007.

In 2008, the annual average sea-surface temperature anomalies were greatest (by ~1°C) over the Labrador Sea and Shelf, similar to 2007. Elsewhere, SST anomalies increased by ~0.5°C over the Grand Banks and the Gulf of St. Lawrence, and by about 0.2°C over the Scotian Shelf. This increase led to above-normal temperatures throughout the region during 2008 by 0.2 to 1.2°C, with the largest values over the central Labrador Sea.

A number of atmospheric (air temperature, the North Atlantic Oscillation [NAO], freshwater runoff at Québec City), ice, and oceanographic variables are summarized as time series (1980–2008) in matrix form in Figure 2. When possible, the variables are displayed as differences (anomalies) relative to 1971–2000 average values; furthermore, because these series have different units (e.g., °C, m³, m²), each anomaly time series is normalized by dividing by its standard deviation (SD), which is also based on the 1971–2000 period. This allows a more direct comparison of the series. Missing data are represented by grey cells, values within 0.5 SD of the average as white cells, and conditions corresponding to warmer than normal (higher temperatures, reduced ice volumes, reduced cold water volumes or areas, negative NAO index) by more than 0.5 SD as red cells, with more intense reds corresponding to increasingly warmer conditions. Similarly, blue represents colder-than-normal conditions. Higher-than-normal freshwater inflow and stratification anomalies are shown as red but are not necessarily indicative of warmer-than-normal conditions.

Air temperatures are an indication of heat transfer between the atmosphere and the ocean. The air temperature pattern across the region is highly coherent, generally cooling from the early 1980s to 1993–94 followed by a warm period marked by strong peaks in 1999 and 2006. In 2008, air temperatures were above normal by 0.7 to 1.7 standard deviations (corresponding to 0.5 to 1.3°C) at five of the six stations (Fig. 2). Only Sept-Îles registered values within 0.5 SD of the 1971–2000 annual mean.

Freshwater runoff in the Gulf of St. Lawrence, particularly within the St. Lawrence Estuary, strongly influences the circulation, salinity, and stratification (and hence upper layer temperatures) in the Gulf and, through the Nova Scotia Current, on the Scotian Shelf. For example, the average 0–20 m salinity in the Magdalen Shallows for the low runoff period of 1999–2007 is ~0.5 more than the average for high runoff years in the 1970s, 80s, and 90s. This represents approximately an extra 17 km³ of freshwater in the upper 20 m of the Shallows. In fact, during 16 of the past 22 years, freshwater inflow at Québec City has been below normal by more than 0.5 SD; in 2008 the inflow returned to normal (-0.02 SD; 12,500 m³ s⁻¹), a significant increase from 2007 (-1.5 SD).

En 2008, tout comme en 2007, la moyenne annuelle des anomalies des températures de la surface de la mer était plus grande (de ~1 °C) au niveau du plateau et de la mer du Labrador. Ailleurs, les anomalies ont augmenté de ~0,5 °C sur les Grands Bancs et dans le golfe du Saint-Laurent et d'environ 0,2 °C sur le plateau Néo-Écossais. Le résultat a été des températures au-dessus de la normale en 2008, de 0,2 à 1,2 °C, pour l'ensemble de la région, avec les valeurs les plus élevées au centre de la mer du Labrador.

Plusieurs variables atmosphériques (température de l'air, oscillation Nord-Atlantique [NAO], débit d'eau douce à Québec), océanographiques et relatives à la glace sont présentées sous forme de séries temporelles (1980 à 2008) dans un tableau synoptique (Fig. 2). Lorsque possible, les variables sont présentées en tant que différences (anomalies) relatives par rapport aux moyennes de la période 1971 à 2000. De plus, comme les séries ont des unités différentes (°C, m³, m², etc.) chaque série temporelle d'anomalies a été réduite en divisant les valeurs annuelles par l'écart-type calculé sur les données de la période 1971 à 2000, afin de permettre une comparaison directe des différentes séries. Une donnée manquante est indiquée par une cellule grise, les valeurs entre 0,5 écart-type de la moyenne sont représentées par les cellules blanches, alors que les conditions plus chaudes que la normale (températures élevées, volumes de glace réduits, aires ou volumes d'eau froide réduits, un indice NAO négatif) par plus de 0,5 écart-type sont en rouge, avec une gamme d'intensités correspondante à des conditions croissantes de réchauffement. De manière semblable, les tons de bleus représentent des conditions plus froides que la normale. Les anomalies du débit d'eau douce et de stratification plus élevées que la normale sont en rouge mais n'indiquent pas nécessairement des conditions plus chaudes que la normale.

Les températures de l'air sont une indication de la quantité de chaleur qui peut être échangée entre l'atmosphère et l'océan. Les températures de l'air montrent une image cohérente sur toute la région, un refroidissement général du début des années 1980 jusqu'en 1993–94, suivi d'une période de réchauffement marquée par des sommets élevés en 1999 et 2006. En 2008, les températures étaient au-dessus de la normale de 0,7 à 1,7 écarts-types (correspondant à 0,5 à 1,3 °C) pour cinq des six sites (Fig. 2). Sept-Îles était le seul endroit où les valeurs se situaient à l'intérieur de 0,5 écart-type de la moyenne à long terme (1971–2000).

Le débit d'eau douce dans le golfe du Saint-Laurent, en particulier dans l'estuaire du Saint-Laurent, influence fortement la circulation, la salinité et la stratification (donc les températures dans les couches supérieures) dans le golfe et, par le courant de la Nouvelle-Écosse, sur le plateau Néo-Écossais. Par exemple, la salinité moyenne entre 0 et 20 m sur le plateau madelinien pour la période de faible débit de 1999 à 2007 est supérieure de ~0,5 unité par rapport à la moyenne des années de forts débits des décennies 1970, 1980 et 1990. Cela représente approximativement un surplus de 17 km³ d'eau douce dans les 20 m supérieurs du plateau. En fait, pour 16 des 22 dernières années, le débit d'eau douce à Québec a été sous la normale par plus de 0,5 écart-type. En 2008, le débit est revenu à la normale (-0,02 écart-type, 12 500 m³ s⁻¹), soit une augmentation significative par rapport à 2007 (-1,5 écarts-types).

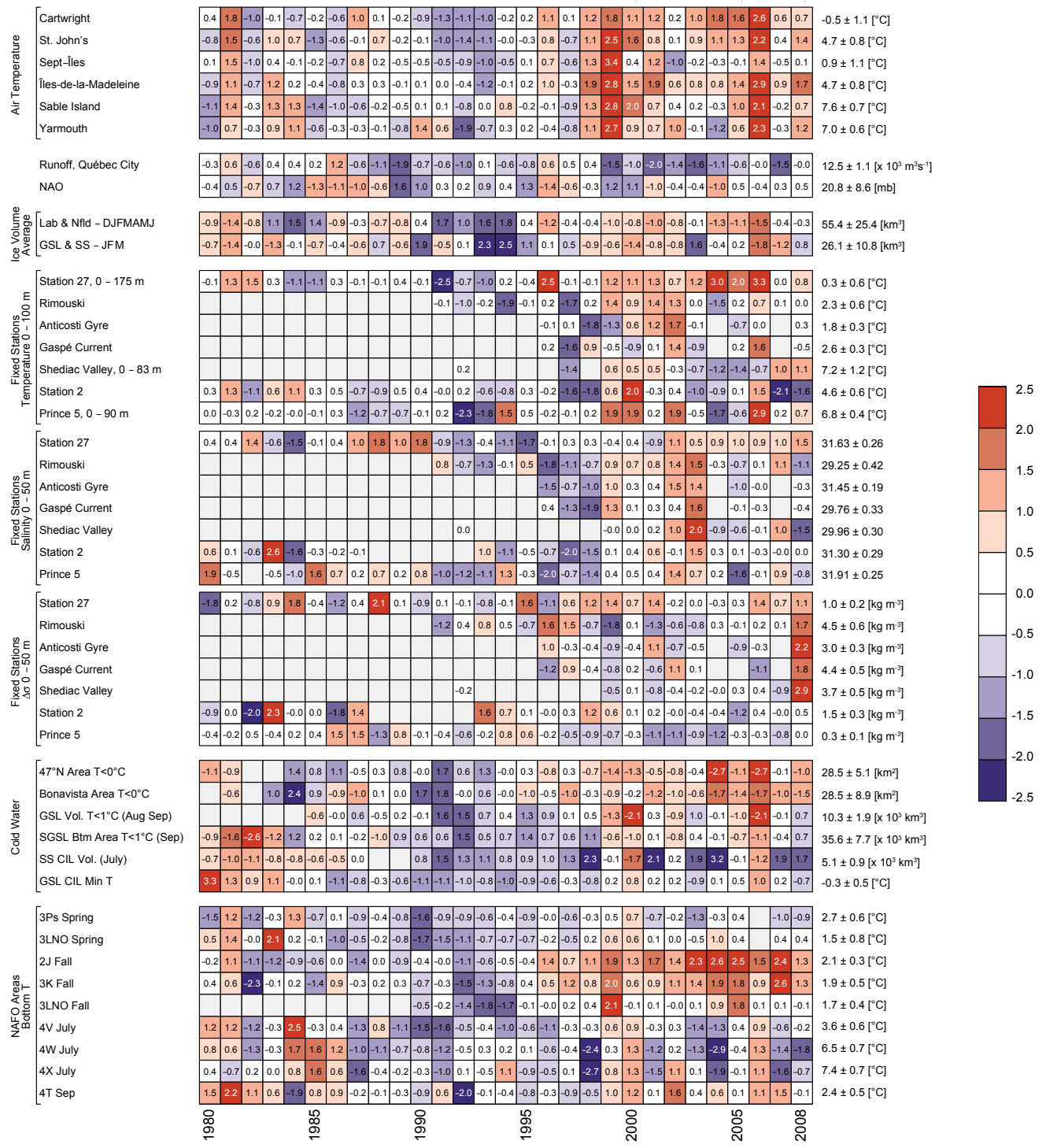


Fig. 2 Time series of atmospheric and oceanographic variables, 1980–2008. A grey cell indicates missing data, a white cell is a value within 0.5 standard deviation of the long-term mean based on data from 1971–2000 when possible; for air temperature, NAO index, ice volumes, fixed station depth-averaged temperature, cold-water volumes and areas, and NAFO areas bottom temperature, a red cell indicates warmer-than-normal conditions, a blue cell colder than normal. More intense colours indicate larger anomalies. For the freshwater inflow, salinity, and stratification, red corresponds to above-normal conditions. The numbers in the cells are the difference from the long-term mean divided by the standard deviation. Long-term means and standard deviations are shown on the right-hand side of the figure. (North Atlantic Oscillation [NAO], GSL [Gulf of St. Lawrence], SGSL [southern Gulf of St. Lawrence], cold intermediate layer [CIL].)

Séries temporelles (de 1980 à 2008) des variables atmosphériques et océanographiques. Une cellule grise indique une donnée manquante, une cellule blanche une valeur entre 0,5 écart-type de la moyenne à long terme calculé, lorsque possible, sur les données de 1971 à 2000 pour la température de l'air, l'indice NAO, les volumes de glace, la température moyenne sur la profondeur aux stations fixes, surfaces et volumes d'eau froide, et la température au fond dans les divisions de l'OPANO. Les cellules rouges indiquent des conditions plus chaudes que la normale, les cellules bleues plus froides que la normale. Les teintes plus fortes correspondent aux plus grandes anomalies. Pour le débit d'eau douce, la salinité et la stratification le rouge correspond aux conditions au-dessus de la normale. Les chiffres à l'intérieur des cellules sont les différences par rapport à la moyenne à long terme divisées par l'écart-type. Les moyennes et écarts-types sont présentés à droite de la figure. (Oscillation Nord-Atlantique [NAO], golfe du Saint-Laurent [GSL], sud du golfe du Saint-Laurent [SGSL], couche intermédiaire froide [CIL].)

The NAO is an index of the dominant atmospheric forcing over the North Atlantic Ocean. It affects winds, air temperature, precipitation, and the hydrographic properties on the eastern Canadian seaboard either directly or through ocean currents. Direct effects occur predominantly to waters of the Labrador Sea and the Newfoundland-Labrador Shelf, where a negative NAO corresponds to warmer-than-average conditions. The tendency of the ocean currents to move from north to south spreads the NAO's influence into the Gulf of St. Lawrence and onto the Scotian Shelf. For the past four years, the NAO has been within 0.5 SD of the 1971-2000 mean; in 2008, the index increased slightly, to +0.49 SD, from its 2007 value of +0.29 SD.

With the exceptions of 1983-85 and 1991, ice volumes on the Newfoundland-Labrador Shelf and in the Gulf of St. Lawrence - Scotian Shelf area have been strongly positively correlated over the past 39 years. The exceptional years featured large ice volumes on the Newfoundland-Labrador Shelf but relatively small volumes in the Gulf. On average, the ice volumes for Newfoundland-Labrador and the Gulf appear to be related to the NAO. Since 1969, there have been 15 years when the NAO has been more than 0.5 SD below (generally milder winters) and 11 years when the NAO has been more than 0.5 SD above (generally colder winters) normal. The difference in the ice volumes between these two groups of years (colder vs. milder) is 6 km³ for the Gulf of St. Lawrence - Scotian Shelf (monthly average for Jan-Mar; not significantly different) and 22 km³ for the Newfoundland-Labrador Shelf (monthly average for Dec-June; significantly different). For the past decade, ice volumes on the Newfoundland-Labrador Shelf and the Gulf of St. Lawrence - Scotian Shelf have generally been lower than normal. This trend persisted during 2008, when the ice volumes were significantly below normal (by 0.7 SD) for the Gulf of St. Lawrence but were within 0.5 SD of normal for the Newfoundland-Labrador region.

There are sufficient data to estimate annual 0-100 m (or 0-bottom if the depth is < 100 m) temperature anomalies for Station 27, Prince 5, and Halifax 2; however, the four series from the Gulf have sufficient data to estimate anomalies for only 35%-60% of the years since 1980. In 2008, temperatures at Station 27, Shédiac, and Prince 5 were above normal, whereas the temperature was below normal by ~1.6 SD at Halifax 2. Temperatures at the other sites were within 0.5 SD of normal values.

The salinity anomalies at Rimouski, Shédiac, and Prince 5 were about 0.8 to 1.6 SD below normal in 2008; on the other hand, salinity was above normal at Station 27 by ~1.5 SD. Salinities at the other sites were within 0.5 SD of normal values. Stratification was stronger than normal (by 1.1 to 2.9 SD) at Rimouski, Anticosti, Gaspé, Shédiac, and Station 27. Prince 5 and Halifax anomalies were positive but within 0.5 SD of normal.

There are a number of indexes, derived from oceanographic sections and ecosystem surveys, that characterize the variability of cold water volumes, areas, and bottom temperatures in the region. For the latest ~30 year period, the highest correlations are for indexes from NAFO areas 2J, 3K, and 3L (see Fig. 3)—the southern Labrador and NE Newfoundland Shelf

Le NAO est un indice des forces atmosphériques dominantes sur l'océan Atlantique Nord. Il influence les vents, les températures de l'air, les précipitations et les caractéristiques hydrographiques de la côte est canadienne, soit directement ou par le biais des courants océaniques. Les effets directs se font sentir surtout sur les eaux de la mer du Labrador et des plateaux du Labrador et de Terre-Neuve où un NAO négatif correspond à des conditions plus chaudes que la normale. La tendance des courants océaniques d'aller du nord au sud étend l'influence du NAO à l'intérieur du golfe du Saint-Laurent et sur le plateau Néo-Écossais. Au cours des quatre dernières années, le NAO est demeuré à l'intérieur de 0,5 écart-type de la moyenne de 1971 à 2000. En 2008, l'indice a augmenté légèrement, passant à +0,49 écart-type par rapport à +0,29 écart-type en 2007.

À l'exception des périodes de 1983 à 1985 et 1991, les volumes de glace sur les plateaux du Labrador et Terre-Neuve et dans le golfe du Saint-Laurent et plateau Néo-Écossais ont été fortement positivement corrélés au cours des 39 dernières années. Les années d'exception sont marquées par des volumes de glace importants sur les plateaux du Labrador et Terre-Neuve mais de petits volumes dans le golfe. En moyenne, les volumes de glace sur le plateau et dans le golfe semblent reliés au NAO. Depuis 1969, il y a eu 15 années où le NAO a été plus de 0,5 écart-type sous (généralement des hivers doux) et 11 années au-dessus (généralement des hivers froids) de la normale. La différence des volumes de glace entre ces groupes d'années (plus froides - plus douces) est 6 km³ (moyenne mensuelle de janvier à mars, différence non significative) pour le golfe du Saint-Laurent et plateau Néo-Écossais et de 22 km³ (moyenne mensuelle de décembre à juin, différence significative) pour les plateaux du Labrador et Terre-Neuve. Pour la dernière décennie, les volumes de glace sur les plateaux du Labrador et Terre-Neuve et dans le golfe du Saint-Laurent et sur le plateau Néo-Écossais ont été plus faibles que la normale. La situation s'est poursuivie en 2008 alors que les volumes de glace étaient sous la normale (de 0,7 écart-type) dans le golfe du Saint-Laurent mais à l'intérieur de 0,5 écart-type de la normale pour la région Terre-Neuve-Labrador.

Il y a suffisamment de données pour l'estimation d'anomalies annuelles des températures (0 à 100 m ou 0 au fond si la profondeur est < 100 m) pour la Station 27, Prince 5 et Halifax 2; cependant pour le golfe depuis 1980 les quatre séries ne sont complètes qu'à 35 à 60 %. En 2008, les températures à la Station 27, vallée de Shédiac et Prince 5 étaient au-dessus de la normale, alors qu'à Halifax 2 les températures étaient sous la normale de ~1,6 écarts-types. Les températures aux autres sites sont demeurées à l'intérieur de 0,5 écart-type des valeurs normales.

Les anomalies de salinité à Rimouski, vallée de Shédiac et Prince 5 étaient d'environ 0,8 à 1,6 écarts-types sous la normale en 2008, alors qu'elles étaient au-dessus de la normale de 1,5 écarts-types à la Station 27. Aux autres endroits, les salinités étaient à l'intérieur de 0,5 écart-type des valeurs normales. La stratification était plus forte que la normale (de 1,1 à 2,9 écarts-types) à Rimouski, gyre d'Anticosti, courant de Gaspé, vallée de Shédiac et la Station 27. À Prince 5 et Halifax 2 les anomalies étaient positives mais à l'intérieur de 0,5 écart-type de la normale.

and the northern Grand Bank. In 2008, the Gulf CIL volume and the southern Gulf bottom area ($T < 1^\circ\text{C}$) were ~ 0.7 SD above normal; the Gulf CIL minimum temperature was 0.71 SD below normal, i.e., all three indexes behaved coherently, tending toward colder conditions. The Scotian Shelf CIL volume, which is strongly influenced by Gulf of St. Lawrence

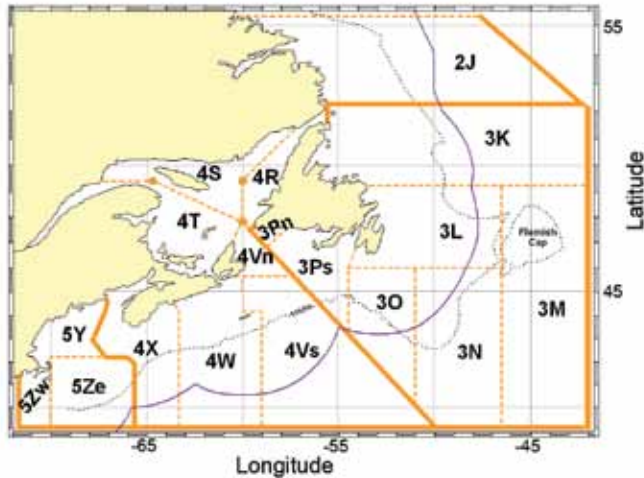


Fig. 3 NAFO areas referenced in text.

Divisions de l'OPANO mentionnées dans le texte.

outflow, also was significantly greater than normal (+1.65 SD), though slightly less than in 2007. On the other hand, the 47°N and Bonavista cross sections ($T < 1^\circ\text{C}$) were significantly below normal (-1 and -1.5 SD).

In 2008, above-normal bottom temperatures continued in the northernmost areas 2J and 3K while temperatures were near normal (within 0.5 SD) in 3LNO, 4T, and 4V, and below normal in 4R and 4S (quantified by the Gulf CIL minimum temperature) as well as 3Ps, 4W, and 4X. Significant (by ~ 1 to 1.6 SD) cooling from 2007 to 2008 occurred in areas 2J, 3K, and the entire Gulf of St. Lawrence; the only significant warming was in 4X (by ~ 0.9 SD).

In summary, air temperatures in 2008 at the six sites were above normal, with five of the six by more than 0.5 SD (Fig. 2). The NAO was positive and ~ 0.5 SD above normal. Ice volumes were below normal (i.e., corresponding to warmer-than-normal conditions), significantly so for the Gulf of St. Lawrence. Indexes of CIL volumes and areas as well as bottom temperatures indicated warmer-than-normal conditions in southern Labrador and the northeast Newfoundland Shelf, changing gradually to colder-than-normal conditions over the southwestern Grand Banks (St. Pierre Bank). Colder-than-normal conditions prevailed in the Gulf of St. Lawrence and on the Scotian Shelf.

Chemical and Biological Environment

The chemical and biological conditions in the Atlantic zone in 2008 have not been fully analyzed and will be reported in a future bulletin. This year's report will instead summarize conditions and trends from previous years utilizing a more condensed format emphasizing key variables and regional patterns. We have adopted the "scorecard" approach that has been employed in previous years to describe physical condi-

De nombreux indices, soit dérivés des transects océanographiques ou des relevés écosystémiques, sont disponibles afin de caractériser la variabilité des volumes et surfaces d'eau froide et des températures au fond dans la région. Pour les dernières 30 années, les corrélations les plus fortes entre les indices sont obtenues pour les divisions 2J, 3K et 3L de l'OPANO (voir Fig. 3), c.-à-d. le sud du plateau du Labrador et le nord-est du plateau de Terre-Neuve et le nord du Grand Banc. En 2008, le volume de la couche intermédiaire froide (CIF) du golfe et la surface d'eau froide ($T < 1^\circ\text{C}$) au fond dans le sud du golfe étaient de 0,7 écart-type au-dessus de la normale, et la température minimale de la CIF du golfe était de 0,7 écart-type sous la normale. Les trois indices montrent une image cohérente d'une tendance vers des conditions plus froides. Le volume de la CIF sur le plateau Néo-Écossais, lequel est fortement influencé par le débit du golfe du Saint-Laurent, était également plus grand que la normale (+1,65 écarts-types), mais légèrement plus petit qu'en 2007. Par contre, les sections d'eau froide au 47°N et de Bonavista ($T < 1^\circ\text{C}$) étaient significativement sous la normale (de -1,0 et -1,5 écarts-types).

En 2008, des températures au fond au-dessus de la normale étaient toujours observées aux limites nord des divisions 2J et 3K, elles étaient près de la normale (à l'intérieur de 0,5 écart-type) dans 3LNO, 4T et 4V, et sous la normale dans 4R et 4S (determinées par la température minimale de la CIF du golfe), 3Ps, 4W et 4X. Entre 2007 et 2008, un refroidissement significatif (de 1,0 à 1,6 écarts-types) est survenu dans les divisions 2J, 3K et pour l'ensemble du golfe du Saint-Laurent. La division 4X a été le seul endroit montrant un réchauffement significatif (de 0,9 écart-type).

En résumé, en 2008 les températures de l'air aux six points de mesures étaient au-dessus de la normale, supérieures à 0,5 écart-type à cinq des six sites (Fig. 2). Le NAO était positif et environ 0,5 écart-type au-dessus de la normale. Les volumes de glace étaient sous la normale (suivant des conditions plus chaudes que la normale), significativement dans le golfe du Saint-Laurent. Les indices de volumes et de surfaces de la CIF et des températures au fond indiquent des conditions plus chaudes que la normale au sud du plateau du Labrador et au nord-est du plateau de Terre-Neuve, changeant graduellement à des conditions plus froides que la normale au sud-ouest des Grand Bancs (banc Saint-Pierre). Des conditions plus froides que la normale ont persisté dans le golfe du Saint-Laurent et sur le plateau Néo-Écossais.

Environnement chimique et biologique

Les conditions chimiques et biologiques de la zone Atlantique pour l'année 2008 ne sont pas complètement analysées. Elles seront présentées dans un prochain numéro du bulletin. En remplacement, le rapport de cette année présente les conditions et les tendances des années antérieures dans un format condensé qui met l'accent sur les événements régionaux et les variables clés. Nous adoptons le format de tableau synoptique utilisé ces dernières années pour décrire les conditions physiques dans l'Atlantique Nord-Ouest (Fig. 2). Pour décrire les conditions chimiques et biologiques (les niveaux trophiques inférieurs), un sous ensemble du grand éventail d'observations récoltées annuellement par le PMZA (de 1999 à 2007) a été choisi afin de présenter : (i) les sels nutritifs qui

tions in the Northwest Atlantic (see Fig. 2). For describing the chemical and biological (lower trophic level) conditions, a subset of the broad spectrum of observations collected annually (1999–2007) by AZMP were chosen to represent (i) nutrients that fuel phytoplankton growth, (ii) phytoplankton biomass and characteristics of their growth cycle (i.e., bloom timing, magnitude, duration), and (iii) abundances of representative groups of zooplankton: large grazers (*Calanus finmarchicus*), small grazers (*Pseudocalanus* spp.), total copepods, and non-copepods. In addition, phytoplankton (colour index, diatoms, and dinoflagellates) and zooplankton (*C. finmarchicus*, *Para/Pseudocalanus* spp.) abundance estimates from the Continuous Plankton Recorder (CPR) were included. This is the longest lower trophic level time series in the NW Atlantic, covering 1960–present.

Interannual and regional variability of chemical and biological conditions in the Atlantic zone can be characterized as complex (Fig. 4A, B). One of the most pronounced patterns, with a high degree of regional coherence, is seen in the CPR record (Fig. 4A), where phytoplankton abundance was well below the long-term mean in the 1960s and 1970s and largely above the mean in the 1990s and 2000s. The highest levels were seen in the mid-1990s with levels declining somewhat in the subsequent years. In contrast, zooplankton abundance was slightly above the long-term mean in the 1960s and 1970s but largely below the mean in the 1990s and 2000s. The lowest recorded levels were seen in the mid-1990s, when phytoplankton levels were highest, and levels appeared to recover in the subsequent years, principally on the southern Newfoundland

alimentent la croissance du phytoplancton; (ii) les caractéristiques du cycle de croissance (le moment, l'amplitude et la durée de la floraison) et la biomasse du phytoplancton; (iii) l'abondance de groupes représentatifs du zooplancton, soit les grands brouteurs (ex. *Calanus finmarchicus*) et les petits brouteurs (*Pseudocalanus* spp.), ainsi que de tous les copépodes et des non copépodes. De plus, les abondances de phytoplancton (l'indice de couleur, les diatomées, les dinoflagellés) et de zooplancton (*C. finmarchicus*, *Para/Pseudocalanus* spp.) tirées du *Continuous Plankton Recorder* (CPR) sont incluses. Il s'agit pour les niveaux trophiques inférieurs de la plus longue série temporelle dans l'Atlantique Nord-Ouest, s'étendant de 1960 à aujourd'hui.

La complexité serait la meilleure caractéristique décrivant la variabilité interannuelle et régionale des conditions chimiques et biologiques dans la zone Atlantique (Fig. 4A, B). Un des événements les plus remarquables, avec un fort degré de cohérence à l'échelle régionale, est observé dans les données du CPR (Fig. 4A), où l'abondance du phytoplancton est bien en-dessous de la moyenne à long terme dans les années 1960 et 1970 et très au-dessus de la moyenne pour les années 1990 et 2000. Les niveaux les plus élevés ont été observés au milieu des années 1990 pour décliner légèrement au cours des années subséquentes. En contraste, l'abondance de zooplancton était légèrement au-dessus de la moyenne à long terme dans les années 1960 et 1970 mais grandement en-dessous de la moyenne dans les années 1990 et 2000. Les niveaux les plus bas ont été observés au milieu des années 1990, alors que l'abondance de phytoplancton était au plus haut, mais un redressement est visible les années subséquentes surtout au sud du plateau de Terre-Neuve et sur le plateau Néo-Écossais. En général cependant, comme pour le phytoplancton une certaine cohérence régionale est présente dans l'abondance du zooplancton. Le milieu des années 1990 est aussi le moment où a débuté un réchauffement significatif et à grande échelle de l'atmosphère et de l'océan, une diminution des conditions de glace et une augmentation de la stratification dans l'Atlantique Nord-Ouest qui ont persisté jusqu'aux années 2000 (Fig. 2).

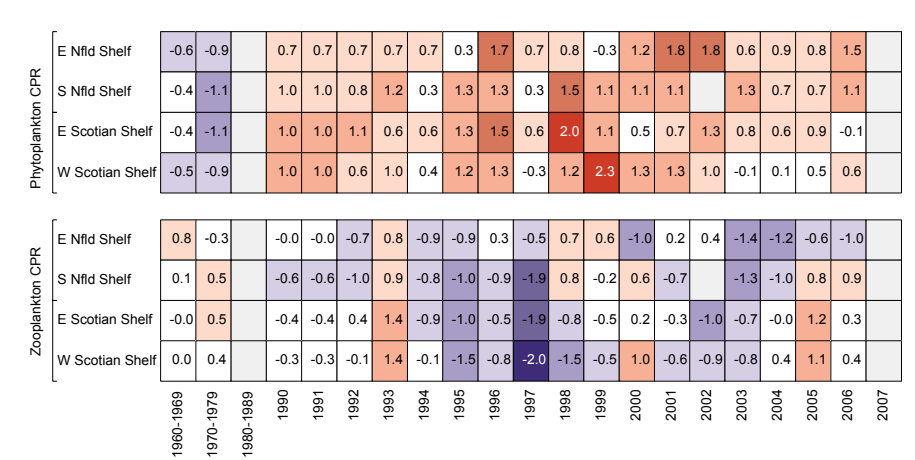


Fig. 4 A) Time series of biological variables from the Continuous Plankton Recorder (CPR), 1960–2006. A grey cell indicates missing data while a white cell is a value within 0.5 SD of the long-term mean based on data from the reference period 1960–2006. A red cell indicates a higher-than-normal level and a blue cell a lower-than-normal level; more intense colours indicate larger anomalies. The numbers in the cells are the anomaly values (differences from the long-term means divided by the standard deviations). Note that CPR data collections in the 1960s–1970s were insufficient to make annual assessments so decadal anomalies were computed; there were no CPR data for the decade of the 1980s.

A) Séries temporelles des variables biologiques tirées du Continuous Plankton Recorder (CPR) de 1960 à 2006. Une cellule grise indique une donnée manquante et une cellule blanche une valeur à l'intérieur de 0,5 écart-type de la moyenne à long terme estimée sur la période de référence de 1960 à 2006. Une cellule rouge indique une valeur plus grande que la normale et une cellule bleue une valeur plus faible que la normale; l'intensité des couleurs indique la grandeur des anomalies. Les nombres à l'intérieur des cellules sont les valeurs des anomalies (les différences entre les moyennes à long terme divisées par les écarts-types). À noter que la récolte de données du CPR était insuffisante dans les décennies 1960 et 1970 pour faire une évaluation annuelle et des anomalies décennales ont été calculées. Il n'y a pas de données du CPR pour la décennie des années 1980.

Ces signaux étaient beaucoup moins évidents dans les données du PMZA, lesquelles sont caractérisées par de grandes fluctuations dans les conditions de sels nutritifs, de phytoplancton et de zooplancton entre les années adjacentes ou parfois pouvant durer deux ou trois ans. Par exemple, des conditions de sels nutritifs au-dessus de la moyenne étaient observées dans le nord du golfe du Saint-Laurent de 2001 à 2003 mais les niveaux étaient bien en-dessous de la moyenne en 2004. Les niveaux de phytoplancton étaient bien en-dessous de la moyenne dans la région de Terre-Neuve en 2003 mais au-dessus de la moyenne la plupart du temps au cours des quatre années subséquentes.

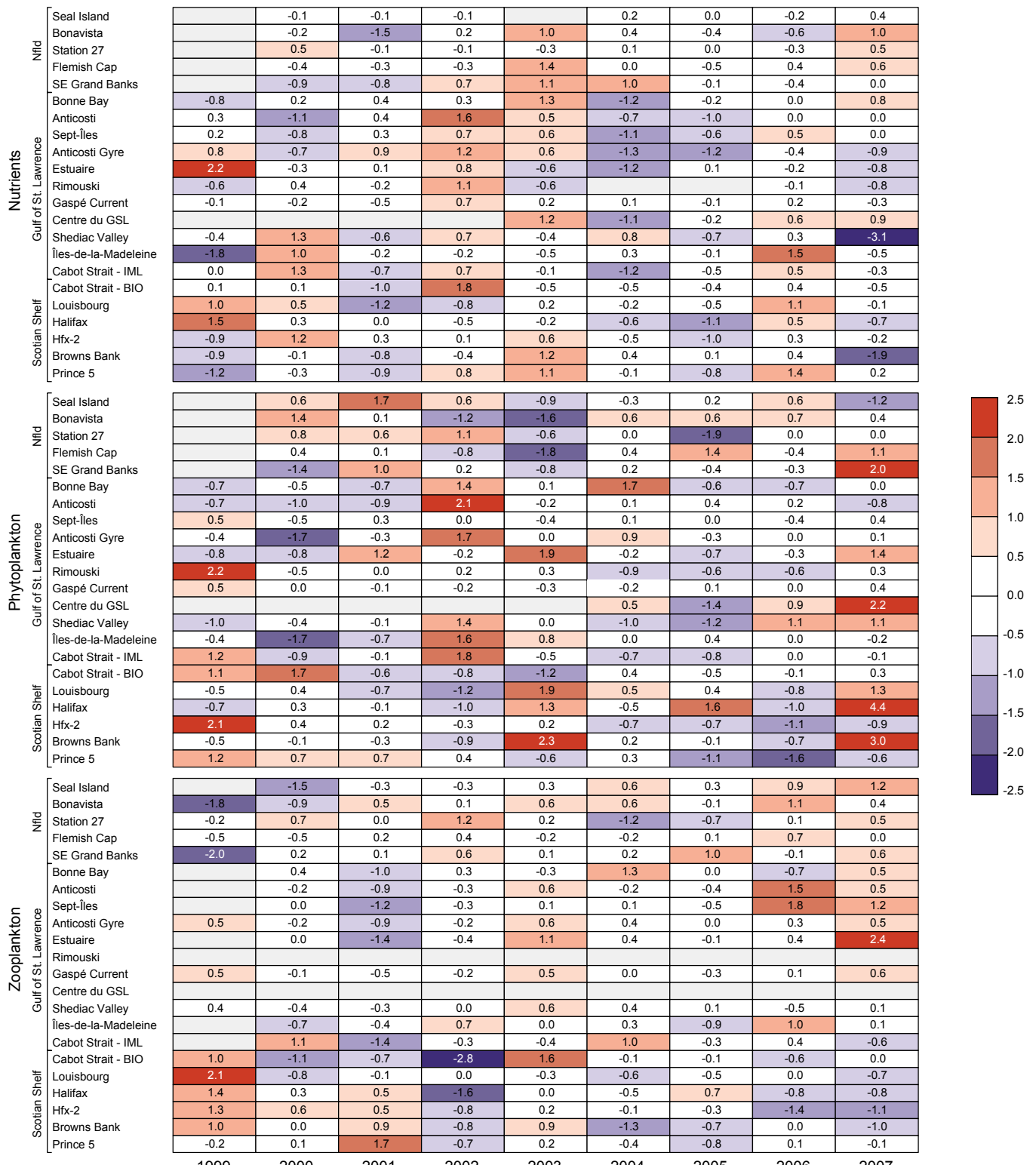


Fig. 4 B) Time series of chemical and biological variables from AZMP fixed stations and transects, 1999–2007. A grey cell indicates missing data while a white cell is a value within 0.5 SD of the long-term mean based on data from the reference period 1999–2006. A red cell indicates a higher-than-normal levels and a blue cell a lower-than-normal levels; more intense colours indicate larger anomalies. The numbers in the cells are the anomaly values (differences from the long-term means divided by the standard deviations).

B) Séries temporelles des variables chimiques et biologiques aux stations fixes et sur les transects du PMZA de 1999 à 2007. Une cellule grise indique une donnée manquante et une cellule blanche une valeur à l'intérieur de 0,5 écart-type de la moyenne à long terme estimée sur la période de référence de 1999 à 2006. Une cellule rouge indique une valeur plus grande que la normale et une cellule bleue une valeur plus faible que la normale; l'intensité des couleurs indique la grandeur des anomalies. Les nombres à l'intérieur des cellules sont les valeurs des anomalies (les différences entre les moyennes à long terme divisées par les écarts-types).

Shelf and the Scotian Shelf. Overall, however, regional coherence characterized zooplankton abundance, as was the case for phytoplankton. The mid-1990s was also the beginning of a period of significant and widespread atmospheric and ocean warming, reduced ice conditions, and increased stratification in the NW Atlantic that persisted through the 2000s (Fig. 2).

Patterns were less clear in the AZMP data, which were often characterized by large swings in nutrient, phytoplankton, and zooplankton conditions between adjacent years or sometimes lasting 2-3 years. For example, above-average nutrient conditions were observed in the northern Gulf of St. Lawrence in 2001-2003, but levels were well below the mean in 2004. Phytoplankton levels were well below the mean in the Newfoundland region in 2003 but above the mean, for the most part, during the subsequent four years. Zooplankton showed the most coherence regionally, i.e., levels in the Newfoundland and Gulf regions were generally above the long-term mean from 2004-2007 but below the mean on the Scotian Shelf. Clearly, the strong, often year-to-year, fluctuations in chemistry and biology are difficult to explain from the physical conditions that often show a more systematic and lower frequency variability, e.g., the cold and fresh mid-1980s through early 1990s and warm and salty late 1990s and 2000s (Fig. 2).

By concentrating on a particular year, regional coherence becomes more apparent (Fig. 5). For example, nutrient inventories on the Newfoundland-Labrador and Grand Banks shelves in 2007 were above the long-term mean, whereas nutrient inventories were generally below the mean throughout much of the Gulf of St. Lawrence and the Scotian Shelf. Phytoplankton showed considerable spatial variability, with below-average conditions on the Newfoundland-Labrador Shelf, at coastal fixed sites off Halifax, and in the Bay of Fundy, and above-average conditions throughout the eastern Newfoundland Shelf, Grand Banks, Gulf of St. Lawrence, and the Scotian Shelf. High overall levels could be linked to strong and widespread spring blooms at many of the AZMP sites. Zooplankton showed the greatest spatial coherence: conditions were above average from Newfoundland through the Gulf of St. Lawrence whereas they were below average from Cabot Strait, across the Scotian Shelf, and into the Bay of Fundy.

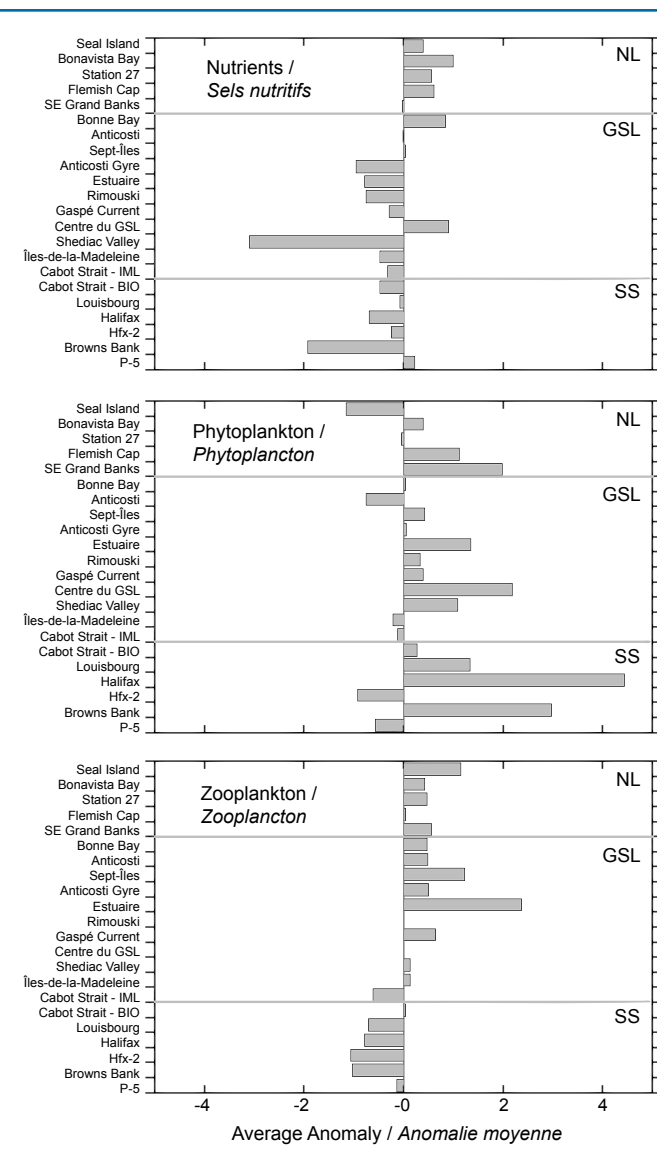


Fig. 5 Zonal summary of the average annual anomalies for nutrients, phytoplankton, and zooplankton for 2007 (NL=Newfoundland Shelf, GSL=Gulf of St. Lawrence, SS=Scotian Shelf/Bay of Fundy).

Résumé pour la zone en 2007 des anomalies moyennes annuelles pour les sels nutritifs, le phytoplancton et le zooplancton (NL=plateau de Terre-Neuve, GSL=golfe du Saint-Laurent, SS=plateau Néo-Écossais/baie de Fundy).

Le zooplancton montrait le plus de cohérence entre les régions, c.-à-d. les niveaux dans les régions de Terre-Neuve et du Québec étaient en général au-dessus de la moyenne à long terme de 2004 à 2007 mais sous la moyenne sur le plateau Néo-Écossais. Évidemment, les fortes fluctuations, souvent d'une année à l'autre, dans la chimie et la biologie sont difficiles à expliquer en relation avec les conditions physiques qui montrent une variabilité plus systématique et une fréquence de variabilité plus faible, c.-à-d. des conditions froides et moins salées du milieu des années 1980 au début des années 1990 et des conditions chaudes et salées de la fin des années 1990 au années 2000 (Fig. 2).

Une cohérence régionale est plus évidente si on se concentre sur une année en particulier (Fig. 5). Par exemple, les inventaires en sels nutritifs sur les plateaux de Terre-Neuve et Labrador et des Grands Bancs en 2007 étaient au-dessus de la moyenne à long terme, alors qu'ils étaient généralement en-dessous de la moyenne pour une grande partie du golfe du Saint-Laurent et du plateau Néo-Écossais. Le phytoplancton montre une variabilité spatiale élevée avec des conditions sous la

moyenne sur le plateau de Terre-Neuve et Labrador, aux stations côtières fixes au large d'Halifax et dans la baie de Fundy, et des conditions au-dessus de la moyenne pour le plateau de l'est de Terre-Neuve, les Grands Bancs, le golfe du Saint-Laurent et le plateau Néo-Écossais. Dans l'ensemble, les hauts niveaux pourraient être liés aux fortes floraisons printanières étendues à plusieurs sites du PMZA. Le zooplancton montrait la plus grande cohérence spatiale; les conditions étaient au-dessus de la moyenne de Terre-Neuve au golfe du Saint-Laurent alors qu'elles étaient sous la moyenne du détroit de Cabot, traversant le plateau Néo-Écossais, jusqu'à la baie de Fundy.

Faits saillants

Les conditions chimiques et biologiques (les niveaux trophiques inférieurs) dans l'Atlantique Nord-Ouest sont très variables dans l'espace et le temps ce qui rend difficile la détection de changements à court terme ou régionalement

Highlights

Chemical and biological (lower trophic level) conditions in the NW Atlantic are highly variable in space and time and tend to make the detection of regional or short-term changes in standing stock difficult. Despite the inherent variability, coherent signals that affect broad areas or that persist for several years have become apparent. For example, events such as a strong phytoplankton blooms (reflected in annual biomass) are seen in some years (e.g., 2007) and are manifest over large geographic areas. Conditions of some biological features (e.g., zooplankton abundance) may persist over longer periods (years) and show regionally distinct patterns, e.g., higher-than-average abundances of zooplankton have been seen off Newfoundland and the northern Gulf over the past four years while lower-than-average abundances have persisted on the Scotian Shelf. CPR results suggest that these conditions may persist for a decade or longer for some taxonomic groups. The linkage of the chemistry and biology of the NW Atlantic to its physical environment is not entirely clear from the scorecard approach, which assesses conditions on an annual time scale. Indicators that take account of processes and linkages on short time scales (daily to seasonal) will have to be considered.

dans l'état des variables. Malgré cette variabilité inhérente, des signaux cohérents sont apparents qui ont affecté de grande surfaces ou qui ont persisté plusieurs années. Par exemple, des événements comme une forte floraison de phytoplancton (réflétée dans la biomasse annuelle) ont été observés certaines années (ex. 2007) et se sont manifestés sur de grandes étendues géographiques. Les conditions pour certaines données biologiques (ex. l'abondance de zooplancton) peuvent persistées sur de longues périodes (des années) et montrent des signatures régionales distinctes; par exemple des abondances de zooplancton plus élevées que la moyenne ont été observées au large de Terre-Neuve et dans le nord du golfe au cours des quatre dernières années alors que des abondances plus faibles que la moyenne ont persisté sur le plateau Néo-Écossais. Les données du CPR suggèrent que ces conditions peuvent persister pour une décennie ou plus selon les groupes taxonomiques. La relation entre la chimie et la biologie dans l'Atlantique Nord-Ouest et l'environnement physique n'est pas claire en se fiant à la méthode des tableaux synoptiques qui évaluent les conditions sur une échelle de temps annuelle. Des indicateurs qui rendent compte des processus et relations à courtes échelles de temps (journalière, saisonnière) devront être considérés.

Physical, Chemical, and Biological Status of the Labrador Sea

Labrador Sea Monitoring Group¹

Bedford Institute of Oceanography, Box 1006, Dartmouth, NS, B2Y 4A2

Sommaire

Une grande partie du matériel présenté dans ce troisième rapport d'état provient de l'échantillonnage annuel réalisé du 23 au 29 mai 2008 sur le transect AR7W, lequel s'étend du Labrador à la côte ouest du Groenland. L'information sur l'historique du transect AR7W peut être consultée dans le premier rapport d'état publié dans le bulletin du PMZA numéro 6.

La partie centrale de la mer du Labrador a connu au cours de l'hiver (janvier à mars) les températures de l'air près de la surface les plus froides des 16 dernières années, alors que pour le reste de l'année les températures ont été au-dessus de la normale et l'été (juillet à septembre) a été le 3^{ème} plus chaud des 61 années de données *NCEP Reanalysis*. La moyenne annuelle des températures de l'air près de la surface en 2008 était la plus froide depuis 2000 mais toujours au-dessus de la normale. Notamment, le couvert de glace a été plus étendu que la normale dans le nord-ouest de la mer du Labrador. Les températures de la surface de la mer se sont refroidies à l'automne 2007 et l'hiver 2008 mais sont demeurées légèrement au-dessus de la normale de 1971 à 2000 pour toute l'année 2008. Des températures de la surface de la mer élevées, presque record, au printemps et à l'été 2008 font en sorte que la moyenne annuelle a été la 5^{ème} plus chaude de la période 1960 à 2008, légèrement plus chaude qu'en 2007. La période de 2003 à 2008 inclut six des sept années de moyennes annuelles des températures de la surface de la mer les plus chaudes de la période 1960 à 2008 (1997 a été la 6^{ème} plus chaude, légèrement au-dessus de 2007). De grandes étendues au centre de la mer du Labrador ont connu une augmentation de la température de l'air de 2 °C et une augmentation de la température de la surface de la mer de 1 °C au cours des deux dernières décennies.

Les données des profils Argo de mars 2008 montrent que le refroidissement et l'augmentation de densité dans les couches supérieures de la partie centre-ouest de la mer du Labrador au cours de l'hiver froid de 2008 ont produit des couches d'hiver mélangées s'étendant jusqu'à 1350 à 1600 m de profondeur. Des quantités accrues d'eau au mode 27,72 à 27,74 kg m⁻³ d'anomalie de densité potentielle ont été observées au centre-ouest de la mer du Labrador en mai 2008. Dans l'ensemble, les couches supérieures de la mer du Labrador sont demeurées chaudes et salées.

Les concentrations de carbone inorganique total dans les couches supérieures du centre de la mer du Labrador ont continué à augmenter, accompagnées d'une décroissance correspondante du pH. Les concentrations d'oxygène dissous dans les mêmes masses d'eau montrent une diminution constante en raison, à part approximativement égale, d'une diminution de la solubilité en réponse au réchauffement et d'autres facteurs pouvant inclure une augmentation de la consommation biologique. L'état des sels nutritifs poursuit les tendances récentes d'une

¹ The Labrador Sea Monitoring Group includes scientists and technicians from Ocean Sciences Division (<http://www.mar.dfo-mpo.gc.ca/science/ocean/osd/osd-e.html>) and Ecosystem Research Division (<http://www.mar.dfo-mpo.gc.ca/science/ocean/erd/erd-e.html>). For further information, please contact John Loder (OSD) John.Loder@dfo-mpo.gc.ca or Glen Harrison (ERD) Glen.Harrison@dfo-mpo.gc.ca.

diminution des silicates et des phosphates, indiquant une diminution de l'influence des eaux arctiques et une augmentation de l'influence d'eaux subtropicales. Les tendances dans les concentrations de nitrates sont toujours faibles et variables. Les tendances observées dans les concentrations relatives de sels nutritifs, telles que l'augmentation des ratios nitrate:silicate et la réduction des phosphates par rapport aux nitrates sont particulièrement frappantes.

La grande variabilité dans toutes les propriétés biologiques rend incertaine l'identification de tendances multi annuelles. Les concentrations de chlorophylle et de bactéries dans la couche supérieure sont demeurées relativement stables au cours de la dernière décennie. Cependant, dans les deux cas une tendance légèrement positive est observée au centre du bassin du Labrador et le plateau et la pente continentale de l'ouest du Groenland et une tendance négative sur le plateau et la pente continentale du Labrador. Les données satellitaires de la couleur de l'océan suggèrent que l'événement principal de croissance de phytoplancton au printemps et l'été 2008 a été plus tôt et plus intense qu'à l'habitude sur le plateau continental et dans le bassin du Labrador mais moins intense sur le plateau continental à l'ouest du Groenland. Les informations préliminaires laissent croire que 2008 n'a pas été une bonne année pour le recrutement de *C. finmarchicus* sur le plateau continental à l'ouest du Groenland.

Introduction

DFO Maritimes Science Branch at the Bedford Institute of Oceanography monitors physical, chemical, and biological conditions in the Labrador Sea with annual occupations of the AR7W section from the Labrador Shelf to Greenland. This is the third annual Labrador Sea status report. Background material on the history of the AR7W section can be found in the initial status report published in AZMP Bulletin No. 6.

The AR7W Section

Figure 1 shows a map of the Labrador Sea and the locations of the standard hydrographic stations. Ice conditions permitting, 28 stations with full chemical sampling and three additional physics-only stations are occupied annually between Hamilton Bank on the Labrador Shelf and Cape Desolation on the Greenland Shelf. The surveys measure temperature, salinity, and a comprehensive suite of chemical variables including dissolved oxygen, nutrients, and dissolved inorganic carbon. Since 1994, biological variables such as dissolved and particulate biogenic (organic) carbon, bacteria, phytoplankton, and zooplankton have been an integral part of the measurement program.

The 2008 AR7W Labrador Sea section was occupied from 23–29 May 2008 on board CCGS *Hudson*. Most of the planned station work was completed, totalling 27 primary CTD stations, 6 shallow biological CTD stations, and multiple net tows per station. Ice conditions prevented the occupation of the four inshore stations on the West Greenland Shelf.

Physical Environment

Surface air temperature

Winter 2008 (defined as January–February–March, JFM) surface air temperatures over the Labrador Sea were notably colder than normal (the 1971 to 2000 normal period is used throughout unless otherwise indicated). NCEP Reanalysis data (Kalnay et al. 1996) showed JFM temperatures up to 6°C below normal in southern Davis Strait and the northern Labrador Sea. JFM 2008 air temperatures over the central Labrador Sea were less extreme but still averaged about 1°C below normal for a representative 5° x 5° box (55° to 60°N, 50° to 55°W) (Fig. 2). Winter 2008 was the coldest since 1993 (16 years) and the 8th coldest in the 61-year NCEP Reanalysis period (1948–2008) for this region. This was a marked change from recent years, since the average 2000–2007 wintertime air temperatures were nearly 2°C warmer than normal and the average 2004–2007 wintertime air temperatures were

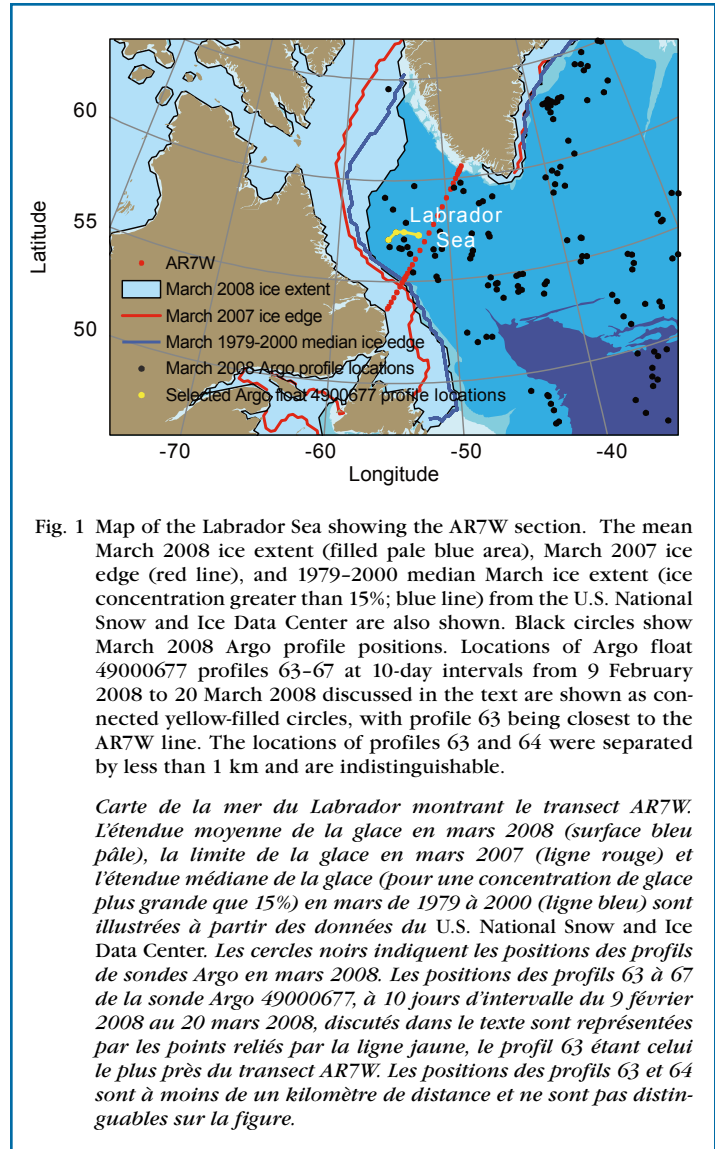


Fig. 1 Map of the Labrador Sea showing the AR7W section. The mean March 2008 ice extent (filled pale blue area), March 2007 ice edge (red line), and 1979–2000 median March ice extent (ice concentration greater than 15%; blue line) from the U.S. National Snow and Ice Data Center are also shown. Black circles show March 2008 Argo profile positions. Locations of Argo float 49000677 profiles 63–67 at 10-day intervals from 9 February 2008 to 20 March 2008 discussed in the text are shown as connected yellow-filled circles, with profile 63 being closest to the AR7W line. The locations of profiles 63 and 64 were separated by less than 1 km and are indistinguishable.

Carte de la mer du Labrador montrant le transect AR7W. L'étendue moyenne de la glace en mars 2008 (surface bleu pâle), la limite de la glace en mars 2007 (ligne rouge) et l'étendue médiane de la glace (pour une concentration de glace plus grande que 15%) en mars de 1979 à 2000 (ligne bleu) sont illustrées à partir des données du U.S. National Snow and Ice Data Center. Les cercles noirs indiquent les positions des profils de sondes Argo en mars 2008. Les positions des profils 63 à 67 de la sonde Argo 49000677, à 10 jours d'intervalle du 9 février 2008 au 20 mars 2008, discutés dans le texte sont représentées par les points reliés par la ligne jaune, le profil 63 étant celui le plus près du transect AR7W. Les positions des profils 63 et 64 sont à moins de un kilomètre de distance et ne sont pas distinguables sur la figure.

more than 3°C warmer than normal. The remainder of 2008 saw air temperatures 1–2°C warmer than normal. Spring 2008 (April–May–June, AMJ) was the 11th warmest spring in 61 years, and summer 2008 (July–August–September, JAS) was the 3rd warmest summer in 61 years; only 2003 and 2006 were warmer. The anomalously cool winter and warm spring–summer temperatures partly offset each other such that the 2008 annual mean Labrador Sea surface air temperature was approximately 0.5°C above normal. This represents a drop of 0.8°C from the 2000–2007 average and makes 2008 the coldest year since 2000 (9 years) and the 22nd coldest in the 61-year NCEP Reanalysis period.

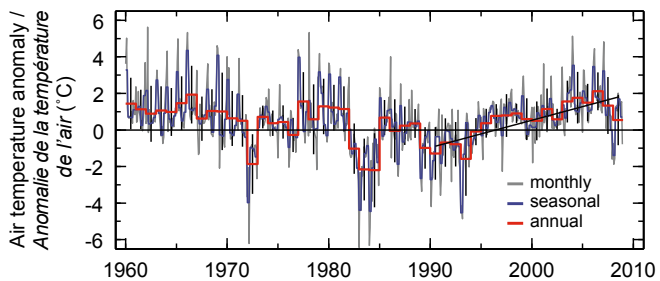


Fig. 2 Surface air temperature anomalies relative to 1971–2000 averaged over the central Labrador Sea for 1960–2008 from NCEP (National Centers for Environmental Prediction) Reanalysis data. Monthly (grey line), seasonal (blue line), and annual (red line) means are shown. A regression line (in black) for the 1990–2008 period gives an increase of about 2.7°C over that period.

Anomalies de la température de l'air au centre de la mer du Labrador de 1960 à 2008 par rapport à la moyenne des années 1971 à 2000 provenant des données NCEP Reanalysis (National Centers for Environmental Prediction). Les moyennes mensuelles (ligne grise), saisonnières (ligne bleu), et annuelles (ligne rouge) sont indiquées. La régression (ligne noire) sur les années récentes, de 1990 à 2000, révèle une augmentation de 2,7 °C pour la période.

Sea ice

The U.S. National Snow and Ice Data Center sea-ice index (Fetterer et al. 2008) shows greater-than-normal March 2008 sea-ice cover in the northern Labrador Sea (Fig. 1). This is consistent with the cold winter conditions detailed above. The mean March 2008 ice edge in the northern Labrador Sea extended about 200 km seaward of the long-term (1979–2000) median location (Fig. 1). At the same time, sea-ice extent on the Labrador Shelf south of about 56°N was close to normal. In contrast, March 2007 ice cover was less than normal for the entire Labrador Sea, with the ice edge in the northern Labrador Sea 100–150 km in retreat of the long-term March median position (Fig. 1).

Sea-surface temperature

Labrador Sea sea-surface temperatures (SST) have increased by about 1°C during the past 20 years (Fig. 3A) according to the HadISST fields from the UK Hadley Centre (Rayner et al. 2003). Record-warm annual means for the 1960–2008 period occurred from 2003–2006. Based on annual means, 2008 was the 5th warmest year since 1960 (49 years), slightly warmer than 2007. The 2003–2008 period included the five warmest years in the 1960–2008 period and 2007 was the 7th warmest, exceeded only by 1997. However, the annual mean anomalies mask an underlying seasonal variability: JFM 2008 was the coldest winter since 2000 (9 years) (Fig. 3A), consistent with the relatively cold winter conditions and increased sea-ice coverage noted above. Seasonal mean SSTs for AMJ and JAS 2008 were respectively the 4th warmest spring and the warmest summer since 1960, consistent with the observed switch to warm surface air temperatures in spring and summer 2008.

The recent warming trend has been dominated by particularly warm conditions in the west-central Labrador Sea (Fig. 3B).

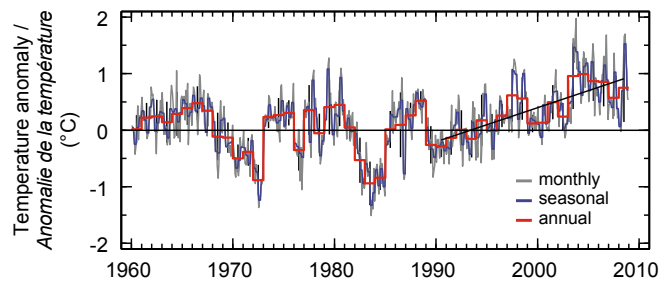


Fig. 3A HadISST sea-surface temperature anomalies relative to 1971–2000 interpolated to the AR7W line and averaged over the distance range 55–915 km (from SW to NE along the transect) for 1960–2008. Monthly (grey line), seasonal (blue line), and annual (red line) means are shown. A regression line (in black) for the 1990–2008 period gives an increase of about 1.1°C over that period.

Anomalies des températures de la surface de la mer HadISST pour 1960 à 2008 par rapport à la moyenne des années 1971 à 2000 interpolées au transect AR7W et moyennes entre le km 55 et le km 915 (du sud-ouest au nord-est) du transect AR7W. Les moyennes mensuelles (ligne grise), saisonnières (ligne bleu) et annuelles (ligne rouge) sont indiquées. La régression (ligne noire) sur les années récentes de 1990 à 2000 révèle une augmentation de 1,1 °C pour la période.

Below-normal sea-surface temperature conditions prevailed over the Labrador Shelf in late 2007 and early 2008, but warmer-than-normal conditions were re-established during the later part of 2008.

Labrador Sea hydrography

The temperature and salinity of the upper layers of the Labrador Sea change from year to year in response to changes

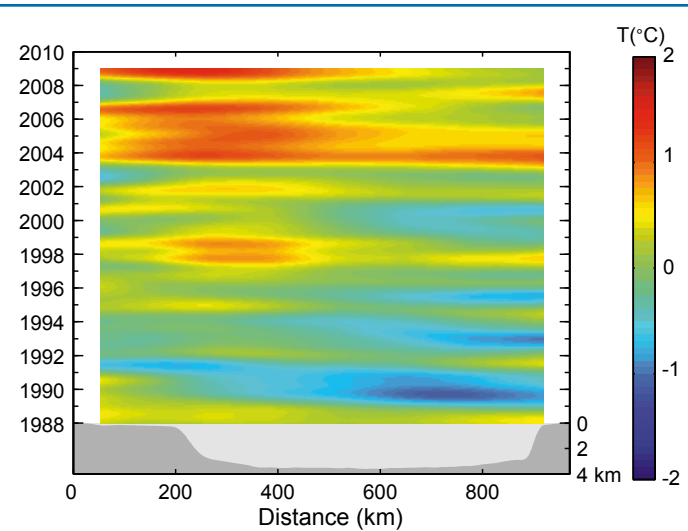


Fig. 3B Low-pass filtered 1988–2008 HadISST sea-surface temperature anomalies relative to 1971–2000 interpolated to the AR7W line. The bathymetry along the AR7W line (from SW to NE) is shown at the bottom of the figure.

Anomalies des températures de la surface de la mer HadISST observées pour 1988 à 2008 par rapport aux années 1971 à 2000; ces données ont été filtrées par un filtre passe-bas et interpolées au transect AR7W. Le profil bathymétrique du transect est illustré au bas de la figure (du sud-ouest au nord-est).

in atmospheric forcing, freshwater inputs from the Arctic and from local sea-ice melt, and changes in the warm and saline inflows in the West Greenland Current. Seasonal cycles in each of these three forcing terms drive a strong seasonal cycle in the properties of the upper layers of the Labrador Sea. During the early 1990s, deep winter convection in the Labrador Sea filled the upper 2 km with cold and fresh water. Recent milder years have produced more limited amounts of warmer, saltier, and less-dense mode waters. Convection in the Labrador Sea is part of the meridional overturning circulation or global conveyor belt that plays an important role in the global climate system.

Vertical overturning associated with the cold winter of 2008 was captured in a number of Argo float profile measurements during March 2008. Våge et al. (2009) and Yashayaev and Loder (2009) exploited these Argo profile measurements in their descriptions of the convection that occurred in the Labrador Sea during this period. Four separate Argo floats whose March 2008 profile positions are included in Figure 1 showed vertical overturning to depths of 1350–1600 m in the west-central Labrador Sea. The deep mixed layers seen in the Argo measurements had a maximum potential density anomaly just greater than 27.74 kg m^{-3} . The associated mode waters had potential temperatures varying between approximately 3.26 and 3.30°C . For example, five February–March 2008 profiles from Canadian Argo float 4900667 at locations also shown in Figure 1 provide a detailed view of the development of a 1450 m deep mixed layer (Fig. 4A).

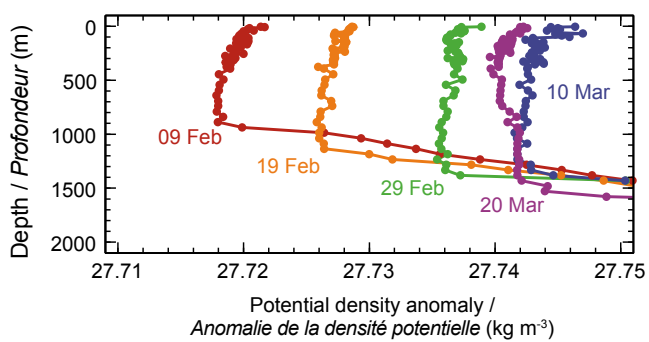


Fig. 4A Observations from Canadian Argo float 4900677 of the deepening of the surface mixed layer in the west-central Labrador Sea from 9 February to 20 March 2008 (profiles 63–67). The float moved approximately 180 km from west to east during this 40-day period. Profile locations are shown in Figure 1. Profile 67 on 20 March 2008 revealed a mixed layer extending from the surface to about 1450 m in depth that was homogeneous in potential density within $\sim 0.002 \text{ kg m}^{-3}$ (27.740 to 27.742), in potential temperature within $\sim 0.017^\circ\text{C}$ (3.261 to 3.278), and in salinity within ~ 0.003 (34.850 to 34.853).

Observations de la sonde canadienne Argo 4900677 du déplacement en profondeur de la couche de surface mélangée entre le 9 février 2008 et le 20 mars 2008 (profils 63 à 67), au centre-ouest de la mer du Labrador. Pendant la période de 40 jours, la sonde s'est déplacée d'approximativement 180 km d'ouest en est. La localisation des profils est illustrée à la figure 1. Le 20 mars 2008, le profil 67 montre une couche mélangée s'étendant de la surface jusqu'à la profondeur de 1450 m, homogène au niveau de la densité potentielle avec un écart limité à $\sim 0.002 \text{ kg m}^{-3}$ (27.740 à 27.742), de la température potentielle avec un écart limité à $\sim 0.017^\circ\text{C}$ (3.261 à 3.278) et de la salinité avec un écart limité à ~ 0.003 (34.850 à 34.853).

The annual AR7W surveys take place as early in the spring of the year as practical to provide a consistent view of interannual change in the face of strong seasonal changes in physical, chemical, and biological properties. Sea ice generally prevents access to the Labrador Shelf before mid-May. The median midpoint date for the 19 spring or early summer surveys completed since 1990 is June 1. The 2008 survey took place slightly earlier than the norm, with a midpoint date of May 27. No sea ice was encountered on the Labrador Shelf, but multi-year ice carried northward by the West Greenland Current prevented the occupation of the four easternmost stations on the West Greenland slope and shelf.

Remnants of the water masses renewed in the winter of 2008 show up in the May 2008 observations in the west-central Labrador Sea as an increased vertical separation of potential density surfaces for particular ranges of potential density (Fig. 4B). Enhanced layer thicknesses with a broad and somewhat bimodal distribution were observed in the 27.72 – 27.74 kg m^{-3} potential density anomaly range. In spite of the cold 2008 winter and the deep mixed layers observed in March 2008, the May survey results suggest that the volume and density range of Labrador Sea water renewal in winter 2008 were similar to those of recent years (with the notable exception of 2007). For example, the mode waters observed at the same stations in the 2003 survey were denser and of a volume similar to the 2008 results (Fig. 4B). This suggests that there was significant spatial variability in the intensity of vertical overturning during the winter of 2008. Both the March 2008 Argo float measurements and the results from the May 2008 AR7W survey suggest that the renewal was confined to the west-central Labrador Sea. The amount and density classes of mode waters formed in recent years contrast with conditions observed in the early 1990s, when a sequence of cold winters filled the upper 2 km of the entire Labrador Basin with cold, fresh, and relatively dense mode waters (range ~ 27.75 to 27.80 kg m^{-3} ; Fig. 4B).

The two modal densities observed in the west-central Labrador Sea in the May 2008 survey are associated with different depths. The less-dense mode (found at two stations) centred at 27.725 kg m^{-3} was found at an average depth of 710 m compared to an average depth of 1150 m for the denser mode (found at three stations) centred at 27.733 kg m^{-3} (Fig. 4C).

The 2008 survey found abundant amounts of the warm and saline Atlantic waters from the Irminger Current that enter the Labrador Sea as an offshore branch of the West Greenland Current and play an important role in the regional heat and salt balance (Fig. 4C). Remnants of these waters also appeared over the Labrador Slope. Overall, the upper layers of the Labrador Sea remain warm and saline.

Chemical Environment

Deep mixed layers formed in the Labrador Sea during winter convection exchange oxygen, carbon dioxide (CO_2), and other gases with the overlying atmosphere. The Labrador Sea acts as a net sink of atmospheric CO_2 because the deeper parts of the gas-enriched winter mixed layers become isolated from the atmosphere by seasonal restratification. Intermediate-depth circulation pathways export the sequestered CO_2 from the Labrador Sea into the adjoining North Atlantic.

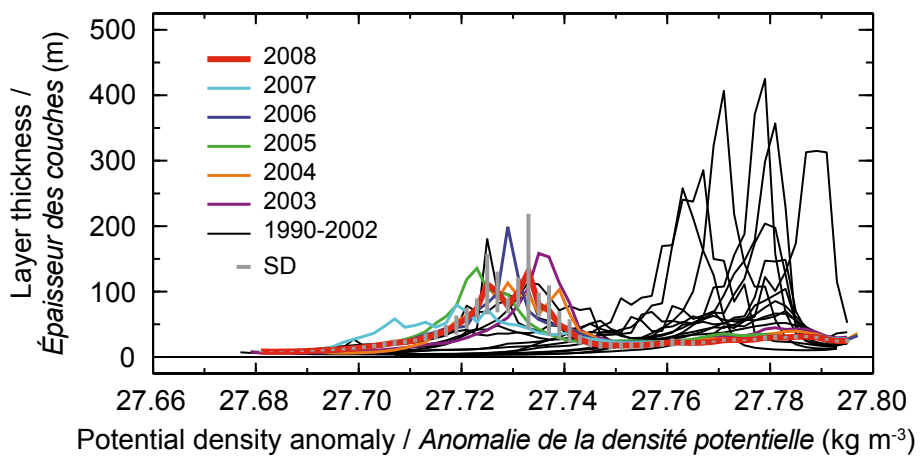


Fig. 4B Average thickness of layers bounded by selected potential density surfaces for spring and early-summer occupations of AR7W from 1990 to 2008. The 27.6800–27.8079 kg m⁻³ range of potential density anomaly is sampled at equal 0.002 kg m⁻³ intervals. The averages are taken over typically five stations in the 325–600 km along-track distance range in Figure 3B. The last six years are colour coded as identified in the legend; years 1990–2002 have the same colour code. Standard deviations for 2008 are also shown as vertical lines. Recent years have seen limited production of mode waters in the 27.72–27.74 kg m⁻³ potential density anomaly range, in contrast to voluminous classes formed in the 27.76–27.79 kg m⁻³ range during the early 1990s. The year 2007 stands out as a year of limited mode water production. The 2008 census shows a bimodal distribution with peaks centred at 27.725 and 27.733 kg m⁻³. The central depths of the thickest layers are marked on the potential temperature section in Figure 4C. The two 2008 modes are associated with mean depths of approximately 700 and 1150 m respectively.

Épaisseur moyenne de couches définies par une sélection de surfaces de densité potentielle pendant les visites du printemps et du début de l'été au transect AR7W entre 1990 et 2008. La gamme de valeurs entre 27,6800 et 27,8079 kg m⁻³ d'anomalie de densité potentielle a été échantillonné par intervalles égaux de 0,002 kg m⁻³. Les moyennes sont calculées normalement à cinq stations entre le km 335 et le km 600 le long du transect (voir figure 3B). Les six dernières années sont identifiées par des couleurs individuelles tel qu'indiqué; les années 1990 à 2002 sont de même couleur. Les écarts-types pour l'année 2008 sont illustrés par les lignes verticales. Au cours des années récentes, il y a eu une production limitée d'eau de valeurs modales 27,72 à 27,74 kg m⁻³ d'anomalie de densité potentielles, en contraste des volumes importants des classes comprises entre 27,76 et 27,79 kg m⁻³ au début des années 1990. L'année 2007 se distingue comme étant une année de production limitée d'eau modale. L'année 2008 montre une distribution bimodale avec des pointes centrées à 27,725 et 27,733 kg m⁻³. Les profondeurs au centre des couches sont indiquées sur les profils de températures potentielles de la figure 4C. Les deux modes de 2008 correspondent à des profondeurs respectives de 700 et 1150 m.

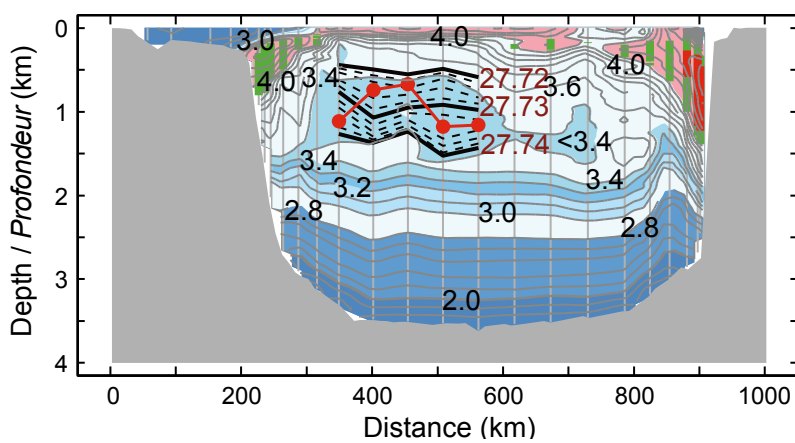


Fig. 4C Section plot of potential temperature from the 2008 occupation of AR7W. Station positions are marked by vertical lines. Waters with potential temperatures in the range 4–6°C are highlighted for salinities in the range 34.95–35.10 (red) or 34.85–34.95 (green). Selected potential density anomaly contours at 0.002 kg m⁻³ intervals are overlaid for five stations in the west-central Labrador Sea. The filled circles indicate the centre depths of the thickest potential density layers for each of the selected stations.

Profils verticaux de la température potentielle au cours de la campagne AR7W de 2008. Les lignes verticales montrent les positions des stations. Les régions colorées indiquent des eaux avec températures potentielles dans l'intervalle 4 à 6 °C dont la salinité est dans l'intervalle 34,95 à 35,10 (en rouge) ou 34,85 à 34,95 (en vert). Les contours de quelques anomalies de densité potentielle à l'intervalle de 0,002 kg m⁻³ sont superposés sur cinq stations du centre-ouest de la mer du Labrador. Les cercles pleins indiquent les profondeurs au centre des couches les plus profondes de densité potentielle à chacune des stations retenues.

Dissolved CO₂ reported as total inorganic carbon (TIC) continues to increase in the upper layers (100–500 m) of the central Labrador Sea (Fig. 5). Increasing levels of dissolved CO₂ lead to ocean acidification, with potential impacts on marine ecosystems. The concentration of total inorganic carbon in this annually ventilated upper layer has increased by about 13 μmol kg⁻¹ from 1996 to 2008. The corresponding decrease of about 0.04 pH units (Fig. 5) is equivalent to an increase in acidity of nearly 10%. If pH continues to decline at this rate, the present century will see the upper layers of the Labrador Sea become corrosive to some marine organisms with calcium carbonate shells and skeletons.

Dissolved oxygen continues to show a negative trend in this same central Labrador Sea water mass (Fig. 6). More than half of the decline can be explained by decreases in oxygen solubility associated with the warming of this layer by about 0.8°C over the past 18 years. Removal of this solubility effect gives the apparent oxygen utilization (AOU) (Fig. 6), which is the difference between the saturation concentration for the observed temperature and salinity and the observed concentration. Decreased air-sea exchanges of oxygen and a reduction in the transport of oxygen to depth are expected in the milder conditions of the recent past. Under these conditions, biological processes (respiration) will consume oxygen and increase AOU. Any oxygen consumption associated with increased respiration will also increase TIC. Both the continuing global increase in atmospheric CO₂ and the local biology play a role in the observed increases in TIC (Fig. 5) in the upper layers of the Labrador Sea.

Nutrient concentrations in the 60–200 m depth range should represent the available supply for phytoplankton growth. An upward temporal trend in nitrate concentration on the Labrador Shelf and a downward trend on the Greenland Shelf were reported in AZMP Bulletin No. 7. Both these trends persist with the addition of the 2008 data, but

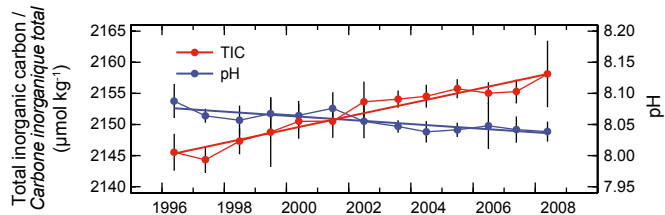


Fig. 5 Total inorganic carbon (left axis) and pH (right axis) in the 150–500 m depth range and corresponding regression lines for stations in the central part of the Labrador Basin for the period 1996–2008.

Concentrations de carbone inorganique total (axe de gauche) et pH (axe de droite) dans l'intervalle de profondeur 150 à 500 m et les lignes de régression correspondantes pour des stations au centre du bassin du Labrador pour la période 1996 à 2008.

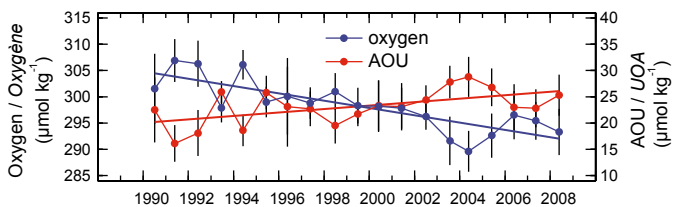


Fig. 6 Dissolved oxygen concentration in the 150–500 m depth range (left axis), apparent oxygen utilization (AOU, right axis), and the corresponding regression lines for stations in the central part of the Labrador Basin for the period 1990–2008.

Concentration d'oxygène dissous (axe de gauche) et utilisation apparente de l'oxygène (UAO, axe de droite) dans l'intervalle de profondeur 150 à 500 m et les lignes de régression correspondantes pour des stations au centre du bassin du Labrador pour la période 1990 à 2008.

it appears that the trend for the Labrador Basin, which was slightly upward until ~2005, may now be slightly downward. None of these trends is significant at $P < 0.05$. Statistically significant downward trends in silicate in all three regions reported in AZMP Bulletin No. 7 continue into 2008. Phosphate (not discussed in AZMP Bulletin No. 7) shows downward trends similar to those of silicate in all three areas, but the trend on the Greenland Shelf is not statistically significant.

The relative concentrations of nutrients as well as the absolute concentrations are important for biological productivity. Increases in the nitrate:silicate ratio described in AZMP Bulletin No. 7 persist with the addition of the 2008 data. A continued reduction of silicate relative to nitrate may eventually affect the community composition of local phytoplankton populations, particularly the dominant silicate-requiring diatoms. The relative concentrations of nitrate and phosphate are also interesting. In most of the Atlantic Ocean, the ratio of nitrate (N) to phosphate (P) concentrations follows the Redfield ratio ($N/P = 16$). On the Labrador Shelf (and to a lesser extent the rest of the Labrador Sea), Arctic Ocean waters with low N/P ratios contribute a substantial amount of “excess phosphate” relative to a prediction based on measured nitrate concentrations and the Redfield ratio (Fig. 7). Downstream, in the warmer waters of the subtropical North

Excess Phosphate / Excès de phosphate ($\mu\text{mol L}^{-1}$)

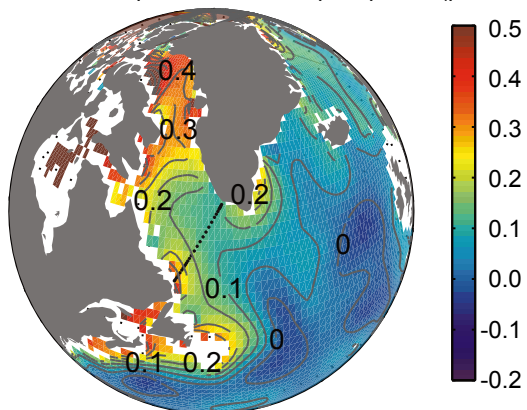


Fig. 7 Climatological annual mean excess phosphate ($[P]-[N]/16$) in the depth range 50–200 m from World Ocean Atlas 2005 (Garcia et al. 2006). Dots mark the positions of the standard AR7W stations.

Climatologie des moyennes annuelles de l'excès de phosphate ($[P]-[N]/16$) pour l'intervalle de profondeur de 50 à 200 m dans l'Atlantique Nord-Ouest selon le World Ocean Atlas 2005 (Garcia et al. 2006). Les positions des stations standards AR7W sont illustrées par les points noirs.

Atlantic, residual phosphate is required to fuel biological nitrogen fixation when nitrate is depleted and phytoplankton switch to molecular nitrogen for nitrogen nutrition. The excess phosphate carried south by the Labrador Current may be an important source of residual phosphate for the subtropical North Atlantic. Concentrations of excess phosphate have decreased by more than 30% on the Labrador Shelf since 1990 (Fig. 8). Weaker but statistically significant declines in excess phosphate are also seen in the Labrador Basin. Excess phosphate has been essentially invariant on the Greenland Shelf.

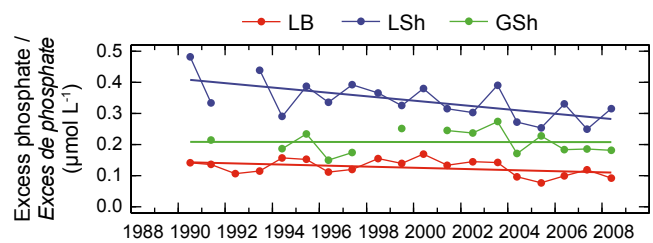


Fig. 8 Excess phosphate ($[P]-[N]/16$) concentrations (60–200 m) and corresponding regression lines for groups of stations for the central Labrador Basin (LB), the Labrador Shelf (LSh), and the West Greenland Shelf (GSh).

Concentrations de l'excès de phosphate ($[P]-[N]/16$), entre 60 et 200 m, et les lignes de régression correspondantes pour un groupes de stations au centre du bassin du Labrador (LB), le plateau du Labrador (LSh) et le plateau de l'ouest du Groenland (GSh).

Biological Environment

Chlorophyll and bacteria

Time series of the 0–100 m mean chlorophyll concentration and water-column mean bacterial abundance for station groups for the central Labrador Basin, the Labrador Shelf/Slope, and the Greenland Shelf/Slope show large scatter partly caused by sampling issues related to seasonal variability

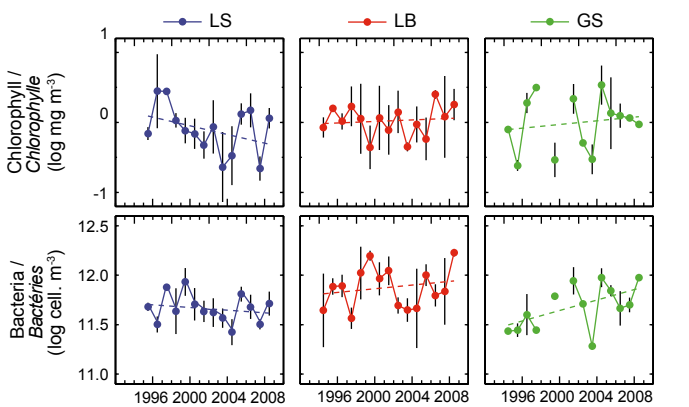


Fig. 9 Chlorophyll concentration (0–100 m) (top) and bacterial abundance (all depths) (bottom) averaged over groups of stations for the central Labrador Basin (LB), the Labrador Shelf/Slope (LS), and the Greenland Shelf/Slope (GS). Standard deviations and regression lines are also shown.

Concentrations de la chlorophylle (entre 0 et 100 m) (panneau du haut) et l'abondance de bactéries (toutes les profondeurs) (panneau du bas) pour des groupes de stations dans le bassin du Labrador (LB) et sur les plateaux et les pentes continentales du Labrador (LS) et de l'ouest du Groenland (GS). Les écarts-types et les droites de régression sont illustrés.

(Fig. 9). Both biogenic carbon pools have remained relatively stable during the 14-year measurement period. Weak positive trends (not statistically significant) for both carbon pools were maintained in the Labrador Basin and West Greenland Shelf/Slope regions. Somewhat stronger negative trends for both chlorophyll and bacteria were maintained on the Labrador Shelf/Slope. Note that incorrect information was provided in the Labrador Sea status report in AZMP Bulletin No. 7. An unfortunate last-minute edit resulted in mixing up the Labrador Basin and Labrador Shelf/Slope series. In the related figure, the legend labels LSh and LB were transposed.

Satellite ocean colour data (SeaWiFS and MODIS sensors) provide a more synoptic view of the regional and temporal dynamics of phytoplankton (surface chlorophyll) in the Labrador Sea. Time series from satellite data (1997–2008) are generally consistent with the ship-based observations, i.e., high interannual variability and weak trends, but they do show that the 2008 spring–summer peak chlorophyll in surface waters was earlier and more intense on the Labrador Shelf and in the Labrador Basin than seen in previous years. On the Greenland Shelf, however, the spring chlorophyll peak was significantly lower than usual.

Increasing temperature, shifts in nutrient levels, and acidification will certainly affect biological processes. These signals will propagate through plankton food webs from the bottom up starting at the level of phytoplankton, which are the primary producers. The possibility that environmental change is driving changes in species composition is a critical point for investigation and is something to look for in future AR7W surveys.

Zooplankton

Zooplankton samples are collected in vertical net hauls between 100 m and the surface at stations along the AR7W

section on the annual surveys. One species dominates the zooplankton biomass, the copepod *Calanus finmarchicus*. Individual *C. finmarchicus* spend the winter at depth as pre-adults in an inactive state. They return to the surface layers in spring to mature, mate, and reproduce. The adults die after reproducing and their offspring develop and feed over the summer, returning to the depths as pre-adults in fall.

The seasonal pattern of *C. finmarchicus* development was examined using data from 1995 to 2006 to calculate a population development index (PDI), defined as the percent of young stage copepodite abundance (stages CI–CIII) of the total abundance (CI–CVI) for the two-week periods over which sampling occurred (Fig. 10). In the central Labrador

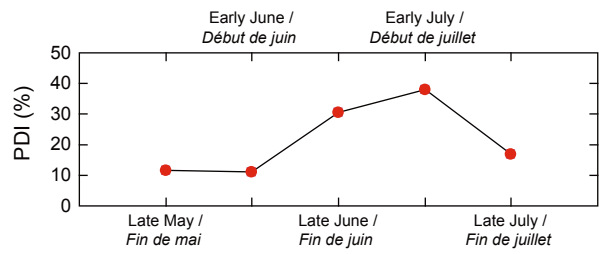


Fig. 10 *Calanus finmarchicus* population development index (PDI) (sum of abundance of young stages [CI–CIII] x 100/sum of all stages) in the central Labrador Sea averaged over two-week sampling periods for annual cruises between 1995 and 2006.

Indice du développement de la population (PDI) de Calanus finmarchicus (somme des abondances des jeunes stades, CI à CIII, x 100 / somme de l'abondance de tous les stades) au centre de la mer du Labrador, moyennes par périodes de deux semaines au cours des missions annuelles de 1995 à 2006.

Sea in late May and early June, the PDI is about 10%, increasing to a peak value of about 40% in early July. Temperatures and food conditions are known to influence reproduction and growth in the laboratory. Sea-surface temperatures increased over the 1995–2006 period and blooms started earlier. Six late-May surveys allow an investigation of the effects of these changing environmental conditions on the *C. finmarchicus* development cycle in the central Labrador Sea (Fig. 11). The

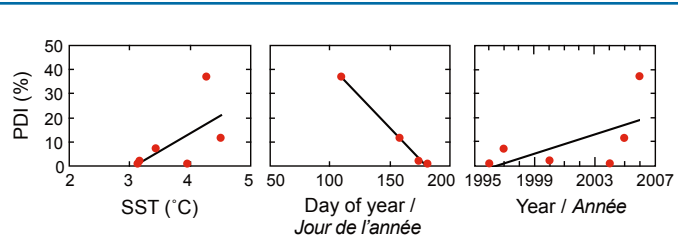


Fig. 11 *C. finmarchicus* population development index (PDI) in the central Labrador Sea in late May in relation to March–May late winter – spring sea-surface temperature (left), bloom start date (defined as the time when sea-surface chlorophyll concentration reached a sustained value of 1 mg m⁻³) (centre), and the trend in PDI from 1996 to 2006 (right).

Indice de développement de la population (PDI) de C. finmarchicus au centre de la mer du Labrador à la fin mai en relation avec les températures à la surface de la mer de mars à la fin mai (fin de l'hiver – printemps) (panneau de gauche), la date du début de la floraison (définie comme le moment où la concentration de chlorophylle en surface atteint et demeure au-dessus de 1 mg m⁻³) (panneau du centre) et la tendance du PDI de 1996 à 2006 (panneau de droite).

late-May PDI varied from 0 to 40%. It increased with increasing late winter-spring sea-surface temperatures and with earlier spring blooms, leading to an increasing trend over time. These results confirm that the effects of food concentration and temperature on reproduction and development rate that can be demonstrated in laboratory studies also occur in situ.

The 2008 survey took place less than one week earlier than the June 1 median midpoint date for spring or early summer surveys since 1990. In most years at this time, an intense spring bloom has usually already occurred or is occurring in the eastern Labrador Sea near the Greenland Shelf, leading to the presence of large numbers of early stage *C. finmarchicus*. In 2008, however, temperatures were lower than in recent years and the intensity and extent (areal coverage) of the bloom in this region were reduced. Preliminary visual inspection of the zooplankton samples suggests that the usually abundant young *C. finmarchicus* were not there in 2008, although more detailed sample and data analysis is required to investigate this apparent recruitment failure. Sampling in 2009 will show any impact the 2008 recruitment may have had on the population dynamics of the species and the overall productivity of zooplankton in the Labrador Sea.

Highlights 2008

The year 2008 was quite variable. The central Labrador Sea experienced the coldest winter (January–March) surface air temperatures in 16 years, but the rest of the year saw above-normal surface air temperatures and the summer (July–September) was the third warmest in the 61-year NCEP Reanalysis period. On an annual average, 2008 surface air temperatures were the coolest since 2000 but still remained above normal. Ice coverage was notably more extensive than normal in the northwestern Labrador Sea. Sea-surface temperatures cooled in fall 2007–winter 2008 but remained slightly above the 1971–2000 normal for all of 2008. Near-record-high sea-surface temperatures in spring and summer 2008 led to the 5th warmest annual average SST in the 1960–2008 period, slightly warmer than 2007. The 2003–2008 period included the warmest five years in the 49-year period from 1960–2008; 2007 was the 7th warmest, slightly cooler than 1997.

Large areas of the central Labrador Sea have seen increases in surface air temperature of 2°C and increases in sea-surface temperature by 1°C over the past two decades.

Cooling and densification of the upper levels of the west-central Labrador Sea during the cold 2008 winter produced winter mixed layers extending to 1350–1600 m depths, as revealed by March 2008 Argo profile measurements. Increased amounts of mode waters in the 27.72–27.74 kg m⁻³ potential density anomaly range were found in the west-central Labrador Sea during the May 2008 AR7W survey. Overall, the upper layers of the Labrador Sea remain warm and saline.

Total inorganic carbon concentrations in the upper levels of the central Labrador Sea continued to increase, with a corresponding decrease in pH. Dissolved oxygen concentrations in the same water mass show a persistent downward trend due in approximately equal parts to reduced solubility caused by warming and by other factors that could include increased

biological consumption. Nutrient conditions followed recent trends indicative of a decreasing influence of Arctic waters and an increasing influence of subtropical waters, with downward trends in silicate and phosphate. Trends in nitrate concentrations remain weak and variable. Observed trends in relative nutrient concentrations such as increasing nitrate:silicate ratios and reductions in phosphate relative to nitrate are especially striking.

High variability in all biological properties makes multi-year trends uncertain. Upper layer chlorophyll and bacteria concentrations have remained relatively stable for the last decade, but both show slight positive trends in the central Labrador Basin and on the West Greenland Shelf/Slope and negative trends on the Labrador Shelf/Slope. However, satellite ocean colour data suggest that the main phytoplankton growth event in spring–summer 2008 was earlier and more intense than usual on the Labrador Shelf and in the Labrador Basin but less intense on the West Greenland Shelf. Preliminary indications are that 2008 may not have been a good year for *C. finmarchicus* recruitment on the West Greenland Shelf.

Acknowledgements

The NCEP Reanalysis data were provided by the NOAA-CIRES Climate Diagnostics Center, Boulder, Colorado, USA, from their Web site at <http://www.cdc.noaa.gov/>. The HadISST 1.1 Global Sea Surface Temperature data were provided by the Hadley Centre for Climate Prediction and Research (<http://www.metoffice.com>). Climatological hydrographic and nutrient data from the World Ocean Atlas 2005 (Garcia et al. 2006) were provided by the U.S. National Oceanographic Data Center (<http://www.nodc.noaa.gov/>). Many staff and associates of Ocean Sciences Division and Ecosystem Research Division at BIO have contributed to the Labrador Sea program. The efforts of the officers and crew of CCGS *Hudson* in support of this work in recent years are gratefully acknowledged.

References

- Fetterer, F., Knowles, K., Meier, W., and Savoie, M. 2002, updated 2008. Sea ice index. Boulder, CO: National Snow and Ice Data Center. Digital media. Available from http://nsidc.org/data/seice_index [accessed 4 March 2009].
- Garcia, H.E., Locarnini, R.A., Boyer, T.P., and Antonov, J.I. 2006. World Ocean Atlas 2005, Volume 4: Nutrients (phosphate, nitrate, silicate). Edited by S. Levitus. NOAA Atlas NESDIS 64, U.S. Government Printing Office, Washington, D.C., 396 pp.
- Kalnay, E., Kanamitsu, M., Kistler, R., and 19 others. 1996. The NCEP/NCAR 40-year reanalysis project. Bull. Amer. Meteor. Soc. 77: 437–470.
- Rayner, N.A., Parker, D.E., Horton, E.B., Folland, C.K., Alexander, L.V., Rowell, D.P., Kent, E.C., and Kaplan, A. 2003. Global analyses of sea surface temperature, sea ice, and night marine air temperature since the late nineteenth century. J. Geophys. Res. 108(D14): 4407, doi10.1029/2002JD002670.
- Våge, K., Pickart, R.S., Thierry, V., Reverdin, G., Lee, C.M., Petrie, B.P., Agnew, T.A., Wong, A., and Ribergaard, M.H. 2009. Surprising return of deep convection to the subpolar North Atlantic Ocean in winter 2007–2008. Nature Geosci. 2: 67–72.
- Yashayaev, I., and Loder, J.W. 2009. Enhanced production of Labrador Sea Water in 2008. Geophys. Res. Lett. 36: L01606, doi:10.1029/2008GL036162.

Using the Long-Term Bottom-Trawl Survey of the Southern Gulf of St. Lawrence to Understand Marine Fish Populations and Community Change

Hugues Benoît¹, Doug Swain¹, and Ghislain Chouinard²

¹Gulf Fisheries Centre, Box 5030, Moncton, NB, E1C 9B6

²Canadian Science Advisory Secretariat, 200 Kent St., Ottawa, ON, K1A 0E6

hugues.benoit@dfo-mpo.gc.ca

Sommaire

Un relevé au chalut de fond est entrepris chaque année au mois de septembre dans le sud du golfe du Saint-Laurent (sGSL). Ce relevé fournit d'importantes données sur l'abondance, la distribution et la répartition des tailles d'un grand nombre d'espèces de poissons et d'invertébrés. De plus, un échantillonnage océanographique synoptique à grande échelle est entrepris lors du relevé. Dans cet article nous résumons quelques aspects de ce relevé. En particulier nous évaluons à quel point il peut fournir un portrait fiable (exacte et précis) des dynamiques de la communauté de poissons du sGSL. Nous discutons ensuite de l'utilité des données récoltées lors du relevé. Pour ce faire, nous présentons en premier lieu une bibliographie qui a récemment été complétée et qui résume les diverses publications produites depuis 1971 à partir des données du relevé du sGSL. Cette bibliographie met en valeur la grande diversité des travaux scientifiques réalisés. Ensuite nous nous concentrons plus précisément sur deux avenues de recherche, à titre d'exemple : les espèces menacées d'extinction et les études sur la dynamique des communautés de poissons marins.

Introduction

Bottom-trawl research vessel (RV) surveys constitute some of the longest, ongoing, annual biomonitoring on Canada's Atlantic coast. They provide data on the abundance, distribution, and demographic composition (size and sometimes age) of fish populations. Increasingly, data for macro-invertebrates are also being collected. These surveys are an important platform for broad-scale synoptic oceanographic data collection.

The history of RV surveys in Atlantic Canada was reviewed in a previous issue of the AZMP bulletin (Chadwick et al. 2007). In the present article, we focus on the RV survey of the southern Gulf of St. Lawrence (sGSL; Fig. 1). First, we begin by providing some brief background information about this survey and the data that are recorded from bottom-trawl sam-

ples. Of course, the survey is also an important platform for physical, biological, and chemical oceanographic sampling, though this is not specifically described here since these data have been the focus of a number of previous AZMP bulletin articles. Second, we briefly review some of the properties that constitute a good survey of marine macrofauna, assessing the degree to which the sGSL RV survey possesses these properties. Finally, having argued that the sGSL RV survey can provide a reliable portrait of abundance and distribution for a large number of marine fish species, we discuss some of the many uses of the data collected during the survey. We begin that final section by introducing readers to a recently compiled bibliography, composed entirely of works based on data collected during the sGSL RV survey. This bibliography highlights the breadth of scientific investigation that such a survey allows. We then follow up with a brief review of two general areas of research on sGSL marine fishes that have relied substantially on the RV survey data: species at risk of extinction and long-term community dynamics.

The sGSL September RV Survey

The RV survey of the sGSL has been conducted annually each September since 1971 and is one of the few bottom-trawl surveys in Atlantic Canada with such a long uninterrupted history. With the addition of three small inshore strata in 1984, the survey covers nearly the entire sGSL with the exception of very shallow waters (<15 m). This degree of coverage is unique in Atlantic Canada and is attributable largely to the relative ease with which the ecosystem can be sampled using a bottom trawl due to the characteristics of the bottom topography in the area (i.e., few rough areas known to damage a trawl).

Since the survey's inception, data on the abundance and distribution of over 70 marine fish species have been collected. In addition, representative length frequencies and individual body weights of all fish species have always been recorded, providing a unique perspective on the size structure of the community. In the early days of the survey, recording of invertebrate species was mostly limited to those that were the object of commercial fisheries. Since the mid-1980s, all

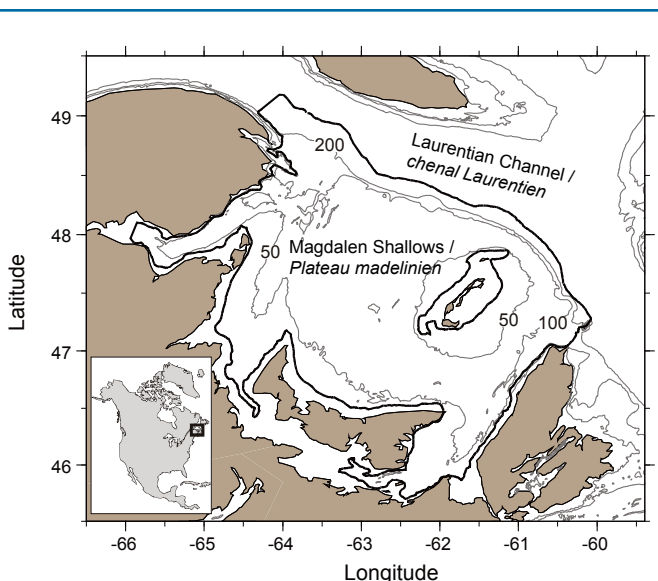


Fig. 1 Southern Gulf of St. Lawrence multi-species bottom-trawl survey area (dark line) with 50, 100, and 200 m isobaths (grey lines).

Aire couverte par le relevé multi-espèces au chalut de fond dans le sud du golfe du Saint-Laurent (ligne grasse) et courbes bathymétriques de 50, 100 et 200 m (lignes fines).

macroinvertebrates captured in the trawl have been sorted into main taxonomic groups and capture weights recorded. More recently, size frequencies for species of certain groups such as decapods (crabs) have also been obtained. That such a breadth of data has been collected for so long—far beyond that required to assess the population dynamics of exploited groundfish—speaks to an early vision to make it as much of an ecosystem survey as logistically possible.

Of course, the length of the survey time series and the number and variety of variables measured are only pertinent to understanding the structure and dynamics of marine communities if the survey provides a reliable (unbiased and precise) picture of the populations being sampled. With a perspective nearing four decades, an assessment of the reliability of the sGSL RV survey is both warranted and generally feasible. In the section that follows, we review the survey with respect to some key aspects we believe relate to a survey's reliability.

Can We Have Confidence in What the Survey is Telling Us?

The purpose of a scientific bottom-trawl survey is to obtain representative samples of fish and invertebrate populations. These observations can then be used to track changes in relative abundance and demographic composition for example. Surveys therefore need to sample in a consistent manner over time, using standardized procedures and gear. Indeed, protocols have remained largely unchanged since 1971 in the sGSL RV survey. Of course, planned changes in vessel and even gear have occurred, though they have always been accompanied by side-by-side comparative fishing experiments aimed at obtaining species-specific calibration coefficients to maintain standardized time series (Nielsen 1994, Benoît and Swain 2003a, Benoît 2006). (Due to the unplanned use of an uncalibrated vessel, data from the 2003 survey are generally excluded from stock assessments in order to maintain the integrity of time series). Likewise, calibration coefficients have been calculated to correct survey data for a change in 1985, from daylight-only to 24-hr sampling (Benoît and Swain 2003b).

In order to obtain unbiased estimates of relative abundance, surveys also need to select fishing locations at random with respect to fish distributions—sampling in areas where fish are rare as well as areas where they are abundant; however, in a truly multi-species survey, there are usually few areas where all species are rare. With very few untrawlable areas and an adherence to a stratified random design, the sGSL RV survey meets this requirement.

A survey should ideally cover all or much of the distributional area for the populations being sampled. Failing to do so, distributional shifts into or out of the survey area would likely be interpreted as changes in relative abundance. Being bordered by land on three sides and the deep waters of the Laurentian Channel on the fourth (Fig. 1), the sGSL has a high potential for containing distinct populations of species that also occur in neighbouring ecosystems. Indeed, for many of the commercially exploited fish species in the ecosystem, the stock management area is the southern Gulf (e.g., Atlantic cod [*Gadus morhua*], herring [*Clupea harengus*], and white

hake [*Urophycis tenuis*]). Likewise, winter skate (*Leucoraja ocellata*) in the sGSL appear to be distinct from winter skate elsewhere (McEachran and Martin 1977). While some of these species exhibit an annual migration outside the Gulf in winter, the timing of the survey is such that it covers the distribution of the species in September.

Abundance and distributional indices must be calculated based on samples obtained from a constant survey area to avoid interpreting sampling artifacts as changes in abundance (e.g., not sampling an area of high abundance is likely to lead to a smaller index value than would otherwise have been obtained). Though three inshore strata were added to the sGSL RV survey in 1984, indices that include these strata are not extended prior to that year. In a small number of cases, survey strata were not sampled due to logistical constraints; however, protocols are in place for adjusting or estimating abundance values for those strata to ensure the integrity of species time series (e.g., Benoît and Swain 2003b).

Obtaining a precise (low variability) representation of the community can be just as important as obtaining an unbiased one. Our ability to detect trends in abundance, for example, will be hindered if the error in the indices dominates the signal that those indices are meant to provide. Precision is affected both by the sampling method and by characteristics of the populations being sampled.

Precision generally increases with sample size. At about one tow per 400 km², the sampling density in the sGSL (total area \approx 73,000 km²) is among the highest in Atlantic Canada RV surveys. As in other DFO regions, considerable effort is expended to ensure the standardization of the fishing gear, and the consistency in its performance during tows is closely monitored. Standardization ensures that there are no changes over time in the gear's ability to fish, which would lead to a biased representation of the populations, whereas performance consistency reduces needless variability in the samples obtained.

Precision on indices of abundance is affected by the number of individuals captured by the survey; it is typically low for species that are rare in the ecosystem or poorly captured by the gear. This problem is largely unavoidable for some species.

The manner in which species are distributed in the survey area, whether aggregated or dispersed, can also have a pronounced effect on precision. We demonstrate this using a simple simulation of two fish populations. Both populations, each consisting initially of 1000 fish distributed in an area of 1000 sampling units, differ only in their pattern of spatial distribution across units, one being aggregated and the other dispersed (Fig. 2A). Abundance in both populations was increased by 100 fish per year for 35 years. Each year, ten units were sampled to calculate a mean abundance and the error about that mean. The resulting abundance index for the dispersed population tracks the true population abundance very well (Fig. 2B), with high levels of annual precision (i.e., small standard error about the mean). In contrast, the abundance index for the geographically aggregated population displays lower levels of annual precision (i.e., larger standard

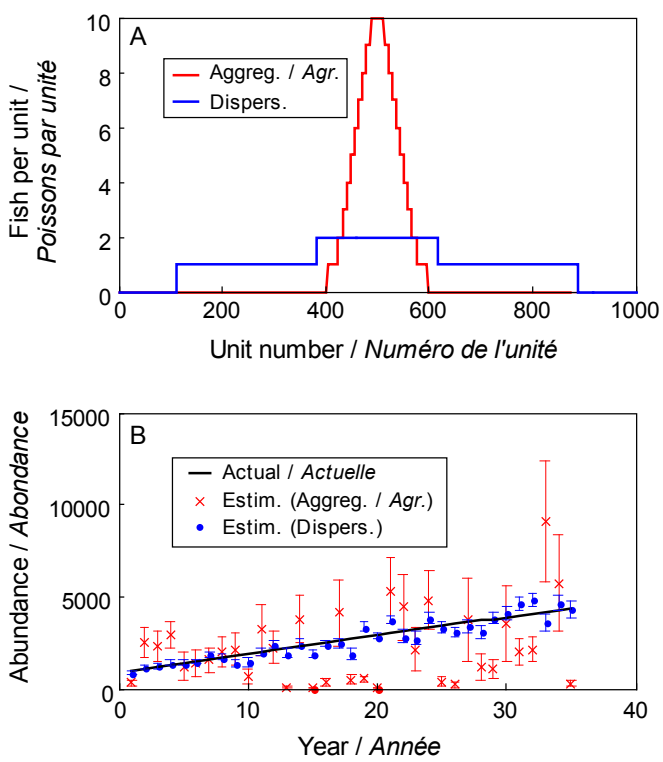


Fig. 2 A simple simulation to illustrate the effect of fish distribution on survey results. A) The distribution of fish across sampling units for an aggregated (red) population and a dispersed (blue) population. B) Annual abundance indices obtained from sampling each of the two populations (mean \pm 2 SE). The black line is the true trend in abundance.

Illustration d'une simulation simple de l'effet de la distribution des poissons sur les résultats du relevé. A) Distribution des poissons sur l'ensemble des unités d'échantillonnage pour une population agrégée (en rouge) et une population dispersée (en bleu). B) Indices annuels d'abondance (moyenne et deux erreurs-types) obtenus par l'échantillonnage de chacune des populations. La ligne noire représente la véritable tendance de l'abondance.

error) and considerably greater interannual variability in mean values. This index for the aggregated population tracks the true abundance trend only coarsely, with much of the year-to-year variation due to sampling error (often termed “year effects”) rather than true population change. To provide the most reliable index of population abundance, a survey should therefore ideally be conducted when fish are most dispersed within the survey area. This is true for most sGSL fish species in summer and early autumn, which subsequently concentrate in the warmer deeper waters of the Laurentian Channel during winter (Clay 1991, Darbyson and Benoît 2003). Winter skate are a notable exception to this pattern, concentrating in warm shallow waters during summer and dispersing throughout the sGSL in winter. Because most species are dispersed and migrations to overwintering grounds appear only to begin in later autumn, September is therefore an ideal time to conduct a multi-species survey in the sGSL.

While we can present arguments for the quality of the indices provided by the sGSL RV survey, the true test of any survey is its ability to track the abundance of fish cohorts (fish from the same species, born during the same year). In a closed population (i.e., no immigration or emigration), the number of fish in a cohort can only decrease over time, as a result of mortality. Furthermore, if a cohort is estimated to be strong at one

age in one year relative to other cohorts at the same age but in other years, it should be estimated to be relatively strong at the next age in the next year providing mortality rates do not fluctuate too much. However, due to sampling error such as that shown in our simulated sampling of an aggregated population (Fig. 2B), cohort size may be perceived to increase from one year to the next. To measure the survey's ability to track cohorts of fish, the correlation between survey catch rates at one age (a) in one year (t) and the catch rates at the next age ($a+1$) in the next year ($t+1$) can be used. A correlation coefficient (r) of 1 indicates a perfect correspondence; a coefficient of 0 indicates no correspondence. For a survey with reliable abundance indices, a high positive correlation would therefore be expected. The analysis can be expanded by considering the correlation with catch rates for a number, n , of ages (i.e., $a+n$) and years ($t+n$) later. As the difference, n , between the ages compared increases, one would expect the correlation to decrease if different cohorts experienced different mortality schedules (e.g., one cohort experienced high mortality rates and another did not).

To define cohorts, an annual estimate of abundance at age is required. We therefore concentrated on the three groundfish species from the sGSL RV survey for which this is the case: cod, American plaice (*Hippoglossoides platessoides*), and white hake. For each species, we calculated r for cohorts at a number of ages and for a number of subsequent years. We contrast this with similar analyses undertaken for cod stocks from 11 other surveys conducted in ecosystems other than the sGSL: seven other research vessel surveys from the Northwest Atlantic, two sentinel (industry) surveys, and two sets of indices from the Northeast Atlantic. (Data for cod were chosen for these contrasts because they are the most readily available and because, for all of these surveys, cod is one of the focal species and we therefore expect the surveys to be most adapted to providing a reliable index of abundance for cod).

For all three sGSL species, we find that the RV survey tracks cohorts of most or all ages exceptionally well from one year to the next (generally, $r \geq 0.7$; Fig. 3). Only one or two of the other surveys perform as well for cod; in fact, for four of these surveys, many of the correlations are not statistically different from $r=0$. For American plaice in particular, but also cod, correlations remain high even as we increase the number of years between which a cohort is observed. This is again uncommon for cod in other surveys. Of course the strength of the correlations in these figures will depend partly on the amount of contrast in the data. Contrast will be greater for stocks that have undergone greater fluctuations in abundance over the history of the survey. An index of the amount of contrast in the data is the ratio of highest and lowest survey catch rates. To minimize the possible influence of “year effects,” we calculated this index, C, as the ratio of age-specific mean abundance in the five most and five least abundant years, averaged across ages. Based on this measure (indicated as blue text in the panels of Fig. 3), contrast is lowest for surveys 2, 3, and 5, partly explaining their poor performance in tracking year-classes (cohorts). Conversely, contrast was highest for survey 4, contributing to its strong performance. However, surveys 1, 7, 8, 10, and 11 have contrasts that are comparable to or considerably greater than

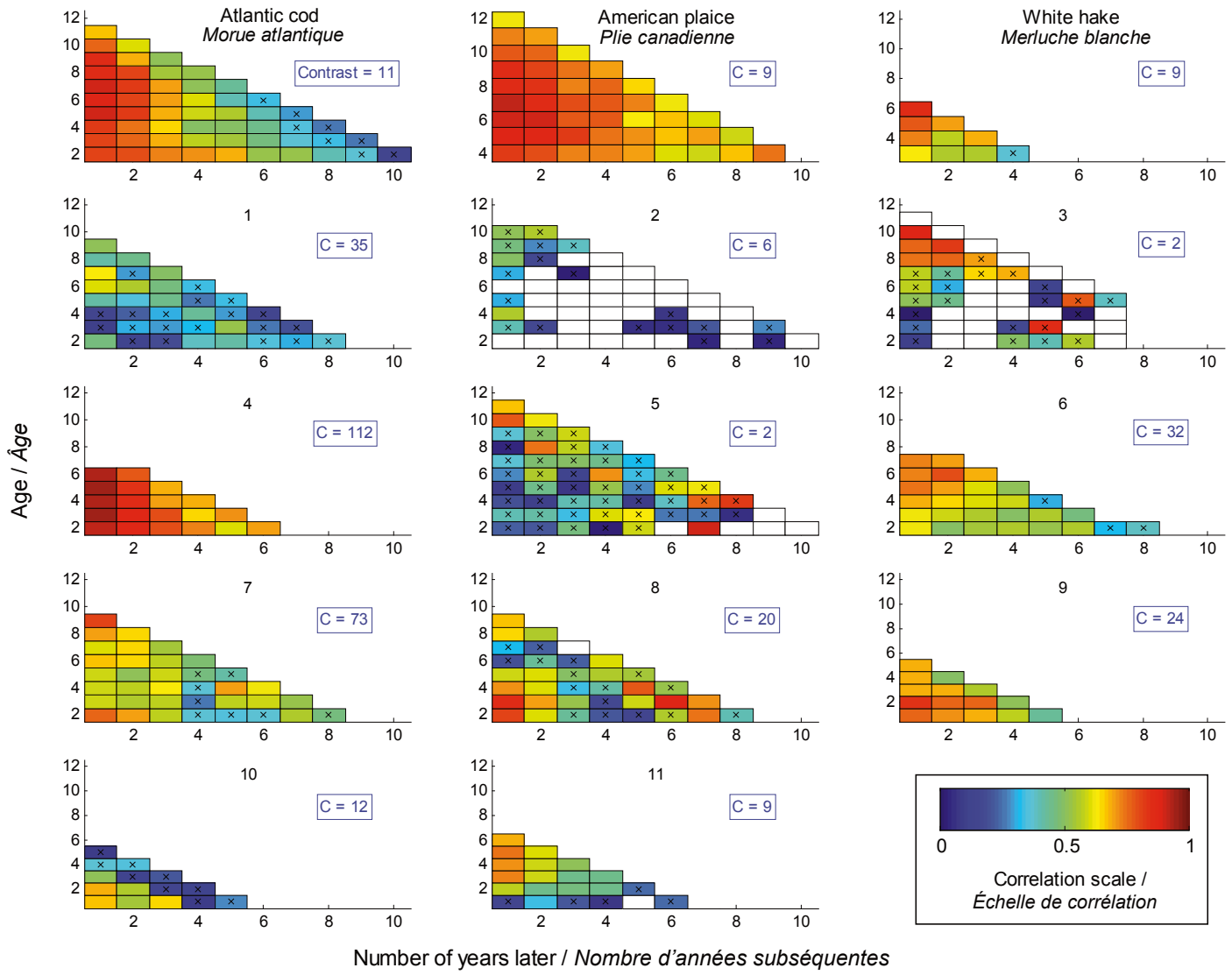


Fig. 3 Comparison of the ability to track year-classes of cod, American plaice, and white hake in the September RV survey (top row) and cod in 11 other surveys (seven other RV surveys from the Northwest Atlantic, two sentinel surveys, and two sets of cod indices from the Northeast Atlantic). Each panel presents data for a single stock and survey. Individual panels summarize the correlations between survey catch rates at age i (vertical axis) versus catch rates of the same cohorts for j number of years later, i.e., at age $i+j$ in year $t+j$ (horizontal axis). As indicated on the scale at the bottom right, orange and red cells represent strong correlations (i.e., a good ability to track the abundance of cohorts), whereas “x” denotes a non-significant positive correlation and white cells indicate a negative correlation. The blue text in each panel represents the contrast in abundance experienced by the stock; high values indicate a stock having undergone a relatively pronounced change in abundance.

Comparaison de la capacité de suivre les classes d'âge de morue, de plie canadienne et de merluche blanche avec le relevé scientifique de septembre (graphes du haut) et pour 11 autres relevés pour la morue (sept autres relevés scientifiques dans l'Atlantique Nord-Ouest, deux relevés sentinelles et deux indices de relevés dans l'Atlantique Nord-est). Chaque graphe présente les données pour un stock et un relevé. Chaque graphe présente un sommaire des corrélations entre le taux de capture du relevé à l'âge i (axe vertical) contre les taux de capture des mêmes cohortes pour un nombre j d'années subséquentes, c.-à-d. à l'âge $i+j$ pour l'année $t+j$ (axe horizontal). Comme l'indique l'échelle au bas à droite, les cellules oranges et rouges représentent de fortes corrélations (une bonne capacité de suivre l'abondance de cohortes), alors qu'un «x» signifie une corrélation positive non significative et une cellule vide une corrélation négative. Pour chaque graphe, le texte en bleu présente le contraste en abondance subi par le stock, une valeur élevée indique que le stock a subi un changement relativement important d'abondance.

those for the three sGSL species, yet all perform substantially more poorly. From this comparison, we conclude that the strong performance of the September RV survey relative to other surveys is not an artifact of unusually high contrast in its catch rates.

The sGSL RV survey provides reliable indices for three commercially important demersal fish species, but is this also the case for the other species sampled? In the absence of data on age composition required for an analysis of cohorts,

we examine a simple measure of the apparent signal-to-noise ratio produced by the survey for each species. Given that all fish species in the sGSL have a multi-year life cycle, reproducing only in years subsequent to their birth year, we would expect abundance to fluctuate somewhat smoothly from year to year. We used the lag-1 autocorrelation (covariance of an abundance index time series and the same series shifted ahead by one year, divided by the series' variance) as a measure of the signal-to-noise ratio (S) of each species' series. For an abundance index that varies smoothly over

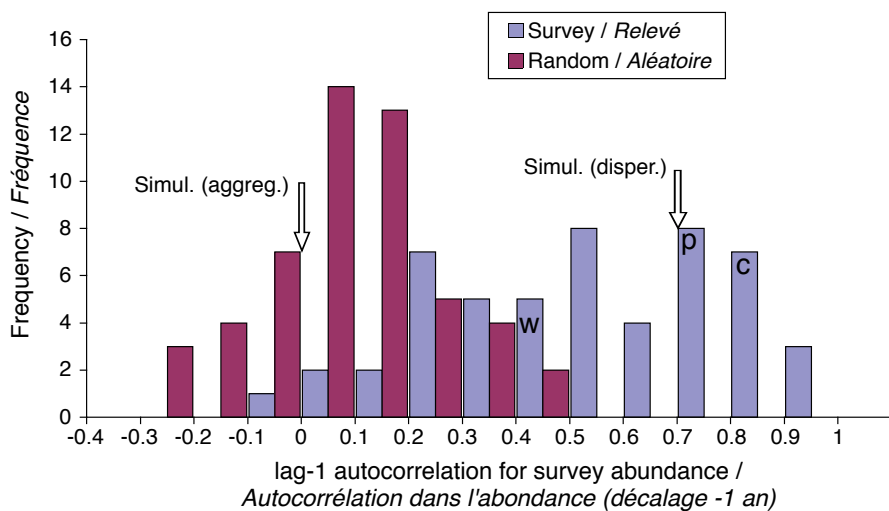


Fig. 4 Histograms of abundance index lag-1 autocorrelation for 52 species in the September RV survey (blue) and 52 randomly generated indices (maroon). The autocorrelation values for the RV indices for white hake (w), American plaice (p), and Atlantic cod (c) as well as for the two simulated populations in Figure 2 are indicated.

Histogrammes des valeurs d'autocorrélation (décalage de 1 an) de l'indice d'abondance pour les 52 espèces du relevé scientifique de septembre (en bleu) et pour 52 indices générés au hasard (en marron). Les valeurs d'autocorrélation des indices du relevé scientifique pour la merluce blanche (w), la plie canadienne (p) et la morue (c) sont identifiées, de même que celles pour les deux populations simulées à la Figure 2.

time, S will tend towards a value of 1. Values of $S \approx 0$ are expected for a constant abundance index or one that fluctuates randomly over time (Fig. 4, maroon bars), as might occur if actual abundance is relatively constant or if the survey is unable to track population change.

For most sGSL species, RV survey values of S are greater than for simulated randomly fluctuating abundance indices (Fig. 4). In fact, S values (mean $S = 0.44$) are generally comparable to those calculated for the three species involved in the cohort-tracking analysis, which might suggest a comparable ability to track abundance. Furthermore, the majority of observed S values more closely resemble the value calculated for the abundance index of our simulated dispersed fish population in Figure 2, compared to the value for the aggregated population. Given that we would expect that in a community of over 50 species of fish, the true abundance of some will have fluctuated without much trend (i.e., $S \approx 0$ even for an ideal survey), we conclude that overall the survey appears to track the local abundance of a large number species.

A good way to appreciate the breadth of scientific study that has relied on data collected during the September survey of the sGSL is to compile a bibliography of pertinent works that have been published since the survey's inception. This has recently been completed for papers, book chapters, and reports published through 2008 (Gautreau et al. 2008). The authors of that bibliography uncovered close to 500 published reports and 74 peer-reviewed journal articles covering a variety of topics (Table 1), a few of which we now briefly review.

The Varied Uses of the September RV Survey Data

By far, the majority of the published reports concern the status assessment of commercially exploited species. The data from the RV survey have been the cornerstone, or at least

complementary, to other sources of information such as commercial catch statistics and acoustic surveys. The themes of the publications range from basic science to applied management, and include topics such as stock status and assessment, survey methodology, science in support of stock assessment and fisheries management, science in support of species at risk of extinction, fish biology and ecology, marine communities, interactions between species and the environment, research and reports on biological, chemical, and physical oceanography, and others.

Stock assessments

For most sGSL species, RV survey values of S are greater than for simulated randomly fluctuating abundance indices (Fig. 4). In fact, S values (mean $S = 0.44$) are generally comparable to those calculated for the three species involved in the cohort-tracking analysis, which might suggest a comparable ability to track abundance. Furthermore, the majority of observed S values more closely resemble the value calculated for the abundance index of our simulated dispersed fish population in Figure 2, compared to the value for the aggregated population. Given that we would expect that in a community of over 50 species of fish, the true abundance of some will have fluctuated without much trend (i.e., $S \approx 0$ even for an ideal survey), we conclude that overall the survey appears to track the local abundance of a large number species.

Table 1 Summary of publications listed in the bibliography by Gautreau et al. (2008). Presented in the table are the numbers, by theme, of technical reports and published working papers and the number of peer-reviewed journal articles and book chapters published since the inception of the sGSL RV survey. Themes are not necessarily mutually exclusive and individual references were attributed to the theme that appeared most appropriate.

Sommaire des publications répertoriées dans la bibliographie par Gautreau et al. (2008). Le tableau présente pour différents thèmes, le nombre de rapports techniques et documents de recherche publiés et le nombre d'articles de journal avec revue par les pairs et de chapitres de livres publiés depuis l'instauration du relevé de recherche dans le sud du golfe du Saint-Laurent. Les différents thèmes ne sont pas mutuellement exclusifs et les références individuelles ont été attribuées au thème jugé le plus approprié.

Thème / Thème	Reports / Rapports	Articles & Chapters / Articles et chapitres
1. Stock status and assessment reports / Rapports d'état et d'évaluation des stocks	283	—
2. Surveys: methodology, standardization and general results / Relevés : méthodologie, étalonnage et résultats	29	4
3. Science in support of stock assessment and fisheries management / Recherche scientifique en appui à l'évaluation et la gestion des pêches	32	15
4. Science in support of species at risk of extinction / Recherche scientifique en appui au risque d'extinction des espèces	8	2
5. Fish biology and ecology / Biologie et écologie des poissons	41	31
6. Marine communities, species interactions, and environmental impacts on abundance and distribution / Communautés marines, interactions entre les espèces et l'influence de l'environnement sur l'abondance et la distribution	27	21
7. Research and reports on biological, chemical, and physical oceanography / Recherche scientifique et rapports sur l'oceanographie biologique, chimique et physique	50	2
8. Others / Autres	13	—

an important component, of the assessment of ten exploited sGSL groundfish species (e.g., Atlantic cod, American plaice). Data collected are also routinely used in the assessments of pelagic species such as herring, capelin (*Mallotus villosus*), and shortfin squid (*Illex illecebrosus*). Given the nature of the forums in which stock status and assessment reports were produced in the past, it is very likely that the 283 reports identified are only a subset of the actual number written. The literature search also uncovered an additional 32 reports and 15 peer-reviewed journal articles that document scientific studies undertaken in support of stock assessments. These include studies on stock identification, assessment methodology, and the estimation of vital rates such as recruitment and mortality.

Species at risk

Commercially important species are but a subset of the species whose population trends are tracked by RV surveys. Some of these species may experience important declines in population status that would otherwise go unnoticed, potentially to the point of extirpation or extinction. It is the mandate of the Committee on the Status of Endangered Wildlife in Canada (COSEWIC) to undertake detailed analyses of species status and recommend a conservation designation.

With hundreds of Canadian marine fish species, a crucial first step in the detailed analysis of species status is prioritization. Those species demonstrating the most pronounced decreases in abundance or facing the largest threats to their viability should be the first to receive a closer examination. In 2003–2004, DFO undertook such an assessment of the general status of Atlantic marine fishes. By considering RV survey trends in population abundance, size structure, and geographic distribution, nine priority species were identified in the sGSL (Benoit et al. 2003). Of these species, two were deemed high priority (winter skate and white hake) and four intermediate priority (Atlantic cod, American plaice, redfish [*Sebastes spp.*], and thorny skate [*Amblyraja radiata*]). All these species have in turn been, or are currently being, evaluated in more detail by COSEWIC.

Once species status has been established, factors affecting population productivity need to be identified in order to plan management activities aimed at halting declines and promoting recovery. Data on population abundance and demographic structure (age or at least body size) are required to examine the key components of productivity: recruitment, somatic growth, and mortality. Fishery-independent standardized surveys are the only source of information that can provide unbiased temporal trends for all three components of productivity. We very briefly illustrate how this has been approached using two contrasting cases: winter skate, a species for which until recently there were neither any firm data on age composition nor an existing population model, and cod, a formally assessed commercially important species.

Data from the September survey show that the distinct population of winter skate that inhabits the sGSL has experienced declines of 96% in adult abundance and >80% in total abundance since 1971 (Benoit et al. 2003, Swain et al. 2006). This led COSEWIC to designate it as *endangered*, i.e.,

facing imminent extinction. Using annual survey numbers at length and prior information on size at maturity and growth rate, Swain et al. (2009) developed a stage-structured model for the population. Model fits to the survey data suggest that population viability has been most affected by the mortality of adults, which increased considerably from the mid 1970s to present (Fig. 5A). Fishery-induced mortality stemming mainly from incidental capture in commercial fisheries directed at other species appears to contribute only a little to adult mortality and actually declined as total mortality increased (Benoit 2006, Swain et al. 2009). The cause of non-fishery-related mortality in adults is not well known, though as we discuss later, there is evidence for an effect of predation by top predators (Benoit and Swain 2008, Swain et al. 2009). Impairment of recruitment did not appear to be a contributing factor to the population status because as adult abundance declined during the 1980s and 1990s, the rate of young skate recruitment was high (Fig. 5A, left panel; Swain et al. 2006, 2009).

The collapse and lack of recovery of cod in the sGSL and NW Atlantic in general is well known. Lack of recovery appears to result mainly from elevated natural mortality, but also from fishing mortality and generally lackluster recruitment (Shelton et al. 2006). Estimating natural mortality (M ; mortality from all sources except accounted fishery removals) is only possible with a standardized fishery-independent survey

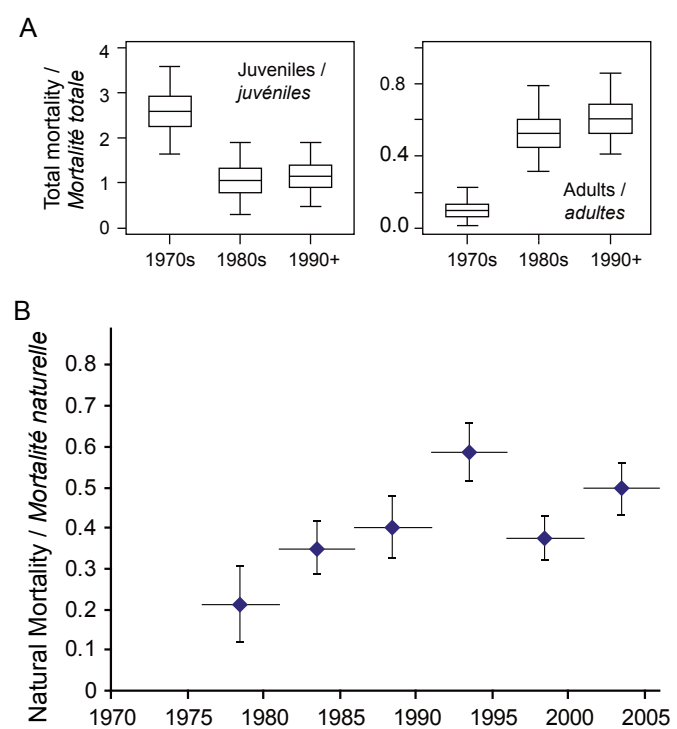


Fig. 5 A) Boxplots of estimates (by decade) of total mortality in juvenile and adult winter skate (see Swain et al. 2009). B) Estimates of natural mortality (M ; mean \pm 2 SE) in adult cod in 5-year blocks, indicated by the horizontal lines (see Chouinard et al. 2006).

A) *Tracé en rectangle et moustaches des estimations de la mortalité totale par décennie chez les juvéniles et les adultes de raie tachetée (voir Swain et al. 2009). B) Estimations de la mortalité naturelle (M ; moyenne et deux erreurs-types) par périodes de cinq ans chez les adultes de morue (voir Chouinard et al. 2006). Les périodes de cinq ans sont représentées par les lignes horizontales.*

(e.g., Sinclair 2001) or a good tagging program, which is difficult to achieve when fisheries and therefore potential tag returns are small. For the period of the 1993–1997 moratorium, almost all of the mortality in sGSL cod estimated from the survey was M. With this independent estimate and another one for an earlier period, it has been possible to estimate in the assessment model fit to the survey data the trends in adult cod M for other blocks of years (Chouinard et al. 2005, 2008). The result is an increasing trend since the early 1980s (Fig. 5B). In fact, recent estimates of M suggest that the sGSL cod population is no longer viable; if its current low productivity persists, the population is projected to become extinct in 40 years or fewer, depending on fishery quotas (Swain and Chouinard 2008). As with winter skate, the causes of elevated M are uncertain, though the strongest evidence again points to an effect of top predators (Chouinard et al. 2005; D. Swain, unpublished analyses).

Community dynamics

The direct effect of fishing (removal of individuals) has been one of the most prominent causes of population change for exploited sGSL fish species. However, interactions with other species and changes in the environment also need to be considered, particularly to understand why many of these species have failed to recover despite strong reductions in fishing (e.g., cod, white hake, American plaice). Furthermore, there is growing interest worldwide to better understand the effects of fishing on non-target species, which can be direct or indirect (i.e., via competitive or predatory release). RV surveys are an integral component of such studies, providing standardized time series of environmental conditions and of the abundance and distribution of a large number of species. Furthermore, these surveys are an important platform for collecting stomach content data to characterize trophic interactions between species. We again turn to examples from the sGSL.

Recently, Benoît and Swain (2008) undertook an analysis of the dynamics of the sGSL marine fish community. Using RV survey time series of abundance spanning 1971–2005 for 52 species, they examined the relative influence on community dynamics of fishing, predation by a top predator (grey seals, *Halichoerus grypus*), changes in bottom-water temperature, and bottom-up effects of changes in prey abundance. A traits-based approach was used, relating similarity among species in their abundance trends to similarities in their ecological traits. Four traits were selected based on a priori beliefs of how each should reflect susceptibility to changes in one of the different external factors potentially affecting the community. Benoît and Swain (2008) interpreted comparable abundance responses among species sharing a trait as an effect of the external factor implied by the trait. The statistical method used allowed for testing both the marginal (i.e., trait by trait) and conditional (i.e., after controlling for the effect of other traits) significance of individual traits.

Benoît and Swain (2008) described dramatic shifts in the species composition of the marine fish community of the sGSL from 1971 to 2005. Some species declined sharply in abundance in the late 1970s and early 1980s, remaining at

low levels since then (e.g., American plaice, winter skate); others increased in abundance in the late 1970s or late 1980s but suffered rapid population collapses in the 1990s (e.g., Atlantic cod, redfish); yet others increased dramatically in abundance in the mid or late 1990s (e.g., capelin). Across species, these trends were independently related to three traits. With few exceptions, species that increased in abundance over the study period were characterized by one or more of the following: little susceptibility to fishing, little susceptibility to seal predation, or a large portion of their biogeographic range occurring in arctic/subarctic waters (i.e., indicative of possible cold-water tolerance) (Fig. 6). Conversely, those species showing an overall decline in abundance were almost all susceptible to both fishing and seal predation, and tended to have a more southerly biogeographic distribution. Species susceptible to fishing included those that were targeted by commercial fisheries as well as incidentally captured ones. Average species' diet, the fourth trait examined and one that was chosen to reflect possible bottom-up effects of changes in prey abundance, was not related to abundance trends.

The apparent trait-dependency of population dynamics reflects trends in the relevant external drivers (Benoît and Swain 2008). Mean bottom-water temperatures cooled throughout the 1980s, resulting in a period of record-low temperatures in the early to mid 1990s (Gilbert and Pettigrew 1997, Drinkwater and Gilbert 2004). The abundance of cooler-water species, particularly arctic species, peaked during or shortly after the period of coldest water temperatures, declining somewhat subsequently as temperatures warmed to more average recent levels (Benoît and Swain 2008). Fishing effort directed towards demersal fish was elevated during much of 1970s and 1980s, increasing rapidly during the late 1980s and early 1990s, followed by a dramatic reduction that has persisted. Much of the decline in abundance of the species most impacted by fisheries occurred during the period of increasingly high fishing effort. The lack of recovery or continued decline of many of these species despite large subsequent reductions in fishing effort appears to correspond with dramatic increases in the abundance of grey seals in the ecosystem (Hammill 2005). Bioenergetic modelling confirms that seals may have indeed largely replaced fisheries in terms of fish removals (Savenkoff et al. 2008). Trends in both cod and winter skate M are consistent with an effect of seals (Chouinard et al. 2005, Swain et al. 2009).

Analyses of RV survey data also suggest that there have been important indirect (i.e., trophic-mediated) effects of fishing on the sGSL fish community. All small-bodied (mean length <15 cm) species in the ecosystem have increased dramatically in abundance (Fig. 6). Though this may be partly environmentally related, as many of these are cooler-water species, trends are strongly consistent with a release from predation by formerly abundant large demersal fish predators (Benoît and Swain 2008, Savenkoff et al. 2008). Similar RV survey trends are observed for large shrimp that are prey for species such as cod and redfish (H. Benoît, unpublished results), again consistent with a trophic-mediated change in abundance (Worm and Myers 2003). Indirect harvesting impacts have also been proposed to explain reduced recruitment success of sGSL cod

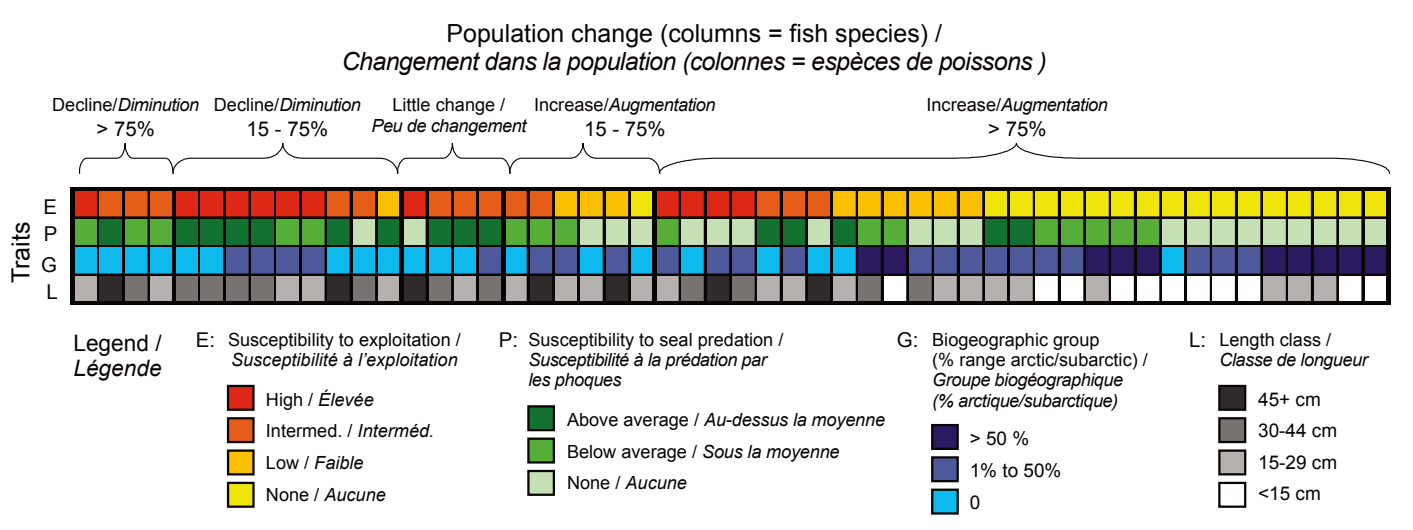


Fig. 6 Values for four traits (rows) in 52 sGSL marine fish species (columns). Species have been grouped according to their major trend in abundance over the period 1971–2005: trait values for species showing pronounced declines are plotted on the left side of the figure; species having undergone large increases are on the right. Trait values are colour coded according to the legend at the bottom of the figure. Susceptibility to fishing and to seal predation are indices calculated based on removals (by fishing and seals respectively) as a function of population biomass and productivity (see Benoît and Swain 2008 for details). Biogeographic group was determined by visually estimating the proportion of individual species' west Atlantic geographic range occurring in arctic/subarctic waters (north of 51°N) based on general accounts and atlases (see Benoît and Swain 2008). Length class is based on the average size of individuals from the survey. Average diet was the other trait considered in the analyses of Benoît and Swain (2008) but is not shown here.

Les valeurs de quatre caractéristiques (lignes) chez 52 espèces de poissons marins du sud du golfe (colonnes). Les espèces ont été regroupées selon leur tendance principale en abondance au cours de la période de 1971 à 2005 : les valeurs des caractéristiques pour les espèces montrant un déclin prononcé sont rapportées sur le côté gauche et les espèces ayant subit une augmentation importante sur la droite. Le code de couleur des caractéristiques est présenté dans la légende au bas de la figure. Les susceptibilités à la pêche et à la prédation par les phoques ont été calculées sur la base des retraits (respectivement par la pêche et les phoques) en fonction de la biomasse et la productivité de la population (voir Benoît et Swain 2008 pour les détails de calcul). Les groupes biogéographiques ont été déterminés par un examen visuel de la proportion de l'aire géographique de l'espèce dans l'ouest Atlantique apparaissant dans des eaux arctiques ou subarctiques (nord du 51°N) selon des rapports généraux et des atlas (voir Benoît et Swain 2008 pour les détails). La classe de longueur est basée sur la taille moyenne des individus observés lors du relevé. La diète moyenne de chaque espèce était une autre caractéristique incluse dans l'analyse de Benoît et Swain (2008), mais n'est pas présentée ici.

since stocks of herring and mackerel, predators of cod eggs and larvae, rebuilt in the 1980s following reductions in harvesting (Fig. 7; Swain and Sinclair 2000).

In summary, the results of the studies described here and the others listed in the bibliography suggest that changes in ocean climate combined with direct and indirect effects of harvesting have dramatically altered the composition of the sGSL marine fish community. Understanding the breadth of the impacts and evaluating multiple hypotheses for the drivers of these changes would not have been possible without a long-running multi-species fishery independent survey.

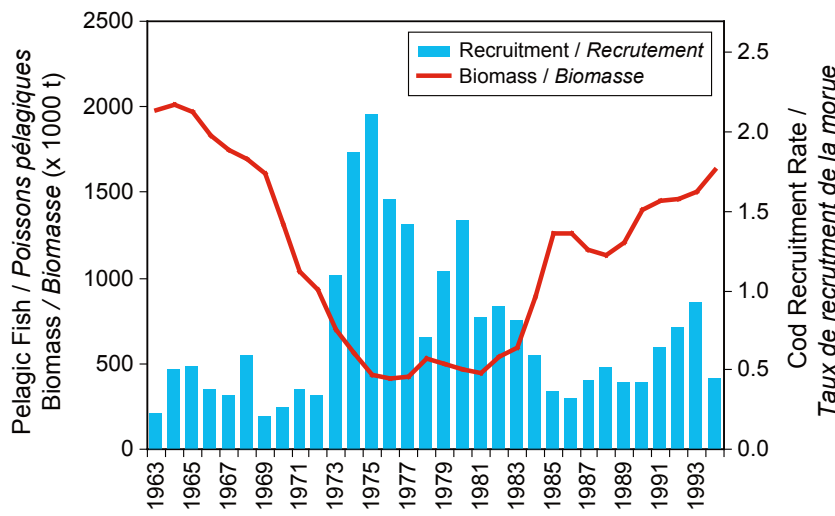


Fig. 7 Total biomass of herring and mackerel and the recruitment rate of cod in the sGSL (see Swain and Sinclair 2000). Recruitment rate is defined as numbers of age 3 cod divided by the spawning stock biomass that produced them, plotted at the year of birth.

Biomasses totales de hareng et de maquereau et le taux de recrutement de la morue dans le sud du golfe du Saint-Laurent (voir Swain and Sinclair 2000). Le taux de recrutement est défini comme étant le nombre de morue de trois ans divisé par la biomasse du stock reproducteur à l'origine de la cohorte, représenté à l'année de naissance.

Concluding Remarks

Though bottom-trawl surveys are both labour and resource intensive, they provide an annual portrait of ecosystem status unmatched in spatial scale, scientific scope, and longevity compared to what is available for the terrestrial realm. Despite being initially founded in the practical world of regular assessments of exploited resources, RV surveys provide us with a strong potential to understand generally the structure and functioning of marine ecosystems as demonstrated by the publications listed in the bibliography presented in Gautreau et al. (2008). Gaining such an understanding will only increase in importance with growing demands on marine resources from an expanding human popu-

lation and increasing pressures from global climate change. A key component to understanding the potential impacts of anthropogenic perturbations and global change is the precision, accuracy, and especially the duration of the surveys. There is therefore a need to regularly assess the reliability of the surveys. We have shown here a few ways in which this can be done; there are others (e.g., comparing results from multiple surveys of the same ecosystem such as Trenkel et al. 2004). Having established that a survey satisfactorily provides an accurate and precise picture of the ecosystem, the key is then to maintain the integrity of that survey. Any methodological change needs to be approached cautiously as it has the potential to change how we perceive the ecosystem and consequently the conclusions we draw about the causes of change over time.

Acknowledgements

We thank Tobie Surette for providing Figure 3. We also acknowledge the hard work of the many people whose dedication has contributed to the success of the southern Gulf of St. Lawrence annual multi-species bottom-trawl survey.

References

- Benoit, H.P.** 2006. Standardizing the southern Gulf of St. Lawrence bottom trawl survey time series: Results of the 2004-2005 comparative fishing experiments and other recommendations for the analysis of the survey data. DFO CSAS Res. Doc. 2006/008.
- Benoit, H.P., and Swain, D.P.** 2003a. Standardizing the southern Gulf of St. Lawrence bottom-trawl survey time series: adjusting for changes in research vessel, gear and survey protocol. Can. Tech. Rep. Fish. Aquat. Sci. 2505, 95 pp.
- Benoit, H.P., and Swain, D.P.** 2003b. Accounting for length and depth-dependent diel variation in catchability of fish and invertebrates in an annual bottom-trawl survey. ICES J. Mar. Sci. 60: 1297-1316.
- Benoit, H.P., and Swain, D.P.** 2008. Impacts of environmental change and direct and indirect harvesting effects on the dynamics of a marine fish community. Can. J. Fish. Aquat. Sci. 65: 2088-2104.
- Benoit, H.P., Abgrall, M.-J., and Swain, D.P.** 2003. An assessment of the general status of marine and diadromous fish species in the southern Gulf of St. Lawrence based on annual bottom trawl surveys (1971-2002). Can. Tech. Rep. Fish. Aquat. Sci. 2472, 183 pp.
- Chadwick, E.M.P., Brodie, W., Colbourne, E., Clark, D., Gascon, D., and Hurlbut, T.** 2007. History of annual multi-species trawl surveys on the Atlantic coast of Canada. AZMP Bulletin PMZA 6: 25-42.
- Chouinard, G.A., Swain, D.P., Hammill, M.O., and Poirier, G.A.** 2005. Covariation between grey seal (*Halichoerus grypus*) abundance and natural mortality of cod (*Gadus morhua*) in the southern Gulf of St. Lawrence. Can. J. Fish. Aquat. Sci. 62: 1991-2000.
- Chouinard, G.A., Currie, L., Poirier, G., Hurlbut, T., Daigle, D., and Savoie, L.** 2006. Assessment of the southern Gulf of St. Lawrence cod stock, February 2006. DFO CSAS Res. Doc. 2006/006.
- Chouinard, G.A., Savoie, L., Swain, D.P., Hurlbut, T., and Daigle, D.** 2008. Assessment of the southern Gulf of St. Lawrence cod stock, February 2008. DFO CSAS Res. Doc. 2008/045.
- Clay, D.** 1991. Seasonal distribution of demersal fish (Osteichthyes) and skates (Chondrichthyes) in the southeastern Gulf of St. Lawrence. In *The Gulf of St. Lawrence: Small Ocean or Big Estuary?* Edited by J.-C. Therriault. Can. Spec. Publ. Fish. Aquat. Sci. 113: 241-259.
- Darbyson, E., and Benoit, H.P.** 2003. An atlas of the seasonal distribution of marine fish and invertebrates in the southern Gulf of St. Lawrence. Can. Data Rep. Fish. Aquat. Sci. 1113, 294 pp.
- Drinkwater, K.F., and Gilbert, D.** 2004. Hydrographic variability in the waters of the Gulf of St. Lawrence, the Scotian Shelf and the eastern Gulf of Maine. J. Northw. Atl. Fish. Sci. 34: 85-101.
- Gautreau, S., Chouinard, G.A., and Benoit, H.P.** 2008. Bibliography of publications based at least in part on data collected during the annual research vessel survey of the southern Gulf of St. Lawrence (last updated December 2008). [Online: 05 February 2009] <http://www.meds-sdmm.dfo-mpo.gc.ca/isdm-gdsi/azmp-pmza/publications-eng.html> (see "Section 5. Other documents"). [accessed 05 February 2009].
- Gilbert, D., and Pettigrew, B.** 1997. Interannual variability (1948-1994) of the CIL core temperature in the Gulf of St. Lawrence. Can. J. Fish. Aquat. Sci. 54: 57-67.
- Hammill, M.O.** 2005. Abundance of Northwest Atlantic grey seals in the Gulf of St. Lawrence and along the Nova Scotia eastern shore. DFO CSAS Res. Doc. 2005/036.
- McEachran, J.D., and Martin, C.O.** 1977. Possible occurrence of character displacement in the sympatric skates *Raja erinacea* and *R. ocellata* (Pisces: Rajidae). Env. Biol. Fishes 2: 121-130.
- Nielsen, G.A.** 1994. Comparison of the fishing efficiency of research vessels used in the sGSL groundfish surveys from 1971 to 1992. Can. Tech. Rep. Fish. Aquat. Sci. 1952.
- Savenkoff, C., Morissette, L., Castonguay, M., Swain, D.P., Hammill, M.O., Chabot, D., and Hanson, J.M.** 2008. Interactions between marine mammals and fisheries: Implications for cod recovery. In *Ecosystem Ecology Research Trends*. Edited by J. Chen and C. Guo. Nova Science Publishers Inc, New York, pp. 107-151.
- Shelton, P.A., Sinclair, A.F., Chouinard, G.A., and Mohn, R.** 2006. Fishing under low productivity conditions is further delaying recovery of Northwest Atlantic cod (*Gadus morhua*). Can. J. Fish. Aquat. Sci. 63: 235-238.
- Sinclair, A. F.** 2001. Natural mortality of cod (*Gadus morhua*) in the Southern Gulf of St Lawrence. ICES J. Mar. Sci. 58: 1-10.
- Swain, D.P., and Chouinard, G.A.** 2008. Predicted extirpation of the dominant demersal fish in a large marine ecosystem: Atlantic cod (*Gadus morhua*) in the southern Gulf of St. Lawrence. Can. J. Fish. Aquat. Sci. 65: 2315-2319.
- Swain, D.P., and Sinclair, A.** 2000. Pelagic fishes and the cod recruitment dilemma in the Northwest Atlantic. Can. J. Fish. Aquat. Sci. 57: 1321-1325.
- Swain, D.P., Simon, J.E., Harris, L.E., and Benoit, H.P.** 2006. Recovery potential assessment of 4T and 4VW winter skate (*Leucoraja ocellata*): biology, current status and threats. DFO CSAS Res. Doc. 2006/003.
- Swain, D.P., Jonsen, I.D., Simon, J.E., and Myers, R.A.** 2009. A stage-structured state-space model to assess threats and management scenarios for data-deficient species-at-risk: Estimating mortality trends in winter skate (*Leucoraja ocellata*, Family Rajidae). Ecol. Applic. (in press).
- Trenkel, V.M., Pinnegar, J.K., Rochet, M.-J., and Rackham, B.D.** 2004. Different surveys provide similar pictures of trends in a marine fish community but not of individual fish populations. ICES J. Mar. Sci. 61: 351-362.
- Worm, B., and Myers, R.A.** 2003. Meta-analysis of cod-shrimp interactions reveals top-down control in oceanic food webs. Ecol. Appl. 84: 162-173.

Macrozooplankton Diel Migration in the Estuary and Gulf of St. Lawrence: Links to Abiotic Factors

Michel Harvey and Peter Galbraith

Institut Maurice-Lamontagne, C. P. 1000, Mont-Joli, QC, G5H 3Z4
michel.harvey@dfo-mpo.gc.ca

Sommaire

Le patron de distribution verticale de différentes espèces de macrozooplancton (euphausiacé, chaetognathe, cnidaire, mysidacé, amphipode) a été examiné à différentes périodes du jour et de la nuit et mis en relation avec certains paramètres physiques. Différentes strates de profondeur ont été échantillonnées à l'aide d'un BIONESS au cours de sept missions successives conduites au printemps et à l'automne de 1998 à 2001, dans deux régions différentes : l'estuaire maritime et le nord-ouest du golfe du Saint-Laurent. Nos résultats indiquent que les différentes espèces de macrozooplancton occupent l'ensemble de la colonne d'eau à différentes périodes du jour et de la nuit dans les deux régions. De plus, trois différents patrons de migration verticale ont été observés au sein de cette communauté zooplanctonique : (1) une ascension verticale pendant la nuit pour l'ensemble de la population; (2) une ségrégation en deux groupes où une partie de la population effectue une ascension verticale pendant la nuit et l'autre partie demeure dans la zone profonde; (3) aucune migration verticale. Nous avons également observé que l'amplitude de la migration verticale de la plupart des espèces de macrozooplancton varie en fonction de certains paramètres physiques, en particulier la profondeur du cœur de la couche intermédiaire froide (CIF). Finalement, les patrons de migration verticale spécifiques observés, couplés avec les différents patrons de circulation des masses d'eau et la topographie du fond peuvent, selon la période du jour ou la saison, amener les animaux dans différents régimes de circulation et contribuer à leur rétention ou dispersion dans différentes régions du système estuaire et golfe du Saint-Laurent.

Introduction

Macrozooplankton are a large contributor to the plankton biomass in the St. Lawrence marine system (SLMS), making up 10 to 20% of the total zooplankton biomass (~123 g ww m⁻²) (Harvey and Devine 2007). They play a significant role in the pelagic ecosystem as food for marine mammals, marine birds, and fish, and as predators on copepods and/or fish larvae. In spite of its importance, our understanding of the macrozooplankton dynamics in the SLMS is severely limited. Apart from a few rudimentary taxonomic studies mainly consisting of brief accounts of occurrence and/or simple listing of specific groups of organisms, and of some studies carried out on different biological aspects of the euphausiids (krill) in northern part of the Gulf of St. Lawrence and at the head of the Laurentian Channel, only one study has systematically examined the composition, abundance, and distribution of macrozooplankton communities in the lower St. Lawrence Estuary (LSLE) and the NW Gulf of St. Lawrence (NW GSL) in relation to the physical environment (Descroix et al. 2005). In that study, the dominant macrozooplankton species found in the LSLE and NW GSL was the mysid *Boreomysis arctica*, but no significant regional or interannual variations in its abundance were observed. Other than this common dominant species, the LSLE and NW GSL were populated by different groups. Two euphausiid species, *Meganyctiphanes norvegica* and *Thysanoessa raschii*, dominated in the LSLE, with abundances 6 and 15 times higher in the LSLE than in the NW GSL. The NW GSL was dominated by chaetognaths, hyperiid amphipods, and siphonophores, all of which were twice as abundant in the NW GSL as in the LSLE. Such inter-regional variations were attributed to different circulation patterns and different trophic systems (Descroix et al. 2005).

A biotic factor that may contribute to the observed population differences between the two regions is the vertical migration of animals; this, coupled with estuarine circulation patterns and bottom topography, may lead to retention

(aggregation) or dispersion of macrozooplankton. Typically, zooplankton vertical migration occurs between the surface layer at night and deeper waters during the day and is well documented in freshwater and oceanic systems. Exogenous and/or endogenous factors such as light intensity, season, lunar phase and tidal cycle, oxygen, hydrology, temperature, salinity, sex, age, and biological rhythms may affect migratory behavior (Cushing 1951, Ohman 1990, Cottier et al. 2006). In addition, vertical migration may confer benefits, including predator avoidance, maximization of food intake and utilization, maximization of fecundity, and various strategies associated with horizontal dispersion and transport (Longhurst 1976). Even though the diel vertical migration (DVM) of many zooplankton species has been well documented in different habitats throughout the world, and the physical and the biological factors that initiate this movement as well as the advantages and the disadvantages for organisms which undertake it have been studied, no data were available on the vertical distribution and the DVM of the various macrozooplankton species of the SLMS prior to this study (with the exceptions of euphausiids at the head of the Laurentian Channel [Simard et al. 1986] and in the northern part of the GSL [Sameoto 1976]).

In order to undertake ecosystemic research of the macrozooplankton in the St. Lawrence estuary, several steps should be taken before considering the system as whole. The first step is to identify and quantify, at least in relative terms, the most abundant species in the LSLE as well as in the Gulf of St. Lawrence region (the Anticosti Gyre region). We have made significant progress concerning this in recent work (Descroix et al. 2005). The second step is to understand what parts of the water column are inhabited by these species, and to what degree these vertical distributions are related and perhaps controlled by environmental factors. This paper summarizes the results published in Harvey et al. (2008), and the reader is referred to that work for more details.

Materials and Methods

Sampling program

The data used in this study originated from seven cruises carried out in spring and fall 1998, 2000, and 2001 and fall 1999 at stations K5 or O4 in the LSLE and at station U2 in the Anticosti Gyre (AG) in the NW GSL (Fig. 1). A temperature and salinity profile was obtained at each station. Zooplankton samples were then collected using a 1 m² BIONESS sampler. Between 7 and 9 depth strata were sampled depending on the survey (details in Harvey et al. 2008).

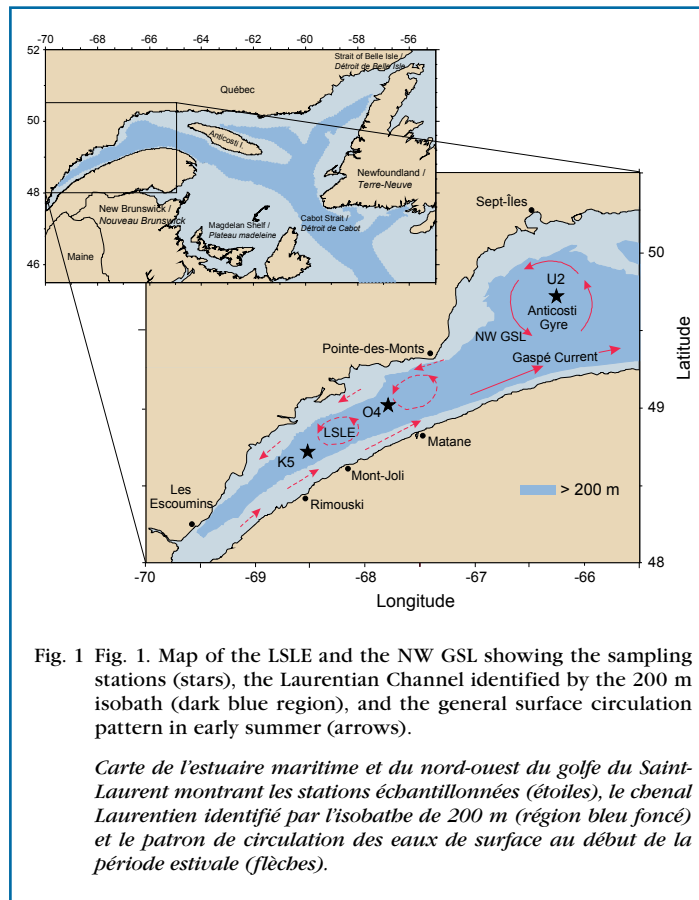


Fig. 1 Fig. 1. Map of the LSLE and the NW GSL showing the sampling stations (stars), the Laurentian Channel identified by the 200 m isobath (dark blue region), and the general surface circulation pattern in early summer (arrows).

Carte de l'estuaire maritime et du nord-ouest du golfe du Saint-Laurent montrant les stations échantillonnées (étoiles), le chenal Laurentien identifié par l'isobathe de 200 m (région bleu foncé) et le patron de circulation des eaux de surface au début de la période estivale (flèches).

To study the vertical distribution and the diel migration of the predominant macrozooplankton species, the BIONESS sampler was towed every three hours during a 24-h period at all stations during three and four surveys in the LSLE and the AG respectively. This paper uses data from 66 BIONESS tows, with a total of 360 nets sampled.

Data analysis

Eight physical variables were used to describe the CIL thermal properties: the upper (Z_i) and the lower (Z_f) depth limit of the CIL at 1 and 3°C, the CIL core temperature (T_{min}), the depth of the CIL core temperature (ZT_{min}), and the CIL thickness at 3°C ($\Delta Z_{3^{\circ}C}$) and 1°C ($\Delta Z_{1^{\circ}C}$).

The daytime and nighttime vertical distributions of the most abundant macrozooplankton species were studied by examining the relative abundance of each species sampled in each depth stratum at all sampling dates in the LSLE and in the AG. Thereafter, the diel migration was studied by calculating the

depth of the centre of distribution (ZCD) for each of the most abundant macrozooplankton species sampled during the 24-h period at station U2 in fall 1999 and at stations O4 or K5, and U2 in spring and fall 2000 and in spring 2001. The ZCD was calculated as

$$ZCD = \sum_{i=1}^n p_i Z_i \quad (1)$$

with p_i = the proportion of the total density (ind. m⁻³) of each species in the i th depth interval, Z_i = the mid-point of i th stratum, and n the number strata sampled depending on the survey.

The diel migration of the most important macrozooplankton species was evaluated by calculating the migration amplitude (ΔZCD) as

$$\Delta ZCD = ZCD_{daytime} - ZCD_{nighttime} \quad (2)$$

where the ZCD during the daytime and the nighttime correspond to the maximum and the minimum centres of distribution observed during the 24-h period for each species. The relationship between the ΔZCD and the CIL thermal properties were examined using Pearson correlations ($p \leq 0.05$).

Results

Daytime and nighttime vertical distribution

Figure 2 shows the daytime and nighttime vertical distributions of the nine most abundant macrozooplankton species in spring and fall (all years combined) in the LSLE and the NW GSL (AG) expressed as the percentage of individuals in each depth interval relative to the total number of individuals sampled at that time (ind. 100 m⁻³). All the macrozooplankton species except the hydrozoan *Aglantha digitale* showed a unimodal vertical distribution pattern during daytime and nighttime for most stations. Most *M. norvegica* and *T. raschii* were distributed between 25 and 250 m and 25 and 150 m, respectively, during the daytime in the LSLE, and between 75 and 250 m and 50 and 200 m in the AG, and ascended to the surface waters (0–50 m) during nighttime. There was no clear difference in the daytime versus nighttime depth distribution pattern of *Themisto abyssorum* except for the fall in the AG, when most were distributed deeper than 150 m during daytime and shallower than 150 m during nighttime. *Themisto libellula* were also distributed deeper in daytime in the AG. Likewise, the chaetognath *Sagitta elegans* was distributed around 25–150 and 25–200 during the daytime in the LSLE and the AG, respectively, and ascended to the surface layer (0–50 m) during the nighttime. On the contrary, the chaetognath *Eukrohnia hamata*, the siphonophore *Dimophyes arctica*, and the mysid *B. arctica* occupied the deep layer during the day and the night and displayed little vertical displacement. *D. arctica* and *E. hamata* were found below 50 m during both daytime and nighttime. There was no distinct day and night difference in the depth distribution of *B. arctica* in the LSLE, but individuals in the AG were mostly found between 200 m and the bottom during the daytime and between 50 m and the bottom (moving up slightly) during the nighttime. Finally, contrary to the other macrozooplankton species, the hydrozoan *A. digitale* showed a unimodal

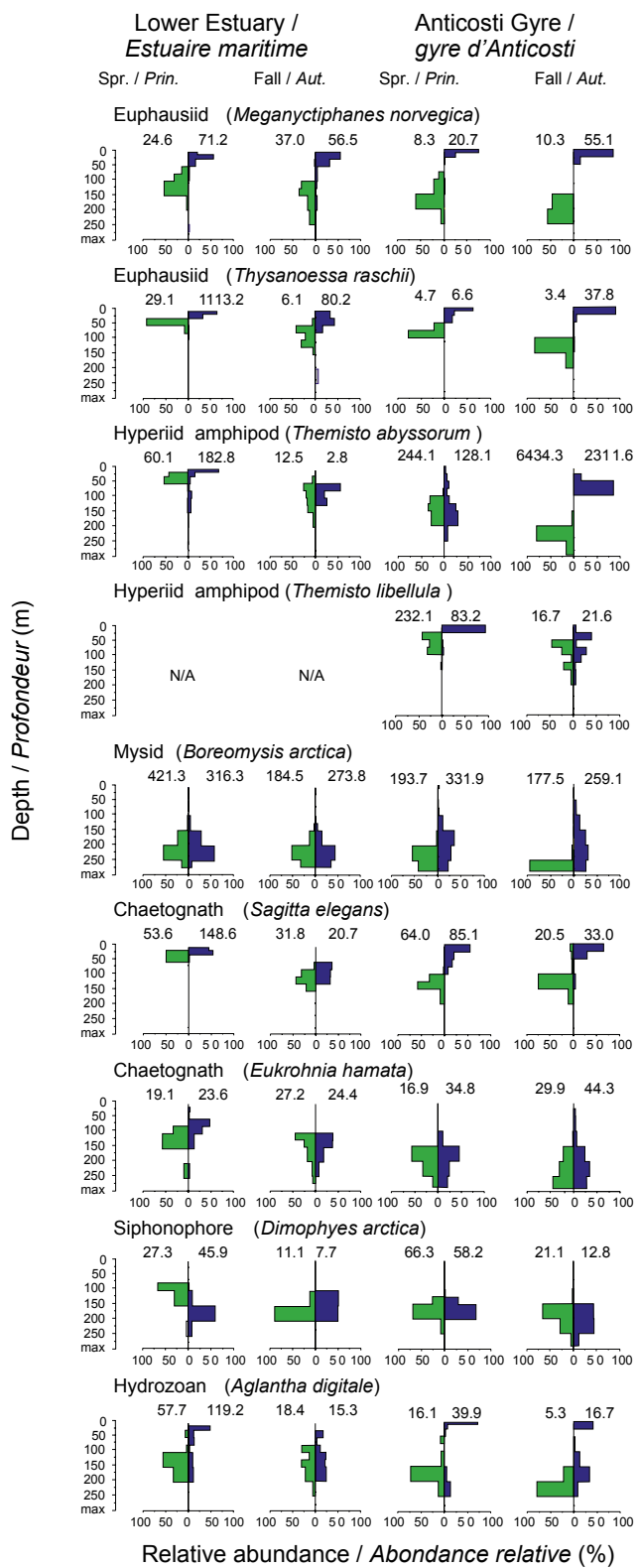


Fig. 2 Day (green) and night (blue) vertical distribution of dominant macrozooplankton species in the Lower St. Lawrence Estuary and the Anticosti Gyre in spring and fall (N/A = insufficient data). Numbers represent the total number of individuals per 100 m^3 of each species sampled during each tow.

Patron de distribution verticale des principales espèces de macrozooplancton de l'estuaire maritime et de la gyre d'Anticosti pendant le jour (vert) et la nuit (bleu) au printemps et à l'automne (N/A = données insuffisantes). Les chiffres représentent le nombre total d'individus par 100 m^3 de chaque espèce échantillonnée à chaque station.

distribution during the day and a bimodal distribution at night. Almost all *A. digitale* individuals were found between 75 and 250 m during the daytime. A fraction of the population varying between 10 and 80% ascended to the surface waters (0–25 m) during the nighttime. The remainder of the population was found between 50 and 250 m in the LSLE and between 100 and 250 m in the AG.

Diel vertical migrations of the most abundant macrozooplankton species

Figure 3 shows the daytime and nighttime depths of the centres of distribution (ZCD) of the nine most abundant macrozooplankton species during a selected 24-h period for both regions. *M. norvegica* and *T. raschii* both exhibited patterns of DVM. For example, in the AG, *M. norvegica* and *T. raschii* were mostly distributed below the CIL (4–5°C), around 150–210 m and 120–180 m respectively, during the daytime, and ascended to 0–50 m, to the surface layer and the upper CIL waters, during the nighttime. In the LSLE, *M. norvegica* and *T. raschii* were distributed in the surface layer or at the upper limit of the CIL during the night (2–6°C) and within the CIL (0–3°C) during the day. Both euphausiid species were distributed at shallower depths in the LSLE than in the AG during the daytime. Moreover, the migration amplitude was generally higher in *M. norvegica* than in *T. raschii*, and the migration amplitude was generally higher for both species in the AG (155 and 107 m, respectively) than in the LSLE (72 and 62 m, respectively). Both *T. abyssorum* and *T. libellula* showed typical patterns of DVM in the AG, with the centre of distribution deeper during the day than at night: the ZCD of *T. libellula* and *T. abyssorum* varied between 30 and 125 m and between 70 and 225 m, respectively, during a 24-h period. With respect to the CIL, *T. libellula* was found in waters around -1 to 0°C during the nighttime and around 2 to 3°C during the daytime, corresponding to the core and the lower part of the CIL respectively. In contrast, *T. abyssorum* was found within the CIL during the nighttime (1–2°C) and in the deep layer during the daytime (4–5°C). There was no clear difference in the depth distribution pattern of *T. abyssorum* during either daytime or nighttime in the LSLE.

The chaetognath *S. elegans* also displayed patterns of DVM during all surveys. Most individuals were distributed in the middle part of the CIL (average ZCD \pm SD = 56 ± 19 m) during the day in the LSLE (fall 2000) and in the lower CIL and the upper part of the deep layer (117 ± 16 m) in the AG (fall 1999). During the night, most individuals ascended to the surface layer and the upper limit of the CIL waters, between 0 and 50 m (22 ± 9 m). In contrast, there was no apparent vertical diel migration of *Eukrohnia hamata*: most were distributed in the lower CIL in the LSLE, between 100 and 175 m ($2\text{--}4^\circ\text{C}$; 131 ± 27 m), and in the upper part of the deep layer (198 ± 21 m) in the AG.

Likewise, both the siphonophore *D. arctica* and the mysid *B. arctica* were always found in the deep layer, between 125 and 275 m. *D. arctica* occupied the upper deep layer just below the CIL, at the same depth as the chaetognath *E. hamata*, and were always found slightly higher than *B. arctica*,

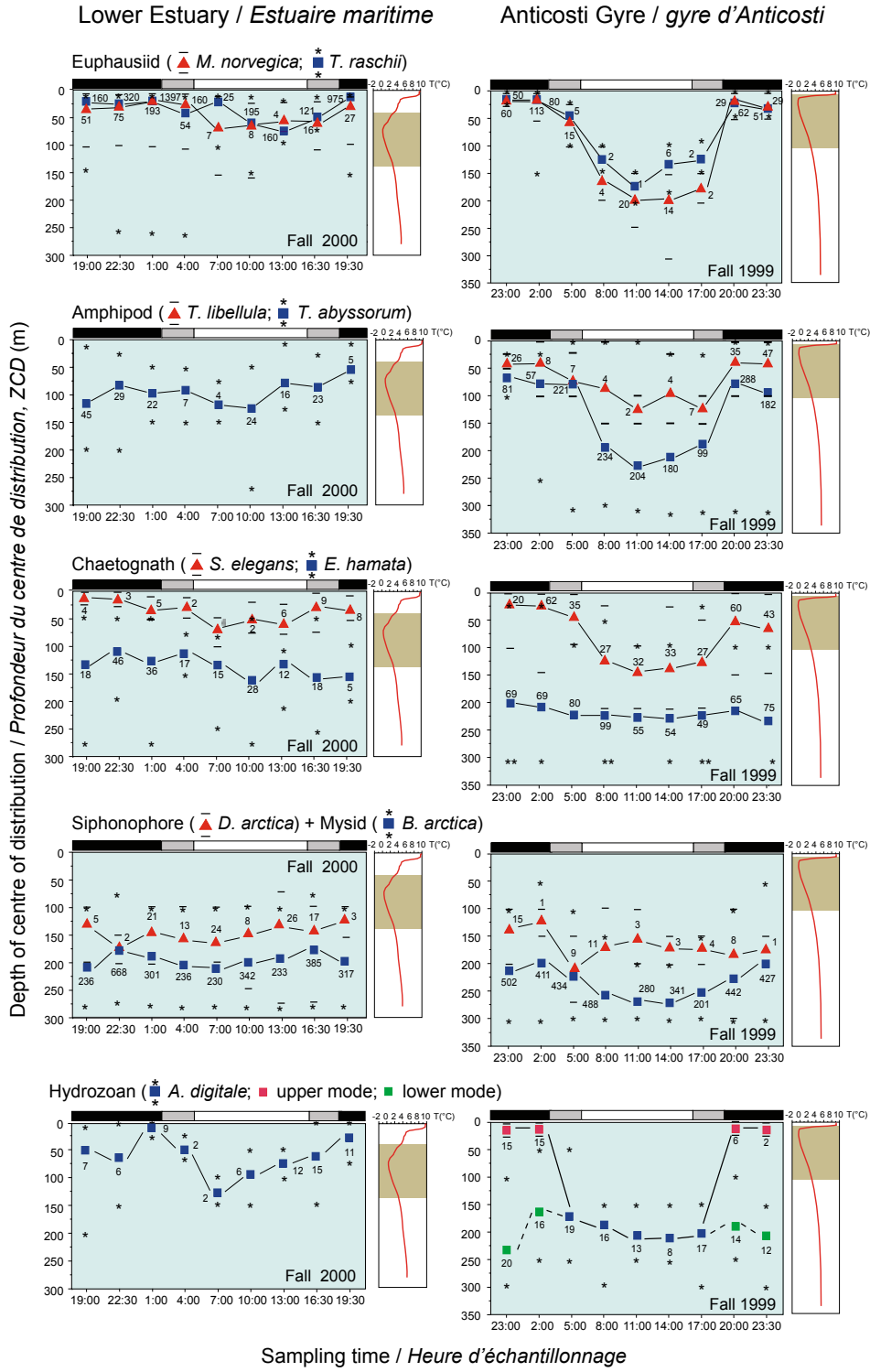


Fig. 3 Depths of the centre of distribution (ZCD; m) of dominant macrozooplankton species in fall 2000 in the LSLE and fall 1999 in the AG. Values next to symbols indicate the number of animals analyzed at each sampling time. Stars and dashed lines above and below the symbols indicate the lower and upper limits of the distributions of the animals at each sampling time. The upper bar indicates daytime (white), periods of sunset and sunrise (grey), and nighttime (black). Average vertical profiles of temperature (T ; $^{\circ}\text{C}$) taken during each sampling period are also shown. The shaded area on the profile panel shows the cold intermediate layer ($\leq 3^{\circ}\text{C}$).

Profondeur du centre de distribution (ZCD, m) des différentes espèces de macrozooplancton pendant l'automne 1999 et 2000 respectivement dans le gyre d'Anticosti (GA) et l'estuaire maritime (EM). Les chiffres près de chacun des symboles indiquent le nombre d'individus prélevés lors de chacun des prélèvements. Les étoiles et les lignes présentes dans la partie supérieure et inférieure de chacun des symboles indiquent la limite supérieure et inférieure de la distribution verticale de chaque espèce de macrozooplancton lors de chacun des prélèvements. L'axe supérieur indique la période journalière (blanc), du lever et du coucher du soleil (gris) et nocturne (noir) lors de chacun des prélèvements. Les profils moyens de température (T ; $^{\circ}\text{C}$) dans l'EM et la GA lors de chacun des prélèvements sont illustrés de même que les limites inférieures et supérieures de la couche intermédiaire froide ($\leq 3^{\circ}\text{C}$).

which were mostly found in the middle of the deep layer. Only *B. arctica* in the AG displayed vertical diel migration. They were always distributed at shallower depths during the night (210 ± 15 m) than during the day (255 ± 16 m), with an average migration amplitude of about 45 m. Since the vertical distribution pattern of the hydrozoan *A. digitale* was typically bimodal during the nighttime and unimodal during the daytime, we calculated both a surface and bottom ZCD for this species. During the daytime, *A. digitale* were below the CIL ($\sim 4^{\circ}\text{C}$) in the AG, between 125 and 225 m (175 ± 26 m), and were within the CIL ($\sim 1^{\circ}\text{C}$) in the LSLE, between 60 and 150 m (106 ± 17 m). During the nighttime, in both the LSLE and the AG, the population segregated into two groups, one that performed a migration to the surface layer and the other that stayed between 100 and 300 m.

Relationships between the diel vertical migration amplitude and the CIL thermal properties

Figure 4 shows the significant correlations between the DVM amplitude of different macrozooplankton species and the CIL core temperature (Z_{Tmin}). While most of the DVM amplitude varies inter-regionally (LSLE versus AG), the source of the difference is surely variability within an underlying abiotic factor, such as the structure of the CIL, that is different between the two regions. The DVM amplitude was negatively correlated with one or more CIL thermal parameters in most of the studied species. The DVM amplitude of all these species decreased significantly as a function of the depth of the CIL core temperature (Z_{Tmin}).

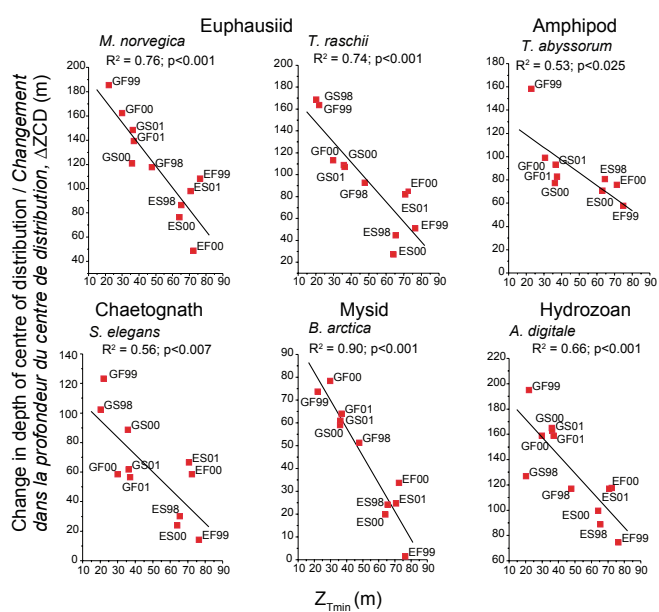


Fig. 4 Significant Pearson correlations between the diel vertical migration amplitude (ΔZCM) and the depth of the CIL core temperature ($Z_{T\text{min}}$) calculated from the CTD profiles measured in spring and fall 1998, 1999, 2000, and 2001 in the Lower St. Lawrence Estuary and the Anticosti Gyre (E: Lower Estuary; G: Anticosti Gyre; S: spring; F: fall; digits: sampling year).

Corrélations (Pearson) significatives entre l'amplitude de migration verticale (ΔZCM) et la profondeur de la température du cœur de la couche intermédiaire froide ($Z_{T\text{min}}$) estimée à partir des profils de CTD mesurés au printemps et à l'automne 1998, 1999 (automne seulement), 2000 et 2001 dans l'estuaire maritime et la gyre d'Anticosti (E: estuaire; G: gyre d'Anticosti; S: printemps; F: automne; chiffre: année d'échantillonnage).

Discussion

Vertical distribution and diel vertical migration of the various macrozooplankton species

Our most important result is that the various macrozooplankton species were distributed throughout the water column, including the surface layer, the CIL, and the deep layer at different times of day and night in both areas. Moreover, three types of migrational patterns were observed within this zooplankton community: (1) nocturnal ascent by the whole population, (2) segregation into two groups—one that performed a nocturnal accent and another that remained in the deep, and (3) no detectable migration.

The two euphausiid species found in the LSLE and the AG, *M. norvegica* and *T. raschii*, have been reported to be important diel vertical migrators in many regions (see review in Harvey et al. 2008). Sameoto (1976) reported that *T. raschii* and *M. norvegica* in the GSL formed distinct, narrow layers between 125 and 200 m during the day but migrated up to the top 50 m at night. At the head of the Laurentian Channel, Simard et al. (1986) observed that the daytime vertical distribution of euphausiids was characterized by two principal modes, at 75 and 150 m. *T. raschii* was the dominant organism in the first mode while *M. norvegica* dominated the second mode. These results are consistent with ours, which showed that *T. raschii* and *M. norvegica* formed two distinct narrow layers during the day, between 125 and 200 m and 50 and 150 m in the AG and LSLE, respectively, and migrated to the surface 50 m during nighttime.

Very little is known about the vertical distribution and the DVM of hyperiid amphipods. *T. libellula* has been generally sampled in the surface layer (< 30 m) and/or the deep layer (<300 m) in different arctic and subarctic seas (see review in Harvey et al. 2008), and a diel vertical movement has only been observed in the eastern Hudson Strait area, where *T. libellula* was mostly sampled in the deep (>200 m) and upper (<100 m) layers during day and night, respectively (Percy and Fife 1993). Our data show that *T. libellula* had limited migration in the AG between depths of 30 m in nighttime and 125 m in daytime, corresponding to the upper and the lower limit of the CIL at ~3°C. Likewise, there is little knowledge about the vertical distribution and the DVM of *T. abyssorum* except for the eastern Hudson Strait area (Percy and Fife 1993), where this species was sampled between 100 and 250 m during both night and day without any apparent DVM. In our study, *T. abyssorum* migrated from the upper part of the deep layer (~ 200 m) to the middle part of the CIL (~ 75 m).

The two chaetognath species found in the SLMS, *S. elegans* and *E. hamata*, have already been reported as exhibiting different diel vertical migrations at Station P in the subarctic Pacific area (Sullivan 1980). There, adult *S. elegans* occupied a deep stratum (200–400 m) during the day and migrated upward at night, mostly to 25 m, whereas adult *E. hamata* live permanently in the deep stratum (200–500 m) without performing diurnal vertical migration. This vertical distribution pattern is consistent with our results showing that *S. elegans* migrated from the upper and the middle part of the CIL to the surface layer in the LSLE and the AG, respectively, and that *E. hamata* remained in the lower part of the CIL in the LSLE and in the upper part of the deep layer in the AG without performing diurnal vertical migrations.

The mysid *B. arctica* was characterized as mesopelagic by Mauchline and Murano (1977); this is in accordance with observations made in many regions (see review in Harvey et al. 2008). However, *B. arctica* was also reported to live epi-benthically or to swim just above the sediment in the Catalan Sea (western Mediterranean) and in several Norwegian fjords (Cartes and Sorbe 1995, Fossa and Brattegard 1990). In the SLMS, *B. arctica* was first characterized as a suprabenthic species that migrates up within the 10 m above the bottom at dusk (Brunel et al. 1998). In the present study, a large number of *B. arctica* were sampled in the deep layer, between 125 and 275 m, during both night and day. This indicates that the *B. arctica* populations of the SLMS have both a hyperbenthic and a mesopelagic element.

Finally, for the two cnidarians, the siphonophore *D. arctica* and the hydrozoan *A. digitale*, *D. arctica* occupied the upper part of the deep layer, just below the CIL, and performed no apparent diel vertical migration. On the contrary, *A. digitale* mostly occupied the lower part of the CIL and the upper part of the deep layer during both night and day, with 38% (LSLE) and 67% (AG) of the population migrating into the surface layer at night. This is the first time that a nighttime bimodal vertical distribution has been observed for this species (see review in Harvey et al. 2008).

Biotic and abiotic factors affecting vertical distribution and diel vertical migration of macrozooplankton species

It is well known that the amplitude of movements and the vertical distribution of coexisting zooplankton species may be very different between species and between ontogenetic stages of the same species. This can be partly attributed to various biotic and abiotic features of their environments, such as light, food and predator abundance, and physical factors (see reviews in Ohman 1990 and Falkenhaug et al. 1997). In the present study, we observed that the DVM amplitude in most of the macrozooplankton species varied as a function of physical factors, in particular the spatio-temporal variations of the CIL thermal properties and especially the depth of the CIL core temperature ($Z_{T\min}$).

We observed that the thermocline/pycnocline did not restrict the upward migration of either euphausiid species (*M. norvegica* and *T. raschii*) or the chaetognath *S. elegans*, which were found in high proportions in the top 10 m. However, the amplitude of the DVM for these three species was negatively correlated with the depth of the CIL core temperature ($Z_{T\min}$). The factors associated with this significant relationship are unknown. Nevertheless, as previously suggested by Mauchline (1980) and Simard et al. (1986), and consistent with the assumption suggesting that the DVM of different macrozooplankton species is a trade-off between food acquisition and predation avoidance, it could be hypothesized that there is a relationship between the concentration of small zooplankton prey and the depth of the CIL, and that prey concentration is actually the factor that explains the high DVM-CIL correlation. For example, if a shallower CIL supported the concentration of prey closer to the surface and a deeper CIL were associated with a less concentrated, more spread out zooplankton prey field, then that could explain the DVM amplitude variability because macrozooplankton would not need to migrate as far at night in the latter case. This hypothesis is supported by the fact that the depth of the fluorescence maximum varied with surface layer thickness and CIL core temperature depth, which affects the distribution of phytoplankton and herbivorous mesozooplankton, in particular the small copepod populations (*Pseudocalanus* spp., *Acartia longiremis* and *Oithona* spp.) and the small copepodite stages (CI–CIII) of some larger species (*Calanus finmarchicus*, *C. glacialis*) that reside in permanency in the surface layer during the daytime and the nighttime (Plourde et al. 2002; M. Harvey unpublished data). However, this factor is unlikely to be the most important because the variability of nighttime predator position in the water column contributes much less to the overall DVM variability than does the variability of the deeper daytime distribution. Moreover, if a shallower CIL coincided with lower light extinction coefficients, then macrozooplankton would have to move deeper during the day to hide from predators. A factor that supports this second part of the hypothesis is the euphotic zone depth, estimated from Secchi disk readings in April and October (1997–2001) (Pierre Larouche, DFO, IML; personal communication). The euphotic zone was found to be shallower in the LSLE (11–14 m) than in the AG (20–32 m). This latter observation is a likely explanation for the fact that *M. norvegica* and *T.*

raschii were distributed twice as deep during the daytime in the AG (~ 125 m) than in the LSLE (~ 65 m), in particular in fall 2000.

T. libellula live almost exclusively within the CIL in the SLMS, at temperatures below 3°C. This is probably related to the arctic origin of this species, where the sea-surface temperature is below 3°C even during summer.

The presence of *S. elegans* in the surface layer during the night and within the CIL (<3°C) during the day also supports the theory by McLaren (1963) that it acquires food at the surface and then returns to deeper cooler waters where the resulting energy savings may be used to increase fecundity. In regards to *E. hamata*, this species apparently needs less food than *S. elegans*, and its vertical distribution is likely restricted by temperature (see Sullivan 1980). These factors would explain the absence of diel migration of *E. hamata* observed in the SLMS during this study.

Patterns in the DVM of *B. arctica* were principally observed in the AG, where the DVM amplitude of this species was negatively correlated with the depth of the upper and the lower limit of the CIL at 1°C ($Z_{i1^{\circ}\text{C}}$, $Z_{f1^{\circ}\text{C}}$) and the depth of the CIL core temperature ($Z_{T\min}$) (see Harvey et al. 2008). These three are highly auto-correlated, but the relevant variable limiting the DVM of *B. arctica* is the probably the lower limit of the CIL at 1°C since this species always occurs below the CIL. According to Mauchline (1980), factors that modify the vertical distribution and migrations of mysids are not well documented but are undoubtedly essentially the same as those that influence the behaviour of other crustaceans.

The specific factors that may initiate the vertical migration of only a part of the *A. digitale* population are unknown but likely include some of the same biotic and abiotic features that we have already discussed for other macrozooplankton species (light, food and predator abundance, physical factors). This is supported by the significant negative correlation between the DVM amplitude and the depth of the CIL core temperature ($Z_{T\min}$) for the portion of the *A. digitale* population that migrated to the top 50 m at night.

Retention or dispersion of macrozooplankton in the LSLE in relation to the DVM

The different DVM patterns observed in this study coupled with estuarine and tidal circulation and bottom topography could place animals in different flow regimes by night and by day and contribute to their retention (aggregation) or dispersion (Longhurst et al. 1984, Ohman 1990). For instance, there is a quasi-permanent rich aggregation of euphausiids (*M. norvegica* and *T. raschii*) at the head of the Laurentian Channel during summer that investigators have related to various retention and aggregation mechanisms (e.g., Cotté and Simard 2005). Likewise, it was previously shown that the euphausiids *M. norvegica* and *T. raschii* were respectively 6 and 15 times more abundant at our study site downstream in the LSLE than in the AG and that these species showed the largest population disparity between the two sites (Descroix et al. 2005). Can aggregation explain the greater abundance of euphausiids in the LSLE than in the AG?

One must be careful to make the distinction between horizontal advection towards the head of the Laurentian Channel and proper aggregation, which would explain our 6- and 15-fold increase in concentration. Aggregation, or the increase in the concentration of a population, can occur for organisms that react passively to horizontal advection but are able to maintain a given depth against vertical currents (for example, when maintaining a given light intensity level in the water column). The currents in the LSLE show estuarine circulation, whereby deep salty waters flow upstream and are gradually mixed upward into the downstream-flowing and fresher surface layer. There is a horizontal salinity gradient in surface waters of the estuary (i.e., surface salinity increases downstream in the estuary). This increase in salinity must be sustained from upwelling and mixing from deeper, more saline waters. This circulation pattern translates into horizontal convergence (divergence) in deep (surface) waters, which compensates for vertical upwelling currents. If deep-dwelling zooplankton are able to swim vertically against the upwelling current and thus maintain vertical position at depth, their population is concentrated by the horizontally convergent currents at depth. *M. norvegica* and *T. raschii* are known to swim at 1.5 to 4 body lengths per second, or several hundred metres per hour (Simard et al. 1986), which is sufficient for this mechanism.

Runge and Simard (1990) were the first to hypothesize that upstream advection of the deep layer by estuarine circulation was the mechanism responsible for zooplankton aggregation in the LSLE. This was subsequently tested by Zakardjian et al. (1999) using a simplified two-dimensional model that included vertical migration. They found that vertical migrants would have to reside on average about four times longer in the upstream-flowing deep layer than in the much faster downstream-flowing near-surface layer, which they argued does not correspond with the DVM pattern observed in the LSLE.

Sourisseau et al. (2006) more recently modelled zooplankton aggregation using a 3D sea ice – ocean circulation model for the entire Gulf of St. Lawrence, in which they added euphausiids with three predetermined DVM behaviours. For deep-dwelling organisms (130–150 m), strong aggregation in the estuary occurred upstream from our LSLE station, closer to the head of the Laurentian Channel, although some aggregation still occurred at our station location. On the contrary—and consistent with the results of Zakardjian et al. (1999)—organisms that carried out some DVM between the deep and the surface layers did not aggregate in the LSLE unless they spent less than 16% of their time in the fast-moving surface layer. However, we found during our study that most macrozooplankton species that performed DVM spent more time than this in the surface layer.

Aggregation areas can also be linked to bathymetric features, such as slopes and sills. In these cases, the horizontal component of the current diverges as it is pushed over the sloping sea floor, and zooplankton that swim against the resulting vertical current aggregate near the slope area. Indeed, many aggregation areas illustrated by Sourisseau et al. (2006) were associated with this mechanism. However, none of our stations are located near such bathymetric features, so this mechanism cannot explain aggregation at the LSLE station.

Our observations showed *M. norvegica* and *T. raschii* to vertically migrate between 25 and 250 m and 25 and 150 m, respectively, during the daytime in the LSLE and around 75–250 m and 50–200 m in the AG and ascend to the surface waters (0–50 m) during nighttime. Our daytime-dwelling depths extend deeper than the 130–150 m used by Zakardjian et al. (1999) and Sourisseau et al. (2006), but that should not be a cause for large differences in the expected outcome. Aggregation is not expected to occur in the highly estuarine circulation of the LSLE downstream from the head of the Laurentian Channel (where local mechanisms come into play; Cotté and Simard 2005) and cannot explain the 6- and 15-fold increase in LSLE abundance compared to those in the AG. Nevertheless, although our LSLE station is not located in a dynamic aggregation site, it is quite possible that the aggregation that does occur at the head of the Laurentian Channel can be carried downstream while in the surface layer and supply the LSLE site with enhanced concentrations. However, since numerical models such as that of Sourisseau et al. (2006) have not predicted that such an advective process could occur, other factors should also be considered, such as food availability, predation, and mortality.

Acknowledgements

This study is a contribution to DFO's Ecosystem Research Initiative and was supported by DFO. The technical contributions of J.-F. St-Pierre, P. Joly, and J.-P. Allard as well as numerous other DFO personnel toward the collection of BIONESS data are gratefully acknowledged. We also wish to thank L. Devine for helping to improve the quality of the text.

References

- Brunel, P., Bossé, L., and Lamarche, G. 1998. Catalogue of the marine invertebrates of the estuary and the Gulf of St. Lawrence. Can. Spec. Pub. Fish. Aquat. Sci. 126, 405 pp.
- Cartes, J.E., and Sorbe, J.C. 1995. Deep-water mysids of the Catalan Sea: Species composition, bathymetric and near-bottom distribution. J. Mar. Biol. Assoc. UK, 75, 187–197.
- Cotté, C., and Simard, Y. 2005. Formation of dense krill patches under tidal forcing at whale feeding hot spots in the St. Lawrence Estuary. Mar. Ecol. Prog. Ser. 288: 199–210.
- Cottier, F.R., Tarling, G.A., Wold, A., and Falk-Petersen, S. 2006. Unsynchronized and synchronized vertical migration of zooplankton in a high arctic fjord. Limnol. Oceanogr. 51: 2586–2599.
- Cushing, D.H. 1951. The vertical migration of planktonic Crustacea. Biol. Rev. 26: 158–192.
- Descroix, A., Harvey, M., Roy, S., and Galbraith, P.S. 2005. Macrozooplankton community patterns driven by water circulation in the St. Lawrence marine system, Canada. Mar. Ecol. Prog. Ser. 302: 103–119.
- Falkenhaug, T., Tande, K.S., and Semenova, T. 1997. Diel, seasonal and ontogenetic variations in the vertical distributions of four marine copepods. Mar. Ecol. Prog. Ser. 149: 105–119.
- Fossa, J.H., and Brattegard, T. 1990. Bathymetric distribution of Mysidacea in fjords of western Norway. Mar. Ecol. Prog. Ser., 67: 7–18.
- Harvey, M., and Devine, L. 2007. Oceanographic conditions in the Estuary and the Gulf of St. Lawrence during 2006: zooplankton. DFO CSAS Res. Doc. 2007/049, 36 pp.
- Harvey, M., Galbraith, P.S., and Descroix, A. 2009. Vertical distribution and diel migration of macrozooplankton in the St.

- Lawrence marine system (Canada) in relation with the cold intermediate layer thermal properties. *Prog. Oceanogr.* 80: 1-21; doi: 10.1016/j.pocean.2008.09.001.
- Longhurst, A.R.** 1976. Vertical migration. In *The ecology of the seas*. Edited by D.H. Cushing and J.J. Walsh. W.B. Saunders, Toronto. pp. 116-137.
- Longhurst, A., Sameoto, D., and Herman, A.** 1984. Vertical distribution of Arctic zooplankton in summer: eastern Canadian archipelago. *J. Plankton Res.* 6: 137-168.
- Mauchline, J.** 1980. The biology of mysids and euphausiids. Academic Press, London.
- Mauchline, J., and Murano, M.** 1977. World list of the Mysidacea, Crustacea. *J. Tokyo Univ. Fish.*, 64: 39-88.
- McLaren, I.A.** 1963. Effects of temperature on growth of zooplankton, and the adaptive value of vertical migration. *J. Fish. Res. Board Can.* 20: 685-727.
- Ohman, M.D.** 1990. The demographic benefits of diel vertical migration by zooplankton. *Ecol. Monogr.* 60: 257-281.
- Percy, J.A., and Fife, F.J.** 1993. Macrozooplankton, particularly species of *Themisto* (Amphipoda, Hyperiidea), and temperature, salinity and density data collected in eastern Hudson Strait in 1987-88. *Can. Data Rep. Fish. Aquat. Sci.* 905, 117 pp.
- Plourde, S., Dodson, J.J., Runge, J.A., and Therriault, J.-C.** 2002. Spatial and temporal variations in copepod community structure in the lower St. Lawrence Estuary, Canada. *Mar. Ecol. Prog. Ser.* 230: 211-224.
- Runge, J.A., and Simard, Y.** 1990. Zooplankton of the St. Lawrence estuary: the imprint of physical processes on its composition and distribution. In *Oceanography of a large-scale estuarine system: the St. Lawrence*. Edited by M.I. El-Sabh and N. Silverberg. Coastal and Estuarine Studies 39. Springer-Verlag, New York, pp. 296-320.
- Sameoto, D.D.** 1976. Distribution of sound scattering layers caused by euphausiids and their relationship to chlorophyll *a* concentrations in the Gulf of St. Lawrence Estuary. *J. Fish. Res. Board Can.* 33: 681-687.
- Simard, Y., Lacroix, G., and Legendre, L.** 1986. Diel vertical migrations and nocturnal feeding of a dense coastal krill scattering layer (*Thysanoessa raschi* and *Meganyctiphanes norvegica*) in stratified surface waters. *Mar. Biol.* 91: 93-105.
- Sourisseau, M., Simard, Y., and Saucier, F.J.** 2006. Krill aggregation in the St. Lawrence system, and supply of krill to the whale feeding grounds in the estuary from the gulf. *Mar. Ecol. Prog. Ser.* 314: 257-270.
- Sullivan, B.K.** 1980. In situ feeding behavior of *Sagitta elegans* and *Eukrohnia hamata* (Chaetognatha) in relation to the vertical distribution and abundance of prey at Ocean Station 'P'. *Limnol. Oceanogr.* 25: 317-326.
- Zakardjian, B., Runge, J.A., Plourde, S., and Gratton, Y.** 1999. A biophysical model of the interaction between vertical migration of crustacean zooplankton and circulation in the Lower St. Lawrence Estuary. *Can. J. Fish. Aquat. Sci.* 56: 2420-2432.

An Evaluation of Operational Sea-Surface Temperature Analyses Using AZMP Data Over the Eastern Canadian Shelves

Yongsheng Wu¹, Dave Senciar², and Charles Tang¹

¹Bedford Institute of Oceanography, Box 1006, Dartmouth, NS, B2Y 4A2

²Northwest Atlantic Fisheries Centre, Box 5667, St. John's, NL, A1C 5X1

wuy@mar.dfo-mpo.gc.ca

Sommaire

La précision des données opérationnelles des températures de la surface de la mer produites par le Centre météorologique canadien (CMC) et le *National Centers for Environmental Prediction* (NCEP) pour le plateau continental de l'est du Canada est évaluée à l'aide des données in situ du Programme de monitorage de la zone Atlantique (PMZA) de 2005 à 2007. L'analyse statistique des données montre qu'à l'échelle régionale le biais moyen est très faible, 0,05 °C pour les données NCEP et 0,06 °C pour les données CMC, alors que l'écart quadratique moyen, 1,0 °C pour le NCEP et 1,04 °C pour le CMC, est grand en comparaison des analyses globales (typiquement 0,4 °C) qui utilisent des données des bouées pour la calibration. Ceci démontre l'avantage d'utiliser les données à haute résolution spatiale des navires pour la préparation des données de températures de surface de la mer à partir des satellites. Les analyses selon les saisons et les transects du PMZA indiquent que les erreurs n'ont aucune tendance saisonnière ou géographique et qu'elles sont du même ordre de grandeur pour les données CMC et NCEP. Les plus grandes erreurs sont observées pour les transects du bonnet Flamant et du sud-est des Grands Bancs. L'examen des statistiques sur ces transects révèle que les erreurs ont une échelle horizontale beaucoup plus petite que la largeur du plateau continental. À la fois le CMC et le NCEP produisent des températures de la surface de la mer trop élevées de 1,6 à 2,9 °C pour le courant du Labrador, alors que le biais pour le plateau continental est typiquement de moins de 1 °C. Nous n'avons pas trouvé de différences notables entre les données du CMC et du NCEP.

Introduction

Satellite-based sea-surface temperature (SST) is one of the most useful data sources in meteorological and oceanographic research (Mesias et al. 2007). The data have been used in fishery applications (Myers and Hick 1990) and assimilated into ocean circulation models to improve predictability (Ezer and Mellor 1997). In weather forecast models, SST is used to set the models' lower boundary conditions (Brasnett 2008). Compared to in situ SST from ships and buoys, a major advantage of satellite-based SST is the global

coverage and near real-time availability; however, in situ data are typically more accurate.

Earlier studies have shown that there are errors in satellite-based SST due to the complexity of oceanic and atmospheric conditions (Robinson et al. 1984, Brown et al. 1985, Minnett 1991, Wick et al. 1992). The errors were found to vary regionally and temporally (Wick et al. 1992). Most of these studies used SST from ocean data buoys at fixed locations for calibration. In this study, we focus on the evaluation of

satellite-based SST on eastern Canada shelves using data from the Atlantic Zone Monitoring Program (AZMP) transects, in which stations are typically separated by 25 km.

Data

In situ SST

The AZMP was implemented in 1998 to provide a seasonal description of marine biological, chemical, and physical variables for Atlantic Canada. Temperature, salinity, nutrients, oxygen, chlorophyll, phytoplankton, zooplankton, and light attenuation are measured. Ship-based surveys along standard sections are one of the main elements of the program (Fig. 1). Since the early 1990s, the sections have been surveyed in spring, summer, and fall, with the SIL section generally limited to a summer survey and the southernmost section (HAL) limited to spring and fall.

Instrumentation for temperature and salinity has been consistently the Sea-Bird SBE 911*plus* high precision CTD system equipped with dual SBE 3 temperature sensors (accuracy of $\pm 0.01^\circ\text{C}$) using factory calibrations and SBE 4 conductivity sensors (accuracy $\pm 0.0003 \text{ S/m}$) in a pumped TC-duct configuration. Temperature and salinity calibrations are validated by comparing the two datasets and by deep water (high homogeneity) checks against a Sea-Bird SBE 35 high precision thermometer (accuracy $\pm 0.001^\circ\text{C}$).

Casey and Cornillon (1999) indicated that care must be taken when comparing satellite-derived SST—a skin (<upper 1 mm) temperature—with ship data. The SST from ships, commonly called bulk SST, usually represents the temperature over the upper few metres (Schlussel et al. 1990, Thomas and Turner 1995). We take the view that under normal oceanographic and meteorological conditions, the skin layer is mostly destroyed by waves and vertical mixing, thus satellite and bulk SST are comparable. This view is consistent with observations made during the AZMP surveys.

Typically, the shallowest CTD records are from $\sim 1.5\text{--}2 \text{ m}$ below the surface due to the physical configuration of the package. The upper 5 m is generally observed to be well mixed ($<0.1^\circ\text{C}$ variability, often $<0.05^\circ\text{C}$). Observations of the near-surface temperature made while retrieving the package suggest that the water above 2 m is similarly mixed. Factors that could lead to differences in the very-near-surface water temperature compared to the bulk SST generally would relate to the proximity to cold freshwater sources such as melting ice fields or icebergs that may resist mixing in low energy sea states. This is principally an issue in areas such as the Nose of the Grand Bank, Flemish Pass, Avalon Channel (western extent of the Flemish Cap line), or the inner Bonavista and Louisburg transects during the spring surveys, where ice is often present. Summer transects could be influenced by localized surface solar heating during calm conditions (as well as the occasional iceberg meltwater), but the lower air temperatures and solar flux combined with often aggressive sea conditions during the spring and fall surveys would in general ensure that the bulk SST is directly comparable with satellite-derived SST. Regions such as the Flemish Cap are also subject to the convergence and interplay of several currents and

water masses within a small area ($\sim 100 \text{ km}$) and are characterized by various transient eddies as well as horizontal shears on scales of tens of kilometres, possibly less than the resolution of the satellite data product we use. Temporal variability less than seasonal is not determined from the AZMP surveys.

Over eastern Canadian shelves, the AZMP sections include, from north to south, Seal Island (SIL), Bonavista (BON), Flemish Cap (FLC), South East Grand Banks (SEG), Louisbourg Line (LOU), and Halifax Line (HAL) (Fig. 1). We compare AZMP and satellite-based data for 2005 to 2007.

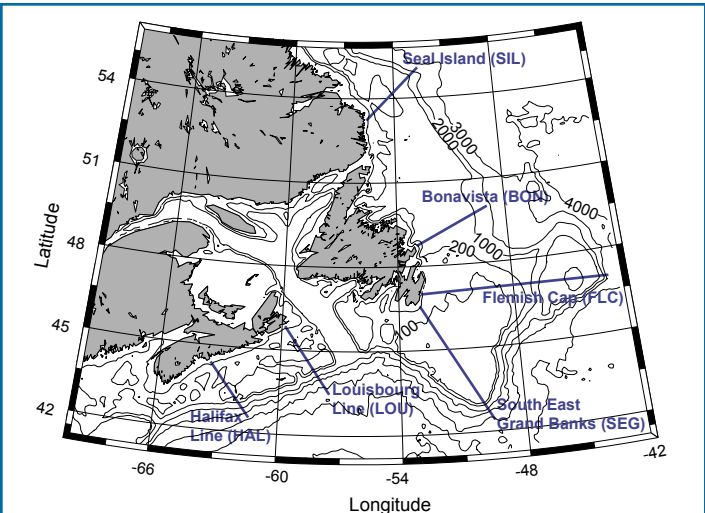


Fig. 1 Locations of the AZMP sections used in the evaluation (bathymetry is in metres).

Localisation des transects du PMZA utilisés pour l'analyse (la bathymétrie est en mètres).

Satellite-based operational SST products

Two sets of SST data are used in this investigation. One is the daily operational SST analysis from the Canadian Meteorological Centre (CMC). This analysis is used as the lower boundary condition in the numerical weather prediction models at CMC. The analysis uses SST retrievals from the A/ATSR (Advanced/Along-Track Scanning Radiometer) aboard the ENVISAT satellite and the AVHRR (Advanced Very High Resolution Radiometer) aboard the NOAA-17 satellite as well as SST measurements from ships and buoys. The analysis is updated every day on a global $1/3^\circ$ ($\sim 30 \text{ km}$ resolution in the study area) grid using optimal interpolation. The first guess or background required by the method is derived from the previous day's analysis, an approach that allows information from recent observations to be carried forward in time. The method is also used to generate SST fields when cloud cover is present. Before data are used in the analysis scheme, biases of daytime and nighttime retrievals are estimated for each satellite and removed. Biases are also estimated for each ship report and removed. A newer version of the analysis that includes retrievals from the AMSR-E (Advanced Microwave Scanning Radiometer for EOS) instrument aboard the Aqua satellite is currently being tested (see Brasnett 2008 for details).

The second dataset is the Real-Time Global Sea Surface Temperature analysis (RTG_SST) produced by the National Oceanic and Atmospheric Administration (NOAA). This

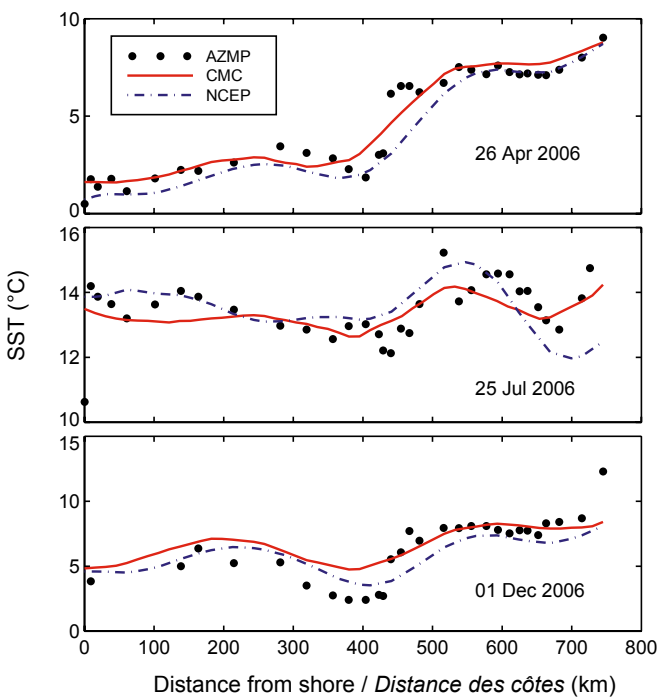


Fig. 2 An example of the comparisons between SST from AZMP, CMC, and NCEP along Flemish Cap in 2006.

Un exemple de la comparaison des données de températures de surface de la mer entre PMZA, CMC et NCEP sur le transect du bonnet Flamant en 2006.

product is a blend of the AVHRR and in situ SST and is produced daily at a resolution of 0.5°. RTG_SST is used as the boundary condition of the weather forecast models at the National Centers for Environmental Prediction (NCEP) and at the European Centre for Medium-Range Weather Forecasts (ECMWF). The development and validation of the dataset are described in Gemmill et al. (2007).

Statistical Analyses

In comparing the operational analyses and in situ SST data, 3-d averaged SSTs from the operational analyses are used. The CMC SSTs are daily products all with a time stamp of 0000 UTC. This time is assigned and does not represent the time of data acquisition. Thus there is an inherent uncertainty of up to 24 h in the assigned time relative to the actual time of the observation. In addition, a correlation analysis indicates that the time between the zero-crossings of the correlation function is approximately three days, and averaging over this time period can reduce the random noise. A more rigorous way to handle the SST products is to perform a space-time optimal interpolation of the data to the ship locations and times.

To evaluate the quality of the operational analyses, two statistical variables, mean bias (satellite mean minus in situ mean) and root mean square difference (RMSD), were computed and analyzed to quantify the accuracy of the SST. For the ship data, only the locations that have temperature data within the upper 3 m were used in the comparison. The averaged temperature within this layer represents the bulk SST. To carry out the statistical analysis, the 3-d averaged satellite SSTs were interpolated linearly to the ship positions. As an illustration, Figure 2 shows the SST from AZMP, CMC, and NCEP across

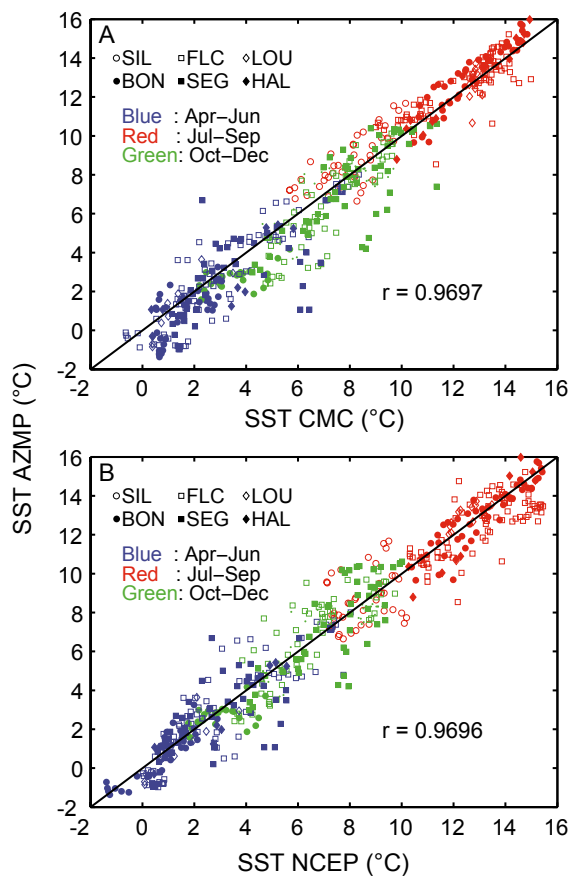


Fig. 3 Scatter plot of all SST data from AZMP transects and operational analyses from A) CMC and B) NCEP.

Diagramme de dispersion de toutes les données des températures de la surface de la mer des transects du PMZA et des analyses opérationnelles A) CMC et B) NCEP.

the Flemish Cap section in 2006. The SST products and in situ data generally agree, but there are noticeable differences. The SST products are smoother, with less spatial structure than the in situ data. The in situ data have strong horizontal gradients at the shelf break (400–500 km) that are not seen in the SST products. We note that the smoothness and weaker horizontal gradients in the SST products are not due to the 3-d averaging alone, but are present in the daily temperature fields as well.

Figure 3 is a scatter plot of all operational and AZMP data used in this work. The figure clearly shows that, on regional scale, both CMC and NCEP SSTs are well correlated with the AZMP SSTs, both with correlation coefficients of 0.97. The biases (root mean square differences, RMSD) are 0.06°C (1.04°C) for CMC and 0.05°C (1.00°C) for NCEP data. The high correlation is a reflection of the strong annual cycle and strong temperature gradient across the region. Other statistical parameters that can be used to quantify the correlation are the slope (optimally 1.0) and intercept (optimally 0) of the line best fitted to the data points (Table 1). For the seasonal comparisons, the CMC data in summer have the best fit, with a slope of 0.93 and an intercept of 0.33. Overall the NCEP product shows the best agreement, with a slope of 0.96 and an intercept of 0.32 (Table 1). There is no obvious seasonal trend from spring to fall for either the CMC or NCEP data, and the differences between the two datasets appear random. The overall slope is closer to 1 in 5 of 6 cases and the overall intercept is smaller in 4 of 6 cases

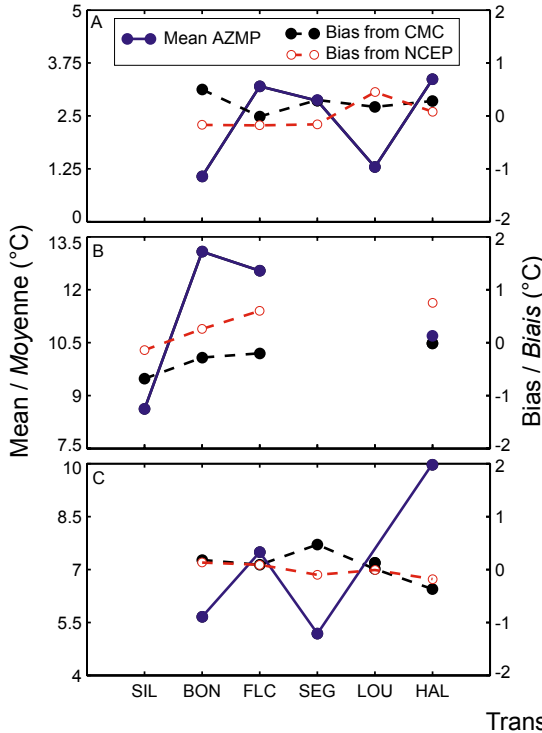


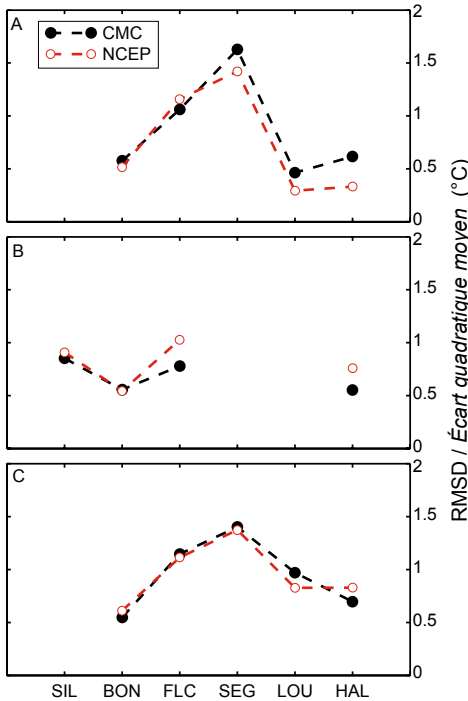
Fig. 4 Variations of the AZMP mean, the CMC bias, and the NCEP bias (left), and the RMSD (right) in A) spring, B) summer, and C) autumn. Transects are listed from north to south on the x axis.

Variations dans la moyenne PMZA, le biais CMC et le biais NCEP (à gauche) et de l'écart quadratique moyen (à droite) au A) printemps, B) à l'été et C) à l'automne. Dans chaque cas, sur l'axe des x les transects sont listés du nord au sud.

in comparison to the seasonal data. We note that the slope and intercept in a linear fit are, in general, scale dependent. If data are selected within a small temporal and spatial range, the range of the SST values will also be small. The slope and intercept calculated from such a subset of data may deviate significantly from the slope and intercept of the overall data.

The RMSDs are 1.04°C for CMC and 1.00°C for NCEP data (Table 1), which are larger than many global analyses, typically 0.4°C (e.g., Brasnett 2008). A possible explanation is that small-scale ocean features are not resolved in the global analyses. Most global analyses utilize SST from ocean buoys at fixed locations. The average distance between the buoys is on the order of 150 km. As a result, small-scale ocean features such as sharp gradients associated with strong currents may not be detected by the buoys. On the other hand, the ocean buoys record over long periods and could sample small spatial scale features advected past them. The scatter plot (Fig. 3) also shows that largest errors are in SEG and FLC in spring.

Our detailed analysis starts with the temporal and regional variability of the mean bias and RMSD from north to south (six sections, from SIL to HAL; see Fig. 1 for locations) in different seasons (spring [Apr-Jun], summer [Jul-Sep], and autumn [Oct-Dec]). Figure 4 shows the mean SST from AZMP data as well as the bias and RMSD from the SST data. In spring (Fig. 4A), in all the sections except FLC, the CMC SST is warmer than AZMP SST. However, the NCEP SST is colder than AZMP SST in the north (BON, FLC, and SEG) but warmer in the south (LOU and HAL). The pattern of change of RMSD from north to south is similar for CMC and NCEP. The RMSD



increases from BON to SEG and then decreases. In summer (Fig. 4B), the CMC SST is colder than AZMP SST in SIL, BON, and FLC but slightly warmer in HAL. The NCEP SST is warmer than AZMP SST for all stations except SIL. In autumn, the biases are in the range -0.2 to 0.5°C, which is slightly smaller than the biases for spring and summer. The RMSD pattern of change is very similar to that for spring, with a maximum at SEG (Fig. 4C).

The analysis presented in Figure 4 and Table 1 indicates that there is no obvious seasonal trend and that the differences between in situ observations and the CMC and NCEP datasets are of similar magnitudes. The biases of the operational analyses are between -0.8 and 0.8°C, and the RMSDs are between 0.3 and 1.7°C. RMSD values greater than 1°C are found in FLC and SEG.

Large errors in FLC and SEG can also be seen in the scatter plot of Figure 3. Despite the large RMSD for FLC and SEG, their biases are comparable to the other stations. This implies that the errors in these two sections occur at horizontal scales much smaller than the length of the sections (also see Fig. 2).

Table 1 Statistics of operational SST data and regressions of AZMP on operational SST data. The root mean square differences (RMSD) and slopes and intercepts from linear regressions are tabulated.

Statistiques pour les données opérationnelles des températures de la surface de la mer et régressions des données PMZA sur les données opérationnelles. Les écarts quadratiques moyens et les pentes et les ordonnées des régressions linéaires sont présentés.

Period / Période	RMSD / Écart quadratique moyen (°C)		Slope / Pente		Intercept / Ordonné (°C)	
	CMC	NCEP	CMC	NCEP	CMC	NCEP
Apr-Jun / avr-juin	0.90	0.85	0.88	0.85	0.50	0.35
Jul-Sep / juil-septembre	0.87	1.15	0.93	0.88	0.33	1.42
Oct-Dec / oct-décembre	1.12	1.02	0.84	0.89	1.60	0.77
Overall / Sur l'ensemble	1.04	1.00	0.92	0.96	0.67	0.32

To show the variation of the statistical properties along FLC and SEG, mean bias and RMSD were calculated (Fig. 5). For the SEG section, the comparisons were based on the spring and fall transects for 2005–07, i.e., six data points per station; for the FLC section, the statistics rest on spring, summer, and fall transects for 2005–07, nine points per station. Large

biases and RMSDs are found in the shelf break areas, where the RMSD reaches 3.0°C in SEG and 2.8°C in FLC, and the bias reaches 2.9°C in SEG and 1.6°C in FLC. In SEG, the large errors occur around the edge of the Grand Banks (460 km). In FLC, there are two regions with large errors, the Flemish Pass (440 km) and the eastern slope of the Flemish Cap (750 km). The edge of the Grand Banks and Flemish Pass have low surface temperatures and large horizontal temperature gradients associated with the Labrador Current (Fig. 5B). There is a trend of increasing RMSD with higher horizontal temperature gradients. The Labrador Current has a width of about 100 km.

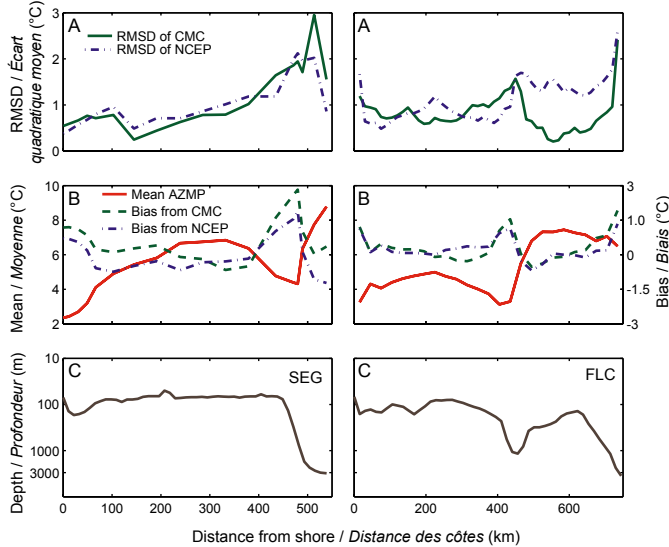


Fig. 5 A) RMSD, B) mean AZMP and CMC, NCEP biases, and C) water depth for SEG (left panels) and FLC (right panels).

A) *Écart quadratique moyen*, B) *moyenne PMZA et biais CMC et NCEP*, et C) *profondeur pour le transect SEG (à gauche) et le transect FLC (à droite)*.

It flows along the edge of Labrador Shelf and the Grand Banks and brings cold and fresh water from the northern Labrador Sea to the southern shelves. Both the CMC and NCEP SSTs in the Labrador Current are too warm by 1.6 to 2.9°C. The large errors may be associated with the large horizontal scale of the operational products relative to that of the Labrador Current. A correlation analysis of the operational SST data gave a correlation scale on the order of 300 km.

Between the CMC and NCEP analyses, CMC has larger RMSDs and biases over the shelf break but smaller RMSDs and biases over the shallow regions of the Grand Banks for the SEG section (left panels of Fig. 5). Along the FLC section (right panels of Fig. 5), the CMC data have significantly smaller RMSDs than the NCEP data over the Flemish Cap (at ~600 km) but comparable RMSDs for the rest of the section. The biases of the two satellite datasets have similar magnitudes.

Conclusions

In this article, the accuracy of operational SST analysis over eastern Canadian shelves from CMC and NCEP is evaluated using data from in situ measurements (AZMP) from 2005 to 2007. On a regional scale, the SSTs from both the CMC and NCEP products are significantly correlated to the in situ SST. The mean biases are small, 0.06°C for CMC and 0.05°C for

NCEP. The root mean squared differences are 1.04°C for CMC and 1.00°C for NCEP, large in comparison to many global analyses. The large errors are attributed to significant variance at small spatial scales in the region and the high horizontal resolution of the AZMP data, which were not incorporated into the operational products. Analyses of the data by season and by AZMP section indicate that the errors have no obvious seasonal or geographic trends and are of similar magnitudes for the CMC and NCEP datasets. Among the sections, FLC and SEG have the largest errors. An examination of the statistics across these sections reveals that the errors occur at horizontal scales much smaller than the width of the shelf. Both CMC and NCEP show SSTs that are too warm by 1.6 to 2.9°C in the Labrador Current, while the bias for the shelf is typically less than 1°C. No appreciable difference is found between the CMC and NCEP products.

Acknowledgements

The authors thank Jeff Spry, Gary Maillet, and Jennifer Higdon for providing the CTD data in 2007, and Bruce Brasnett for information about the CMC data.

References

- Brasnett, B. 2008. The impact of satellite retrievals in a global sea-surface-temperature analysis. *Q. J. Roy. Meteor. Soc.* 134: 1745–1760; DOI: 10.1002/qj.319.
- Brown, O.W., Brown, J.W., and Evans, R.H. 1985. Calibration of the advanced very high resolution radiometer infrared observations. *J. Geophys. Res.* 90: 11667–11677.
- Casey, K.S., and Cornillon, P. 1999. A comparison of satellite and in situ-based sea surface temperature climatologies. *J. Climate* 12: 1848–1863.
- Ezer, T., and Mellor, G.L. 1997. Data assimilation experiments in the Gulf Stream region: How useful are satellite-derived surface data for nowcasting the subsurface fields? *J. Atmos. Ocean. Tech.* 14: 1379–1391.
- Gemmell, W., Katz, B., and Li, X. 2007. Daily real-time global sea surface temperature - high resolution analysis at NOAA/NCEP. NOAA / NWS / NCEP / MMAB Office Note No. 260, 39 pp.
- Mesias, J.M., Bisagni, J.J., and Brunner, A.M.E.G. 2007. A high-resolution satellite-derived surface temperature climatology for the western North Atlantic Ocean. *Cont. Shelf Res.* 27: 191–207.
- Minnett, P.J. 1991. Consequences of sea surface temperature variability on the validation and applications of satellite measurements. *J. Geophys. Res.* 96: 18,475–18,489.
- Myers, D., and Hick, P. 1990. An application of satellite-derived sea surface temperature data to the Australian fishing industry in near real-time. *J. Remote Sens.* 11: 2103–2112.
- Robinson, I.S., Wells, N.C., and Charnock, H. 1984. The sea surface thermal boundary layer and its relevance to the measurement of sea surface temperature by airborne and spaceborne radiometers. *J. Remote Sens.* 5: 19–45.
- Schlüssel, P., Emery, W.J., Grassl, H., and Mammen, T. 1990. On the bulk-skin temperature difference and its impact on satellite remote sensing of sea surface temperature. *J. Geophys. Res.* 95: 13,341–13,356.
- Thomas, J.P., and Turner, J. 1995. Validation of Atlantic Ocean sea surface temperatures measured by the ERS-1 Along Track Scanning Radiometer. *J. Atmos. Ocean. Tech.* 12: 1303–1312.
- Wick, G.A., Emery, W.J., and Schlüssel, P. 1992. A comprehensive comparison between satellite-measured skin and multichannel sea surface temperature. *J. Geophys. Res.* 97: 5569–5595.

A Preliminary Investigation of Two Potential Stability Data Products for AZMP

Jim Helbig and Jennifer Higdon

Northwest Atlantic Fisheries Centre, Box 5667, St. John's, NL, A1C 5X1
james.helbig@dfo-mpo.gc.ca

Sommaire

Deux produits dérivés de données relatifs à la stabilité verticale de la colonne d'eau ont été étudiés dans la perspective de leur utilité pour le PMZA et sont présentés en espérant stimuler la discussion sur leur valeur. Il s'agit de la fréquence de Brunt-Väisälä ou de stabilité N et du nombre de Richardson Ri . Le premier est bien connu, à une interprétation dynamique et peut être calculé directement des données de CTD, même si ceci est fait rarement. Le second demande en plus l'estimation de la cisaille verticale du courant tel que l'on peut l'obtenir des mesures de l'ADCP utilisé lors des relevés du PMZA. Il semble cependant que cette valeur n'a jamais été présentée auparavant sur une grande échelle géographique. Plusieurs considérations pratiques sont discutées pour le calcul des deux variables. De plus, on présente six sections verticales de N^2 et Ri pour trois saisons, sur deux années, sur le transect Bonavista du PMZA. Les variables montrent une variabilité saisonnière importante mais aussi une forte cohérence entre les années.

Introduction and Background

Although the biological importance of the vertical stability of the upper ocean to mixing is well known, the AZMP does not routinely report any measure of it, except at fixed stations (e.g., see Environmental Overview in this and previous issues). The purpose of this note is to consider two stability measures that can be derived from transect data in the hope of stimulating discussion as to their utility.

The Brunt-Väisälä frequency N , commonly called the stability or buoyancy frequency, and the gradient Richardson number Ri are defined by formulas 1a and 1b.

$$N^2 = -\frac{g(\partial \rho / \partial z)}{\rho_*} \quad Ri = \frac{N^2}{(\partial u / \partial z)^2 + (\partial v / \partial z)^2} \quad (1a, 1b)$$

Here g is the acceleration due to gravity, ρ is the density, ρ_* is a constant reference density, u and v are the two components of the horizontal velocity, and z is the vertical coordinate (positive upward). N is a scaled version of the density gradient, has dimensions of s^{-1} , and is a measure of gravitational stability; the water column is gravitationally unstable where $N^2 < 0$, i.e., when more dense water overlays less dense water. Physically, N is the frequency with which a parcel of water would oscillate if subjected to a small vertical displacement; it is also an important parameter that appears naturally in the equations of motion. It is readily calculated from CTD data using widely available routines and tends to be highly variable. In a review of the effect of physical processes on primary productivity, Gargett and Marra (2002) suggest that N should be routinely reported as part of marine observations.

The gradient Richardson number is a measure of the dynamic stability of the water column. It is closely related to the flux Richardson number, which is the ratio of the destruction by buoyancy forces to the production by vertical shear of turbulent kinetic energy. In regions of high stratification (large N) or weak shear, both Richardson numbers are large and turbulence tends to decay. Conversely, in regions of small N

or large shear, turbulence tends to grow. The computation of Ri requires measurement of the squared vertical shear $\Sigma^2 = (\partial u / \partial z)^2 + (\partial v / \partial z)^2$. This is a difficult measurement, but Σ^2 can be estimated from the vertical profiles of current collected by ship-mounted ADCPs on AZMP surveys.

Ri is a dimensionless number with theoretical significance for the stability of steady, vertically sheared flows. The Miles-Howard theorem states that a vertically sheared flow is linearly stable if $Ri > 0.25$ everywhere in the flow (e.g., Kundu 1990). In practice, laboratory and field experiments have shown that both steady and unsteady flows are stable if Ri is greater than a critical value somewhat smaller than 0.25 (e.g., Thorpe 2005), although there are field experiments showing that the critical Richardson number is close to one (e.g., Mack and Schoeberlein 2004).

Among AZMP and other DFO-led studies that have considered stability is the work by Greenan et al. (2004, 2008), who estimated Ri by combining moored ADCP data with hydrographic data from a profiling CTD. They used these estimates in a site-specific examination of the relative importance of mixing and upwelling in initiating phytoplankton blooms. Colbourne et al. (2007) presented highly provocative horizontal sections of mixed layer depth (estimated from the maximum density gradient) and stratification index (the density difference between the surface and 50 m divided by 50 m). Their results were derived from tow-mounted CTD measurements made during the multi-month DFO multi-species spring and fall Newfoundland-Labrador surveys. As well, Craig and Gilbert (2008) considered a variety of methods for determining mixed layer depth.

Method

Both N^2 and Ri were estimated along the Bonavista transect¹ for six AZMP surveys (spring, summer, and autumn in 2002 and 2003). CTD data collected at standard hydrographic stations and ADCP data collected continuously along the transect were used in the computations. For

¹ See the AZMP website <http://www.meds-sdmm.dfo-mpo.gc.ca/isdm-gdsi/azmp-pmza/index-eng.html>

each hydrographic station, we interpolated density to a 0.5 m grid and used the openly available MATLAB routine² bvfreq.m written by R Pawlowicz to estimate N^2 . This routine computes a best fit over a “smooth” number of consecutive points. Estimates were made every metre, but we chose smooth = 8, thus effectively obtaining values averaged over 4 m; we did this to suppress noise and for compatibility with the ADCP data.

ADCP vertical profiles of horizontal velocity are routinely made on many AZMP surveys. Currents are vertically averaged within the instrument into bins that are typically 4 m in thickness. For AZMP data, the first bin is at 12 m for the instrument used aboard the *Teleost* and 16 m for that on the *Hudson*. The data are also averaged over an ensemble time, generally 5 min (~1.8 km), while the ship steams. The resultant datasets thus comprise a number of ensembles, each with a fixed number of depth bins. The depth range of an ADCP varies with model, but in ocean depths of less than about 350 m, the instrument also measures ship speed relative to the ocean floor (bottom tracking); this allows an absolute estimate of water velocity to be made.

ADCP data are noisy and their quality control (QC) is labour intensive. To avoid QC, we restricted our analysis to those portions of the transects for which the bottom tracking was available. This limits the present analysis to depths less than 350 m and effectively means that the main branch of the Labrador Current is missed. This is unfortunate, and when QC procedures are implemented for data without bottom tracking as part of the PERD-supported DFO project “Vessel Mounted ADCP Currents for the Atlantic Offshore,” the analysis will be extended offshore. It is important to realize, however, that an Ri estimate does not require knowledge of the absolute current, only its vertical shear. Bottom tracking or highly accurate navigation is not required.

Our first QC step was to accept only velocity estimates for which the percent good indicator³ was at least 50%. Our second measure was to use the bottom track record to detect and delete ensembles during which the ship’s heading changed by more than 30°; experience has shown that ship turning often leads to erroneous velocity estimates.

The vertical gradient of current was estimated for each ADCP ensemble by differencing the velocity estimates between adjacent bins. These estimates were then linearly interpolated at each depth onto a 1 km by 4 m grid extending from the coast to the outermost station. N^2 was linearly interpolated onto the same grid, and estimates of Ri were made by simple division.

Some discussion of method is merited, as it is not obvious that N^2 should be interpolated onto a 1 km grid. The mean hydrographic station separation is about 17 km. If N^2 were highly correlated over this scale, one could justifiably interpolate between stations. Although satellite sea-surface temperature (averaged over 13 km x 19 km) exhibits long cor-

relation scales over the continental shelf (> 100 km; Ouellet et al. 2003), it is not clear what scale the vertical derivatives of water properties might have, especially since N^2 is known to be highly variable. High-quality measurements of N^2 from the Sargasso Sea thermocline suggest a correlation scale less than 10 km (Mack and Schoeberlein 2004). This should be an upper limit for the N^2 scale. However, closely spaced estimates of N^2 from the shelf are not available to us, and its

Table 1 Correlation length scales as e-folding lengths in kilometres. Variables are as follows: u , v : components of the horizontal velocity; Σ^2 : squared vertical shear; Ts : continuous temperature record.

Échelles de longueurs de corrélation exprimées comme distances de réponse e en kilomètre. Les variables sont, dans l’ordre : u et v , composantes de vitesse verticale; Σ^2 , cisaille verticale au carré; Ts , les températures enregistrées en continu.

	Apr/avr 2002	Apr/avr 2003	Jul/juil 2002	Jul/juil 2003	Nov/nov 2002	Nov/nov 2003
u	19.0	20.8	14.6	29.5	15.8	12.7
v	14.6	11.1	16.9	15.9	16.4	8.2
Σ^2	2.8	2.2	3.0	3.0	2.2	2.4
Ts	50.0	7.3	6.7	29.8	23.9	15.4

correlation scale cannot be determined. As a poor alternative, we analyzed the continuous temperature record, Ts , made by the ADCP at about 10 m depth. As seen in Table 1, the e-folding length for Ts varies from about 7 to 50 km, with a mean value greater than 20 km. For the ADCP, the mean ensemble length when the ship is steaming between stations was close to 2 km; interpolation onto a 1 km grid

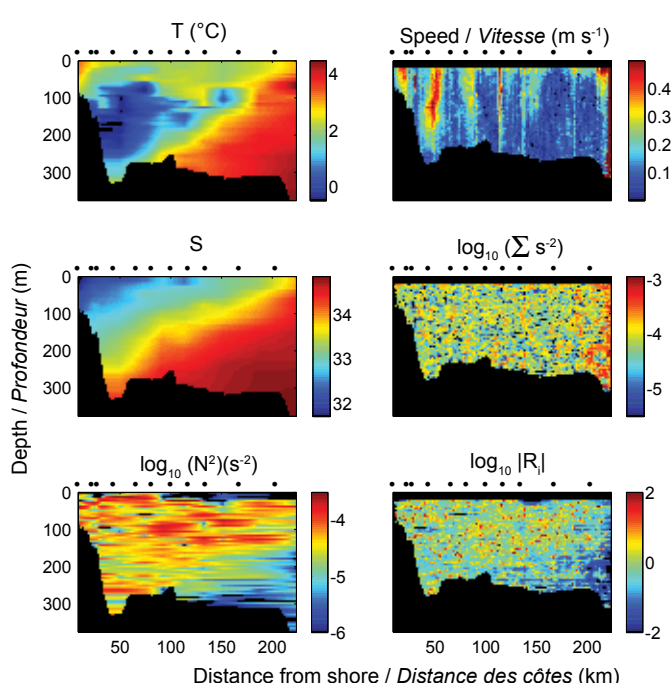


Fig. 1 Results for the November 2003 Bonavista transect. Negative values of N^2 and Ri were blanked and are depicted in black.

Résultats sur le transect de Bonavista en novembre 2003. Les valeurs négatives de N^2 et Ri ont été masquées et sont représentées en noir.

² Available at [ftp://acoustics.whoi.edu/pub/Matlab/oceans/](http://acoustics.whoi.edu/pub/Matlab/oceans/)

³ See <http://www.rdinstruments.com/> for further information about ADCPs used in the AZMP

Table 2 Summary statistics for Ri , N^2 , and Σ^2 . $Q^{1/4}$ and $Q^{3/4}$ are the first and third quartiles, SD is standard deviation. All units are SI.

Résumé des statistiques sur Ri , N^2 et Σ^2 . $Q^{1/4}$ et $Q^{3/4}$ sont le premier et le troisième quartile, SD est l'écart-type. Toutes sont en unité SI.

	Apr/avr 2002	Apr/avr 2003	Jul/juil 2002	Jul/juil 2003	Nov/nov 2002	Nov/nov 2003
Ri	19.0	20.8	14.6	29.5	15.8	12.7
min.	-0.19	-0.01	-0.02	-10.29	-3.31	-0.82
max.	>1000	>1000	>1000	>1000	>1000	>1000
med.	0.94	1.06	0.38	1.51	0.36	0.57
SD	>100	>100	>100	>100	>100	>100
$Q^{1/4}$	0.17	0.30	0.08	0.36	0.13	0.24
$Q^{3/4}$	3.25	3.09	2.09	4.93	1.03	1.46
$N^2 \times 10^4$						
min.	-0.06	-0.01	-0.15	-0.49	-0.03	-0.19
max.	2.73	2.87	15.00	12.00	5.25	8.01
med.	0.24	0.21	0.29	0.34	0.27	0.37
SD	0.28	0.27	1.53	1.34	0.39	0.47
$Q^{1/4}$	0.13	0.11	0.17	0.20	0.12	0.18
$Q^{3/4}$	0.41	0.40	0.53	0.57	0.48	0.61
$\Sigma^2 \times 10^4$						
min.	0.000	0.000	0.000	0.000	0.000	0.000
max.	124.0	19.0	294.0	42.0	13.0	11.0
med.	0.25	0.20	0.75	0.29	0.77	0.70
SD	5.85	1.08	13.00	2.15	0.85	0.91
$Q^{1/4}$	0.09	0.05	0.20	0.11	0.32	0.30
$Q^{3/4}$	1.10	0.81	2.88	0.86	1.37	1.24

is thus somewhat ambitious. ADCP velocities exhibit length scales of 10–30 km, while Σ^2 has scales in the range of 5 to more than 30 km.

Results and Discussion

The purpose here is to present examples of N^2 and Ri so that their potential utility can be evaluated. Figure 1 shows the work-up to the actual data products for the November 2003 transect. Temperature and salinity are distributed as one would expect: both T and S tend to increase with distance offshore, and a cold intermediate layer is apparent. N^2 , Σ^2 , and Ri all exhibited large dynamic ranges and skewed distributions (Table 2) and are shown here on a logarithmic scale. N^2 shows distinct areas of high and low values, although the horizontal extent of the layers is partially an artefact of the linear interpolation at each depth. Near-surface stability decreases offshore as does the depth of maximum N^2 .

The currents also display a typical, somewhat columnar pattern of stronger and weaker speeds. Note the sharp increase in speed at the offshore edge of the transect, indicative of the offshore branch of the Labrador Current. Σ^2 and Ri are both patchy, and the former could be characterized as string-like. Like current speed, Σ^2 is largest near the offshore Labrador Current.

The patchy nature of Ri suggests that it should be smoothed or classified in order to generate a useful product. We classified Ri into four ranges: unstable for $Ri < 0$, potentially unstable for $0 \leq Ri < 0.25$, stable for $0.25 \leq Ri < 1$, and very stable for $Ri \geq 1$. As discussed later, these intervals might not be the best choice. However, in this format (Fig. 2), distinct patterns are revealed, and there are similarities and differences between years and seasons. Focusing first on interannual comparisons, we see that spring 2002 and 2003 are almost equivalent over the section where they overlap. The same is true for the autumn transects.

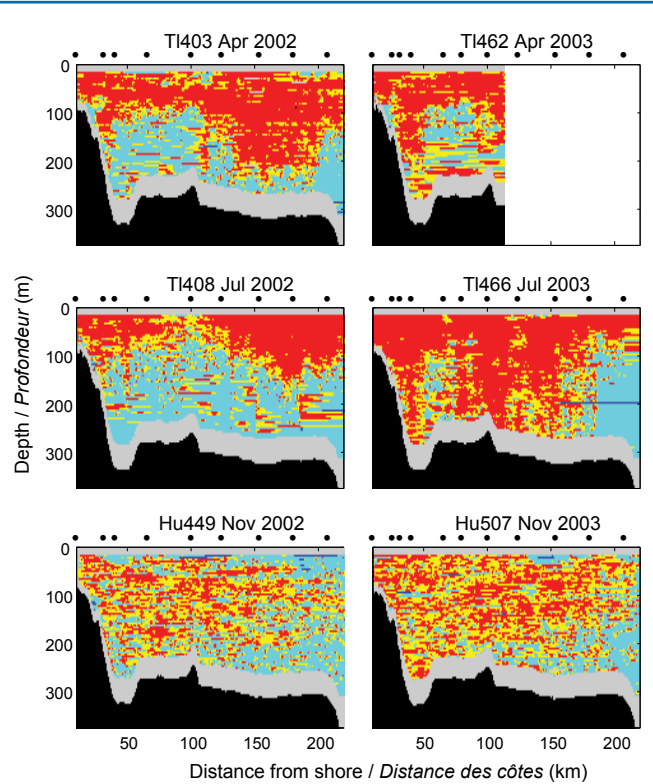


Fig. 2 Vertical cross sections of Ri on the Bonavista transect. Ri was classified into the following segments: unstable ($Ri < 0$, dark blue), potentially unstable ($0 \leq Ri < 0.25$, light blue), stable ($0.25 \leq Ri < 1$, yellow), and very stable ($Ri \geq 1$, red). Black denotes the bottom and the grey zone indicates segments of the water column not sampled by the ADCP.

Sections verticales de Ri sur le transect de Bonavista. Les valeurs ont été classées en différentes catégories : instable ($Ri < 0$, bleu foncé), potentiellement instable ($0 \leq Ri < 0.25$, bleu pâle), stable ($0.25 \leq Ri < 1$, jaune) et très stable ($Ri \geq 1$, rouge). Le fond est en noir et les zones grises indiquent les segments de la colonne d'eau non échantillonnés par l'ADCP.

In contrast, summer 2003 is much more stable over most of the water column than summer 2002. In terms of a seasonal progression, spring and summer are similar, although summer 2003 displays higher stability than summer 2002. By autumn, however, one can see a dramatic lessening of stability over the full water column. In all the transects, there is a region of lower stability at depth over the shelf break.

Except for a few phenomena, we tend to think in terms of time and not frequency. Consequently, we chose to display N as its inverse, the buoyancy period $T_b = 2\pi/N$. Again there are clear similarities between years (Fig. 3), and differences between seasons are most pronounced near the surface, as would be expected. Overlaid on each figure is the depth of maximum

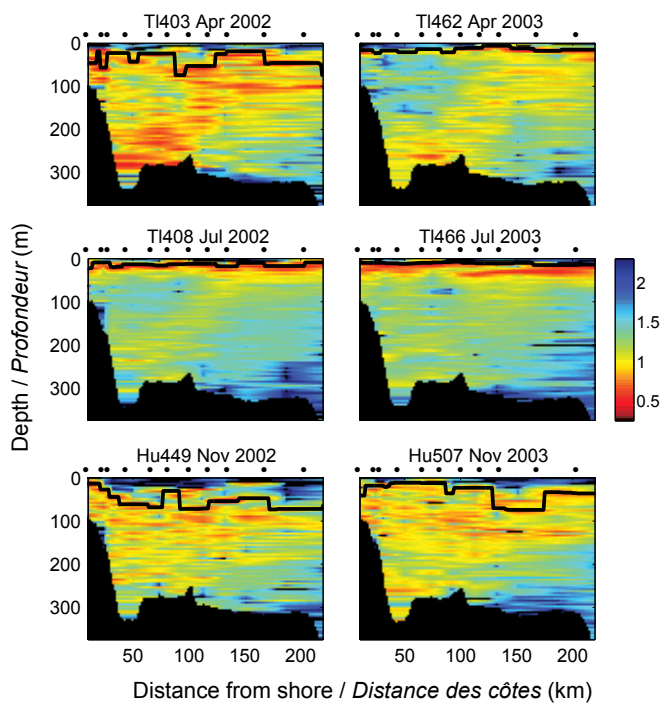


Fig. 3 Vertical cross sections of \log_{10} (Tb) (in minutes) on the Bonavista transect. Imaginary values of Tb (corresponding to negative N^2) were blanked and are depicted in black. The heavy black line denotes the depth of maximum N^2 in the upper water column.

Sections verticales du \log_{10} de Tb (en minutes) sur le transect de Bonavista. Les valeurs imaginaires de Tb (les valeurs négatives de N^2) sont masquées et apparaissent en noir. La ligne noire épaisse démarque la profondeur maximale de N^2 dans la partie supérieure de la colonne d'eau.

N in the upper 75 m, which is a measure of the mixed layer depth. Its step-like character is partly due to the fact that the depth profile of N often has multiple maxima and partly due to the linear interpolation scheme. This estimate is essentially equivalent to a maximum density gradient calculation.

Conclusions and Recommendations

Vertical sections of the buoyancy period and the Richardson number were calculated for three seasons and two years; they show marked seasonal variation and considerable similarity between years. This suggests that such estimates are meaningful and could form the basis for standard AZMP data products. However, the question of their utility has yet to be answered. Two obvious steps need to be taken. First, the Richardson number computation should be geographically extended to deeper waters for which ADCP bottom tracking is not available. Second, more sections need to be generated to see if they reveal significant interannual variations.

In addition, the choice of classification scheme for Ri needs further study. Field estimates of the critical Richardson number suggest that the value of 0.25 is not universal (e.g., Mack and Schoeberlein 2004). Moreover, the data collected on AZMP cruises are relatively crude compared with research-grade measurements made in turbulence studies. Our estimates, averaged over 4 m and 5 min, may underestimate the real Richardson number. This would also affect the choice of classification. Finite differences always underestimate actual

derivatives, so both the numerator and denominator in Eq. 1b are underestimated. Since N^2 is computed on a finer grid, its error should be smaller than the error in Σ^2 . Therefore their ratio should be smaller than the true value. On the other hand, the ADCP signal contains a proportionately larger noise contribution than does the CTD signal, and this probably biases Ri estimates towards smaller values. The turbulence community should be consulted on this issue.

It is also clear that the computations and display could be improved, but that is not the point here. As stated in the introduction, the primary goal is to stimulate a discussion of the utility of these two data products.

It would, however, seem appropriate to routinely compute vertical sections of N^2 (or Tb) as a measure of static stability because they provide information over the full water column. This differentiates sections of N^2 from the commonly used stratification index or mixed layer depth. In theory, the Richardson number should give an even more meaningful measure of vertical stability because it includes the effect of current shear. However, our experience with field estimates of Ri, including those from research studies made at fixed locations, is small. Moreover, Ri varies with time, especially in the upper ocean where the wind episodically drives strong currents (e.g., Greenan et al. 2004, 2008). More examples of Ri sections are required to build our knowledge of it and to allow us to judge its value.

Acknowledgements

We thank the editors and an anonymous reviewer for their constructive comments that led to a much improved manuscript.

References

- Colbourne, E., Fitzpatrick, C., Senciali, D., and Stead, P. 2007. Oceanographic observations from trawl-mounted CTDs on multi-species surveys in the Newfoundland and Labrador Region. AZMP Bulletin PMZA 6: 43–47.
- Craig, J., and Gilbert, D. 2008. Estimation of mixed layer depth at the AZMP fixed stations. AZMP Bulletin PMZA 7: 37–42.
- Gargett, A., and Marra, J. 2002. Effects of upper ocean physical processes (turbulence, advection and air-sea interaction) on oceanic primary production. In *The Sea, Volume 12. Biological-physical interactions in the sea*. Edited by A.R. Robinson, J.J. McCarthy and B.J. Rothschild. John Wiley and Sons, New York. pp. 19–49.
- Greenan, B.J.W., Petrie, B.D., Harrison, W.G., and Oakey, N.S. 2004. Are the spring and fall blooms on the Scotian Shelf related to short-term physical events? Cont. Shelf Res. 24: 603–625.
- Greenan, B.J.W., Petrie, B.D., Harrison, W.G., and Strain, P.M. 2008. The onset and evolution of a spring bloom on the Scotian Shelf. Limnol. Oceanogr., 53: 1759–1775.
- Kundu, P.K. 1990. Fluid Mechanics. Academic Press, San Diego, CA.
- Mack, S.A., and Schoeberlein, H.C. 2004. Richardson number and ocean mixing: Towed chain observations. J. Phys. Oceanogr. 34: 736–754.
- Ouellet, M., Petrie, B., and Chassé, J. 2003. Temporal and spatial scales of sea-surface temperature variability in Canadian Atlantic waters. Can. Tech. Rep. Hydrogr. Ocean Sci. No. 228: v + 30 pp.
- Thorpe, S.A. 2005. The turbulent ocean. Cambridge University Press, Cambridge.

Currents and Temperature Variability From Moored Measurements on the Outer Halifax Line in 2000–2004

John W. Loder and Yuri Geshelin

Bedford Institute of Oceanography, Box 1006, Dartmouth, NS, B2Y 4A2
john.loder@mar.dfo-mpo.gc.ca

Sommaire

La variabilité des courants océaniques et de la température sur le plateau Néo-Écossais entre l'été 2000 et le printemps de 2004 est décrite en utilisant les observations d'un programme de mesures par instruments ancrés, complétées par différentes bases de données disponibles grâce au Programme de monitorage de la zone Atlantique. Les instruments ont été déployés à trois sites à la limite extérieure du transect Halifax (HL), à des profondeurs de 300, 1100 et de 2000 m. Une attention particulière est donnée à la variabilité saisonnière et de basse fréquence en utilisant les moyennes saisonnières des données fixes. Contrairement aux données des températures de la surface de la mer dominées par un cycle saisonnier très marqué, il y a peu d'indications d'un cycle saisonnier des températures sous la surface (sous les 80 m). Par contre, il y a des indications de la présence d'un cycle saisonnier dans l'écoulement le long du plateau. Cependant, l'interprétation d'une variabilité durant la période d'ancrage des instruments est confondue avec une interruption de l'écoulement équatorial de la masse d'eau subpolaire au printemps et à l'été 2002 et, également, à l'été et l'automne 2003, en raison de l'intrusion d'une masse d'eau chaude de la pente associée aux méandres du Gulf Stream. Pour la période de l'automne 2001 au printemps 2004, le transport moyen net le long du plateau entre les isobathes de 150 et 2300 m est évalué à 2,1 Sv vers le sud-ouest, avec un maximum saisonnier de 3,5 Sv en hiver et un minimum de 0,1 Sv en été. Toutefois, la représentativité à long terme du transport moyen pour le printemps et l'été est incertaine en raison des deux interruptions survenues sous l'influence du Gulf Stream. Des cartes bimensuelles des températures de la surface de la mer, des données hydrographiques saisonnières à HL et les indices de la position du front pente/plateau sont utilisés afin de compléter la description de la structure spatiale et temporelle et l'origine de la variabilité observée.

Introduction

It is well known that multiple large-scale factors contribute to the oceanographic variability of the Scotian Shelf, Gulf of Maine, and adjacent slope areas. These areas are located in the downstream tail of the western boundary current of the North Atlantic's subpolar gyre (e.g., Loder et al. 1998), and it has been shown that variable transport of the Labrador Current around the Tail of the Grand Bank can result in large changes in their temperature and salinity (Petrie and Drinkwater 1993). On the other hand, these areas are within reach of rings and eddies shed from the meandering Gulf Stream, which carries water of subtropical origin northeastward across the Atlantic (Smith and Petrie 1982). Oceanographic variability in the region is further complicated by the seasonally varying influences of solar radiation, atmospheric conditions in the lee of the North American continent, and run-off and outflow from the Gulf of St. Lawrence. These factors result in pronounced variability that makes a systematic long-term observation program like the Atlantic Zone Monitoring Program (AZMP) of paramount importance to our understanding of climate and ecosystem issues.

AZMP and earlier hydrographic observation programs have now provided multi-decadal time series of variability on representative sections across the Atlantic Canadian shelf and slope, while multi-year research programs have provided moored measurement time series that fully resolve temporal variability at a few local sites in the region. Some of these moored measurement sites have been located on the long-term monitoring sections, but in general this is not the case. On the Halifax Line (HL), which is the Scotian Shelf monitoring section with the longest record, there have been moored measurements across the Nova Scotian Current on the inner shelf (e.g., Anderson and Smith 1989) that have revealed significant variability associated with atmospheric forcing and a

frontal/upwelling system. However, prior to 2000, there had been no moored measurements on the section over the shelf edge and continental slope, where the shelf/slope front and the Labrador Current extension—the primary conduit for the equatorward transport of subpolar water—are located. This gap has been problematic when the objective is to provide a good quantitative description and understanding of oceano-

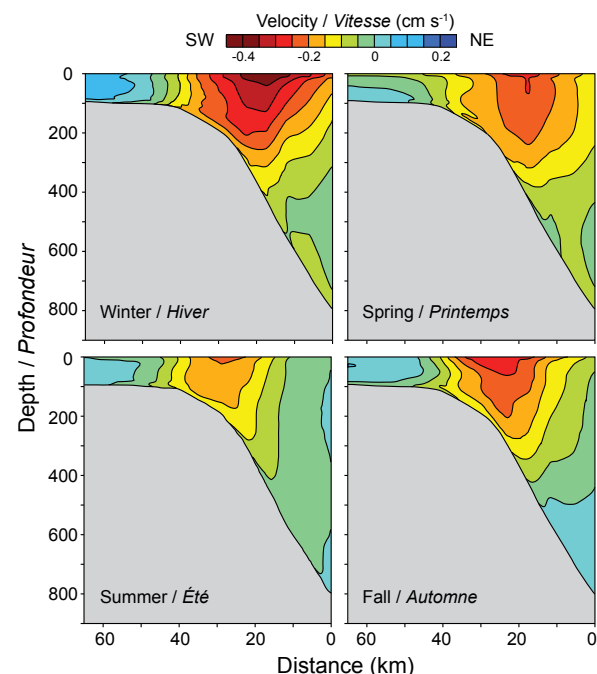


Fig. 1 Along-shelf flow (positive northeasterward) on the outer HL from the seasonal-mean circulation fields obtained by Hannah et al. (2001) (courtesy of C. Hannah).

Écoulement le long du plateau (positif vers le nord-est) à la limite extérieure du transect HL, tiré des champs de circulation saisonniers moyens de Hannah et al (2001) (courtoisie de C. Hannah).

graphic variability in the region, such as in estimations of interannual variability in the southwestward flow of subpolar water (e.g., Loder et al. 2003) or in numerical model diagnoses of the three-dimensional seasonal-mean circulation in the region (e.g., Hannah et al. 2001).

During the early 2000s, there was an increasing interest in petroleum exploration on the Scotian Slope in waters deeper (>500 m) than those of earlier surveys. With funding from the federal Program on Energy Research and Development (PERD) and several petroleum companies, BIO's Ocean Sciences Division carried out a multi-year moored current and hydrographic measurement program on the outer HL from 2000 to 2004. The HL was chosen because of its extensive archived hydrographic dataset and as a representative section across the central Scotian Slope. Here, we provide a brief overview of the temperature and current variability from the moored measurements, with a focus on seasonal and interannual variability.

The paradigm for circulation in the Scotian Shelf/Slope region has been that, averaged over weather-band variability (~2–10 d variability in this region), there is substantial persistence of current pathways along the shelf edge and inner shelf, with strong topographic steering around banks and basins and episodic disruptions from Gulf Stream influences over the slope. For the outer HL, a circulation model (Hannah et al. 2001) has suggested a seasonally varying, surface-intensified southwestward flow along the shelf edge centred near the 300 m isobath (Fig. 1), with much weaker flow in deeper water.

Methods

Moored measurements were made at three sites on the upper-middle continental slope of the HL and in close proximity to HL stations 5–7 (Fig. 2) starting in June 2000 with a single mooring at a central site (denoted A) with water depth of 1100 m near station HL6. In June 2001, a mooring was

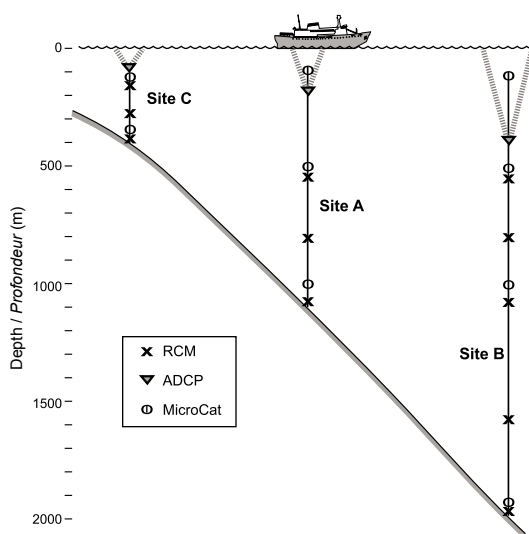


Fig. 2 Schematic representation of the 2001–2002 mooring array. After the staggered initial deployments at each site, a mooring array similar to this was maintained until April 2004.

Schéma représentant les lignes d'instruments ancrés en 2001–2002. Après les déploiements initiaux décalés à chaque site, une ligne d'instruments comme celle illustrée a été maintenue jusqu'en avril 2004.

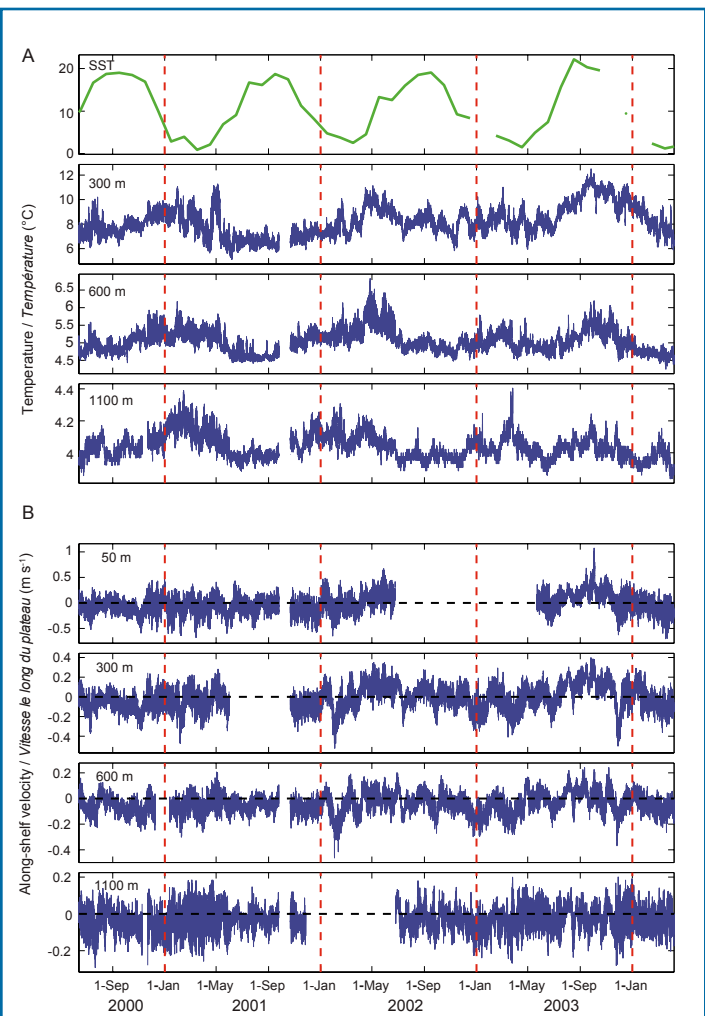


Fig. 3 Merged time series of (A) temperature at three depths and (B) along-shelf velocity (positive northeastward) at four depths from hourly moored measurements over four years at the central mooring site A. Monthly mean SST (green) from the Pathfinder satellite dataset (courtesy of B. Petrie) is included in the top panel of (A). Note the different temperature and velocity scales at each depth. Red-dotted vertical lines indicate 1 January of each year.

Combinaison des séries temporelles de (A) températures à trois profondeurs et (B) de la vitesse le long du plateau (positive vers le nord-est) à quatre profondeurs tirées des données boraires mesurées aux instruments ancrés pendant quatre années au site central A. Les moyennes mensuelles de températures de la surface de la mer (ligne verte) tirées de la base de données du satellite Pathfinder (courtoisie de B. Petrie) sont présentées dans le tableau du haut, en (A). Noter les différentes échelles pour la température et la vitesse selon la profondeur. Les lignes verticales rouges marquent le 1er janvier de chaque année.

deployed at a second site (denoted B), with water depth of 2000 m, approximately halfway between stations HL6 and HL7. Then in October 2001, a third mooring (denoted C) was deployed on the 300 m isobath (expected centre of the shelf-edge jet shown in Fig. 1), approximately one-third of the way from HL6 to HL5. Moorings were redeployed at these sites at 6–12 month intervals until April 2004, when the field phase of the project was completed. The typical mooring configuration at each site was an upward-looking Acoustic Doppler Current Profiler (ADCP) at 75–150 m with a Sea-Bird MicroCAT (MC) temperature-salinity recorder near or above the ADCP, and Aanderaa current meters (RCM8s) and MCs spaced at 200–500 m intervals below, down to an RCM8 at 25 m above bottom. To protect the site C moorings from fish-

ing activity, three guard buoys were maintained around it. Fifteen of the seventeen deployed moorings were recovered as planned, while the other two were apparently struck by vessels and recovered prematurely. The program provided time series of 46-, 33- and 30-month durations at sites A, B, and C, with some data gaps due to the aborted moorings and instrument failures (or limitations).

Results From the Moored Measurements

The data return, temporal variability, and vertical structure at the central mooring site (A) are illustrated by time-series plots of hourly temperature and along-shelf velocity at selected depths (Fig. 3). A time series of monthly mean SST (from satellite data) is included for comparison, showing the strong upper-ocean seasonal cycle that is common in mid latitudes. There is variability in the subsurface temperature and currents on a range of time scales, from high-frequency fluctuations associated with tides and winds, to events and wave-like variations of weeks to months, to seasonal and interannual changes. Although the range (magnitude) of variability varies strongly with depth for both temperature (especially) and currents, there is similarity in the relative magnitudes of the fluctuations on different time scales at the various depths shown. This suggests that seasonal snapshots of the hydrographic structure have the potential for indicating spurious low-frequency variations because of aliasing of the higher-frequency variability (e.g., Mann and Needler 1967).

The higher-frequency variability will not be discussed further, but it should be noted that most of the lower-frequency changes discussed below also have associated variability on shorter time scales. For example, the above-average temperatures observed at 300 and 600 m in spring 2002 and summer-fall 2003 were associated with some relatively abrupt changes. Many of the temperature and velocity fluctuations on time scales of days to seasons are coherent over much of the water column, but there is also variability that is more restricted to the shallow, mid-depth, or deeper layers.

In order to focus on seasonal and interannual variability, we provide the seasonal-mean values of temperature and along-shelf velocity in Figures 4 and 5 for selected depths at the three mooring sites. At the depths shown (85 m and deeper), there is little indication of a seasonal cycle (1-y period) in subsurface temperature like that which dominates the SST variability. Note, however, that there are limited multi-year data in the upper 80 m from this program, and the data at site C are limited in duration. There is some suggestion of a seasonal cycle in along-shelf velocity between summer 2000 and winter 2003 at sites A and C, with the strongest southwestward (henceforth SWward) flow in fall or winter. This shows some similarity to the seasonal variation in the model fields, but not in any detail.

The variability of both the temperature and along-shelf velocity between spring 2002 and spring 2004 was dominated by two major events whose influence persisted longer than a single season. In both spring-summer 2002 and summer-fall 2003, there were pronounced increases in temperature (Fig. 4) and northeastward (henceforth NEward) flow (Fig. 5) anomalies at depths shallower than 600 m at all three sites.

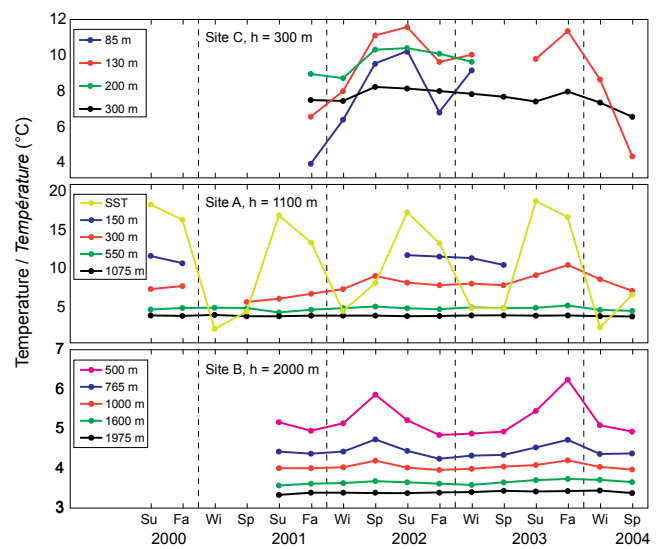


Fig. 4 Time series of seasonal-mean temperature at selected depths at the three mooring sites. SST from satellite data is included in the middle panel. Seasons (three-month periods) are abbreviated as summer (Su, 15 June to 15 September), fall (Fa), winter (Wi), and spring (Sp).

Séries temporelles de la moyenne saisonnière des températures à des profondeurs sélectionnées aux trois sites d'instruments ancrés. Les températures de la surface de la mer des données du satellite sont présentées dans le panneau du milieu. Les saisons (des périodes de trois mois) sont identifiées par les abréviations Su (été, du 15 juin au 15 septembre), Fa (automne), Wi (hiver) et Sp (printemps).

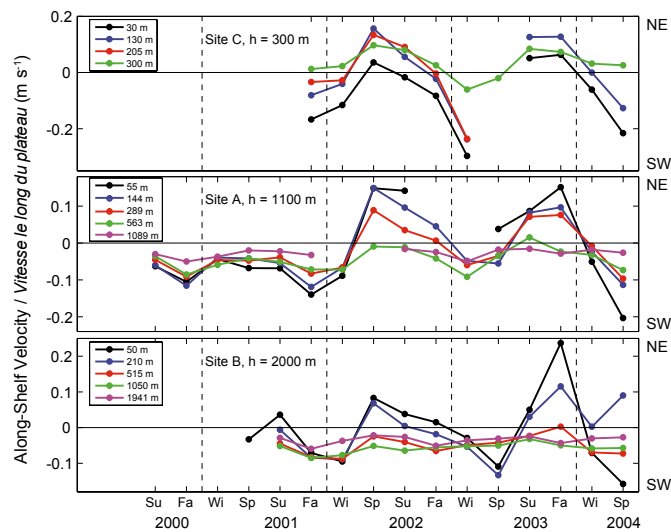


Fig. 5 Time series of seasonal-mean along-shelf velocity (positive NEward) at selected depths at the three mooring sites.

Séries temporelles de la moyenne saisonnière de la vitesse positif vers le nord-est à des profondeurs sélectionnées aux trois sites d'instruments ancrés.

These were associated with the presence of anomalously warm slope water on the outer HL that was related to meso-scale variability in the Gulf Stream and slope water. In spring 2002, the anomalously warm water extended below 1000 m at the offshore site B; flow in the upper 300 m at all three sites was directed NEward, and there was reduced SWward flow at all other depths at the mooring sites. The anomalous conditions persisted into summer at most positions (although

the warmer water and reduced SWward flow may have been partly related to the seasonal cycle seen in the SST and/or one in the Labrador Current extension). Starting in late summer and peaking in the fall of 2003, there was a somewhat similar occurrence of anomalously warm water and increased NEward (or reduced SWward) flow at all three sites, with magnitudes at the offshore site (B) exceeding those of the spring 2002 anomalies. A remarkable aspect of these events from a circulation perspective is that the equatorward flow of subpolar water was shut down in the upper 300 m or so over the Scotian Slope (from seaward of the 2000 m isobath to shoreward of the 300 m isobath) for a period of 4–5 months in successive years, and was fairly weak at depths down to at least 600 m during these periods.

The moored measurements can be used to provide estimates of the along-shelf transports on the outer HL, either for particular water masses or for particular areas. Figure 6 shows the seasonal-mean transports for each mooring site and for combinations of the sites. The currents at each position are assumed to represent a vertical and horizontal interval encompassing the position, extending a total distance of 49 km from the 150 m isobath at the shelf edge to the 2300 m isobath.

The magnitude of the depth-integrated transport at each site (Fig. 6) generally increases in the offshore direction, as might be expected from the increasing water depths (but not from model results in Fig. 1). The temporal variability is heavily influenced by the warm slope water disruptions of the SWward flow in spring-summer 2002 and summer-fall 2003. During these periods, the depth-integrated transports at sites A and C were NEward and that at site B was less than 1 Sv SWward. As a result, there was a net NEward transport of about 1 Sv across the mooring section in both spring 2002 and summer-fall 2003, which is opposite to the conventional

climatology of equatorward flow of waters of subpolar origin over the Scotian Slope. This is not the first observation of a net NEward transport on the Scotian Slope: the mean transport of “shelf” water (taken as having salinity < 34.8) was found to be 0.05 Sv NEward during the 1975–1978 Shelf Break Observation Program (Smith and Petrie 1982, Loder et al. 1998). It is clear that variability in the Gulf Stream system can have large influences on the equatorward transport of subpolar water along the Scotian Slope.

On the other hand, the moored measurements also indicate that, when there are not large disruptions from Gulf Stream influences, there is a tendency towards a seasonal cycle in the transport of subpolar water along the Scotian Slope, as inferred from the climatological hydrography (Hannah et al. 2001, Loder et al. 2001). There is a clear suggestion in Figure 5 of increased SWward flow at all depths at site A in the falls of 2000 and 2001. The transports at each mooring site as well as the net transports across the section during 2001–2002, 2002–2003, and 2003–2004 (Fig. 6) had annual maxima in fall, winter, or spring, with peak seasonal-mean net transports of 4.2, 4.3, and 3.1 Sv in these years, respectively. Sites A and B were the primary contributors to these seasonal maxima in the SWward flow, with an additional small contribution from site C.

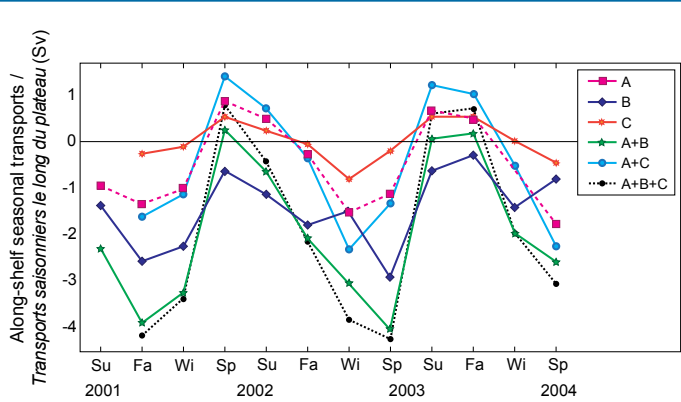


Fig. 6 Seasonal-mean net along-shelf transports (positive NEward) at each of the mooring sites and for combinations of the sites. Transports are given in units of Sverdrups ($1 \text{ Sv} = 1 \times 10^6 \text{ m}^3 \text{ s}^{-1}$). It has been assumed that mooring sites A, B, and C are representative of adjoining cross-slope intervals between the 150 m and 2300 m isobaths, with magnitudes of 19, 16, and 14 km, respectively.

Moyenne saisonnière du transport net le long du plateau (positif vers le nord-est) à chaque site d'instruments ancrés et pour une combinaison de sites. Le transport est présenté en unités Sverdrups ($1 \text{ Sv} = 1 \times 10^6 \text{ m}^3 \text{ s}^{-1}$). On assume que les sites A, B et C sont représentatifs de sections adjacentes de la pente entre les isobathes de 150 et 2300 m de l'ordre de 19, 16 et 14 km, respectivement.

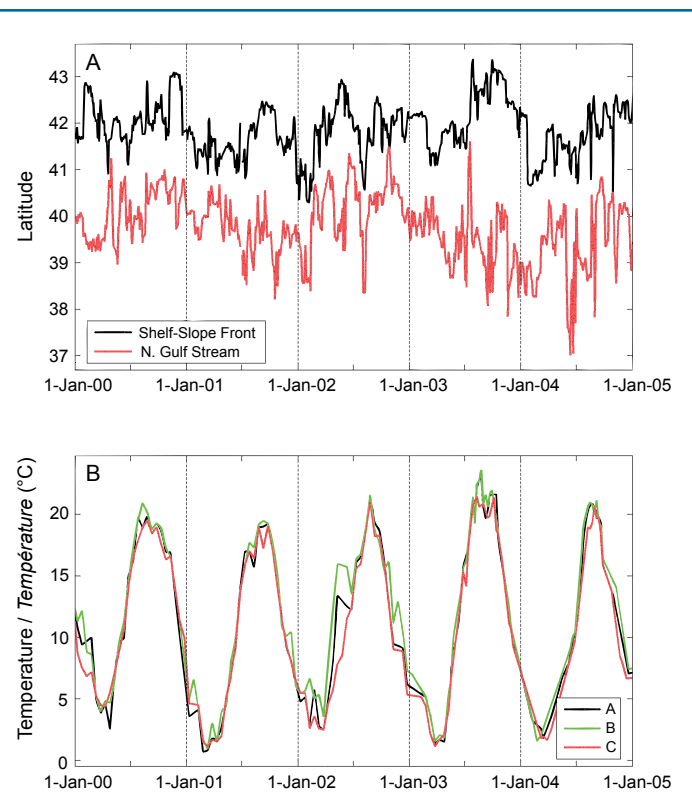


Fig. 7 Time series of (A) the latitude of the shelf-slope front and the north wall of the Gulf Stream at the longitude of the outer HL (courtesy of R. Pettipas), and (B) SST at the mooring sites from satellite AVHRR (Advanced Very High Resolution Radiometer) data (courtesy of B. Petrie).

Séries temporelles de (A) la latitude du front plateau/pente et du flanc nord du Gulf Stream à la longitude de la limite extérieure de HL (courtoisie de R. Pettipas), et (B) températures de la surface de la mer aux sites d'instruments ancrés tirées des données AVHRR (Advanced Very High Resolution Radiometer) du satellite (courtoisie de B. Petrie).

Averaged over the period from fall 2001 to spring 2004, the net transport across the section was 2.1 Sv SWward, with a maximum seasonal mean of 3.5 Sv in winter and a minimum of 0.1 Sv (also SWward) in summer. The transports for sites A and C only, which represent a more comparable (though still larger) domain to that in previous climatological studies, had an annual mean of 0.7 Sv (SWward), a winter maximum of 1.3 Sv, and summer minimum of 0.2 Sv (NEward). These values are only 20%-50% of the annual mean (1.8 Sv), winter maximum (2.5 Sv), and summer minimum (1.0 Sv) estimated by Hannah et al. 2001. Part of this discrepancy may be that there was SWward flow farther up the slope at the shelf edge that was missed by the 2000–2004 moored measurements. It also appears that there must be one or more other important factors, such as the 2002 and 2003 slope water disruptions and/or decadal-scale variability (Loder et al. 2001), that make the 2001–2004 transport estimates low relative to the long-term mean. Collectively, the recent moored measurements and the earlier climatological estimates indicate that the actual long-term mean equatorward transport of subpolar water over the Scotian Slope is greater than the 2 Sv estimated from the 2000–2004 moored measurements.

Interpretations Using AZMP Data

Data and products from the AZMP help substantially with the interpretation of the variability in the moored measurements. The AZMP time series of the latitudes of the shelf-slope front and the north wall of the Gulf Stream at the longitude of the outer HL (Fig. 7A) as well as the satellite SST time series for mooring sites (Fig. 7B) provide hints as to the origin of the warm-water disruptions in spring-

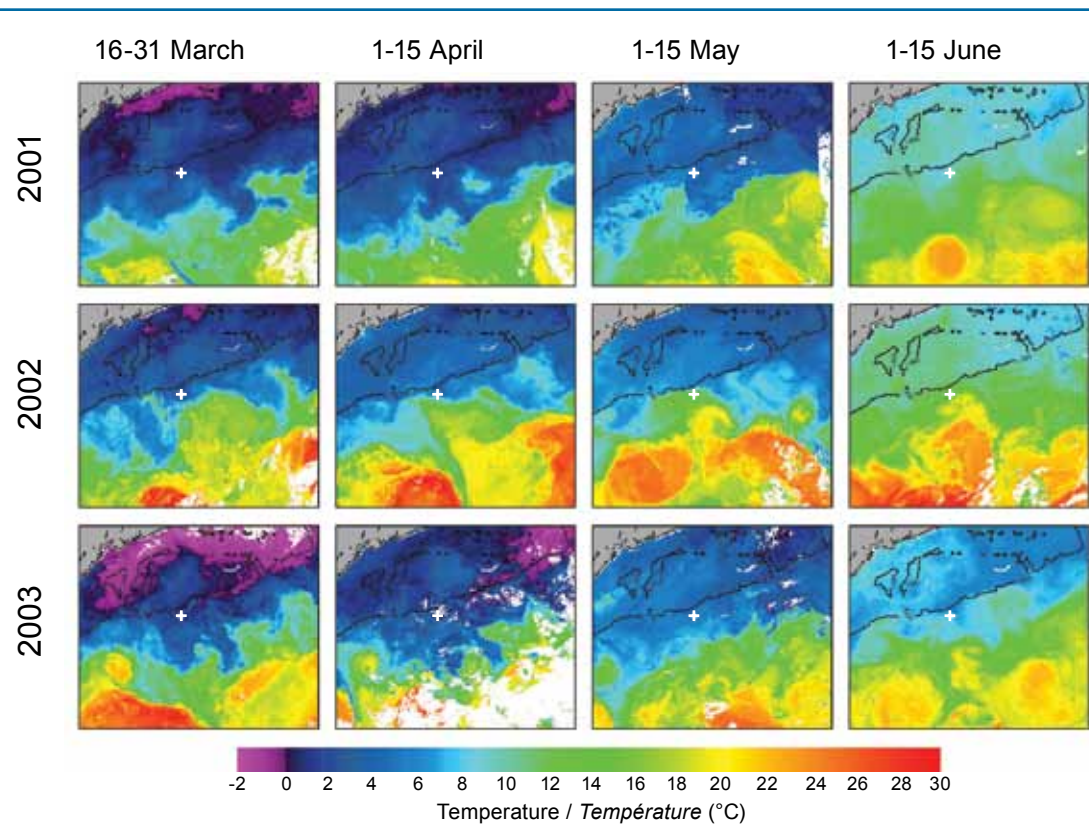


Fig. 8 Composite SST maps for four two-week periods in the springs of 2001, 2002, and 2003 derived from AVHRR data from the AZMP. The Nova Scotia coast is in the upper left corner, the black lines are the 200 m isobath, and a white "+" sign indicates the mooring area (courtesy of C. Caverhill).

Cartes composites des températures de la surface de la mer pour quatre périodes bimensuelles au printemps de 2001, 2002 et 2003, obtenues des données AVHRR du PMZA. La côte de la Nouvelle-Écosse apparaît au coin supérieur gauche, les lignes noires indiquent l'isobathe de 200 m et les symboles + blancs indiquent les sites des mesures d'instruments ancrés (courtoisie de C. Caverhill).

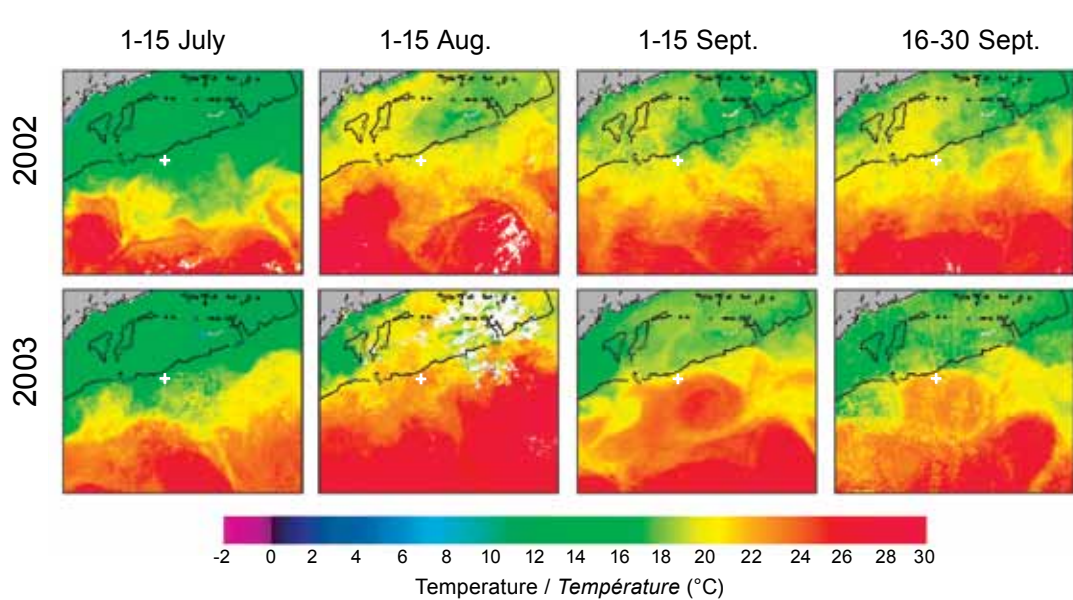


Fig. 9 SST maps like those in Figure 8, but showing four two-week periods in the summers and early falls of 2002 and 2003.

Cartes des températures de la surface de la mer semblables à celles de la figure 8, mais pour quatre périodes bimensuelles à l'été et au début de l'automne en 2002 et 2003.

summer 2002 and summer-fall 2003. During summer-fall 2003, the shelf-slope front extended (and persisted) farther northward than at any other time during the five-year period displayed, and during spring-summer 2002, it was also dis-

placed northward (although not much more than average). There were northward displacements of the Gulf Stream during these periods that may have contributed to those of the shelf-slope front, but they were of shorter duration than the frontal displacements (probably due to Gulf Stream rings drifting by, rather than persisting at, the longitude of the outer HL).

The SST indices (Fig. 7B) also show the warm anomalies, superimposed on the dominant annual cycle. In spring-summer 2002, there was a period of earlier-than-usual warming at sites A and B, which was more pronounced at the offshore site B. In the late summer and early fall of 2003, there was warmer surface water at all three mooring sites than at any other time during the five-year period shown, including extreme anomalies at the offshore sites A and B. It is noteworthy that this is the period when Hurricane Juan reached Atlantic Canada, which has been in part attributed to warmer-than-usual surface temperatures over the Scotian Slope and Shelf (Fogarty et al. 2006).

Satellite SST imagery can provide remarkable information on the spatial structure of upper-ocean features in frontal zones such as the subpolar-subtropical confluence zone off Atlantic Canada. Figure 8 shows two-week composite images of SST for four periods during the springs of 2001, 2002, and 2003, when broad-scale seasonal warming was occurring. Prior to the onset of the near-surface stratification in May-June, it can be seen that cold subpolar waters bathed the Scotian Shelf and Slope each year. Mesoscale intrusions of relatively warm water varied from year to year, linked to Gulf Stream meanders and rings and related frontal features. The relatively warm waters did not reach the mooring area (denoted by a "+" sign in each image) in the springs of 2001 and 2003, when the Scotian Slope remained dominated by subpolar water, but did reach the area in the spring of 2002, as Gulf Stream meanders west and east of the outer HL's longitude (the red features in the March and April images) evolved into rings that severely distorted the shelf-slope front. In particular, it appears that the clockwise flow in the meander/eddy to the southeast of the outer HL resulted in warm slope water (green) on its western side being pushed or entrained shelfward into the mooring area, with a clockwise (locally NEward) flow that is consistent with the disruption of the SWward flow observed at the mooring sites.

Similar SST imagery for the summers and early falls of 2002 and 2003 (Fig. 9) indicates that the warm water disruption at the mooring sites in summer-fall 2003 was associated with Gulf Stream meanders towards the shelf in August and a warm-core Gulf Stream ring that reached the mooring area in September. The NEward flow in the upper 300 m at all three sites (Fig. 5) resulted from the moorings being in the outer (northern) part of the clockwise flow of the ring near the shelf edge. The images for the corresponding summer-fall periods in 2002 indicate that the meander/eddy that was influencing the mooring area in the spring (Fig. 8) had moved westward by summer and relatively cool water was reappearing on the outer HL by September, consistent with the moored measurements.

Complementary information on the vertical and cross-slope structure of the water masses is provided by the hydrographic observations from the AZMP seasonal surveys of HL. Figure 10 contrasts the temperature distributions over the slope from the spring (May), summer (June-July), and fall (October) surveys in 2001, 2002, and 2003. Besides the seasonal near-surface warming, relatively warm water generally appears as a 200–400 m thick layer extending from offshore towards the shelf, centred at about 200 m below the surface. In most cases, this layer has the temperature-salinity (T, S) characteristics of "Warm Slope Water (WSW)" (Gatien 1976), which typically overlies the colder "Labrador Slope Water (LSW)" of

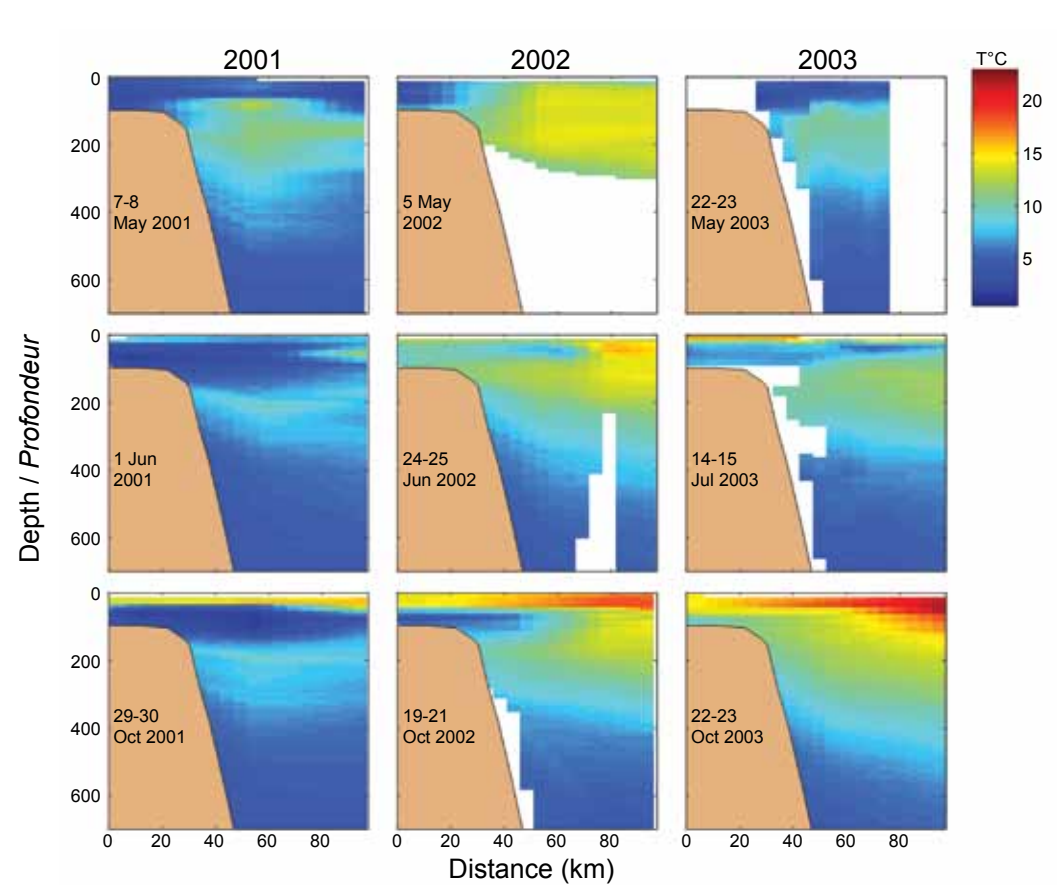


Fig. 10 Temperature (°C) in the upper 700 m on the outer HL from the spring, summer, and fall AZMP surveys in 2001, 2002, and 2003.

Température (°C) sur les 700 m supérieurs à la limite extérieure de HL pour les levés de printemps, d'été et d'automne en 2001, 2002 et 2003.

a predominantly subpolar origin. During periods of increased transport of LSW into the region over the slope, the WSW may not reach the shelf edge (e.g., Loder et al. 2003).

The HL survey data (Fig. 10) indicate that WSW extended northward to the shelf edge during the spring–fall of all four years of the moored measurement program, suggesting that they were not years of exceptional inflow of subpolar water (also supported by the moored temperature measurements). The data confirm that the peak springtime amount of WSW over the HL upper slope occurred in 2002 and was spread over the upper 300–400 m; the amount of WSW then gradually decreased during summer and fall. In 2003, only a modest layer of WSW extended towards the shelf edge in spring, but the quantity and intensity (higher T and S) of WSW increased during summer and early fall until an anomalously large volume of warmer-than-usual WSW lay over the HL outer slope in October. This temperature variability is (at least) qualitatively consistent with that observed in the moored and SST data, which collectively point to the pronounced four-dimensional structure of water mass and circulation variability on the outer HL in the spring–fall periods of 2002 and 2003.

Discussion

This cursory examination of multiple datasets points to the potential for and challenges of describing and understanding the hydrographic and circulation variability over the Scotian Slope. The variability on seasonal and longer time scales described here is suggestive of both an underlying seasonal cycle associated with air-sea fluxes and the subpolar gyre, and episodic disruptions on the time scale of months associated with Gulf Stream meanders. The moored measurements at depths below 80 m show little indication of the strong seasonal variation in temperature that is prominent in near-surface waters. The current measurements provide support for the paradigm of a seasonally varying surface-intensified equatorward flow along the slope, but also indicate that this pattern can be disrupted during (at least) spring through fall by Gulf Stream influences. Thus, while the seasonal transports estimated here appear to be in part indicative of a larger-scale persistent seasonal cycle, their magnitudes are almost certainly influenced by the Gulf Stream-related disruptions in 2002 and 2003 and so probably underestimate the longer-term means.

It is tempting to speculate that the presence of the warm-core rings near the shelf edge in 2002 and 2003 contributed to the reappearance of deep water with temperatures exceeding 10°C in Emerald Basin in those years. On the other hand, there is along-slope variability in the hydrographic structure associated with the ring locations and topography that may influence the warm-water interactions with the shelf at the longitude of the Scotian Gulf (a deep channel between Emerald and Lahave Banks, west of the HL), where

on-shelf slope water intrusions primarily occur. Clearly, the features identified here and many other aspects of oceanographic variability over the Scotian Slope (and the Atlantic Canada slope in general) need to be examined further in order to understand large-scale ocean climate influences on regional ecosystems. The AZMP is providing an invaluable observational record that can be used in conjunction with other observations and models to describe, understand, and eventually predict ocean (and related marine ecosystem) variability off Atlantic Canada.

Acknowledgements

We are grateful to the many individuals and organizations who have contributed to the moored measurement program and to the AZMP datasets. In particular, we thank Murray Scotney and the Technical Operations group at BIO for the execution of the field program, and Carla Caverhill, Charles Hannah, Brian Petrie, Roger Pettipas, and Victor Soukhovtsev for providing data or graphics for this article. Funding for the moored measurement program was provided by DFO, PERD's Offshore Environmental Factors subprogram, Marathon Canada, Shell Canada, ChevronTexaco, EnCana, Kerr-McGee Canada, and BP Canada.

References

- Anderson, C., and Smith, P.C. 1989. Oceanographic observations on the Scotian Shelf during CASP. *Atmos.-Ocean* 27: 130–156.
- Fogarty, C.T., Greatbatch, R.J., and Ritchie, H. 2006. The role of anomalously warm sea surface temperatures on the intensity of Hurricane Juan (2003) during its approach to Nova Scotia. *Mon. Weather Rev.* 134: 1484–1504.
- Gatien, G. 1976. A study in the slope water region south of Halifax. *J. Fish. Res. Board Can.* 33: 2213–2217.
- Hannah, C.G., Shore, J.A., Loder, J.W., and Naimie, C.E. 2001. Seasonal circulation on the western and central Scotian Shelf. *J. Phys. Oceanogr.* 31: 591–615.
- Mann, C.R., and Needler, G.T. 1967. Effect of aliasing on studies of long-term variability off Canada's coasts. *J. Fish. Res. Board Can.* 24: 1827–1831.
- Loder, J.W., Petrie, B., and Gawarkiewicz, G. 1998. The coastal ocean off northeastern North America: a large-scale view. *In* The Sea, Vol. 11. Edited by A.R. Robinson and K.H. Brink. John Wiley & Sons, Inc., New York, pp. 105–133.
- Loder, J.W., Shore, J.A., Hannah, C.G., and Petrie, B.D. 2001. Decadal-scale hydrographic and circulation variability in the Scotia-Maine region. *Deep-Sea Res. II* 48: 3–35.
- Loder, J.W., Hannah, C.G., Petrie, B.D., and Gonzalez, E.A. 2003. Hydrographic and transport variability on the Halifax section. *J. Geophys. Res.* 108(C11), 8003, doi: 10.1029/2001JC001267.
- Petrie, B.D., and Drinkwater, K.F. 1993. Temperature and salinity variability on the Scotian Shelf and in the Gulf of Maine 1945–1990. *J. Geophys. Res.* 98: 20079–20089.
- Smith, P.C., and Petrie, B.D. 1982. Low-frequency circulation on the edge of the Scotian Shelf. *J. Phys. Oceanogr.* 12: 28–46.

La station de monitorage de Rimouski : plus de 400 visites et 18 ans de monitorage et de recherche

Stéphane Plourde, Pierre Joly, Liliane St-Amand et Michel Starr

Institut Maurice-Lamontagne, C. P. 1000, Mont-Joli, QC, G5H 3Z4

stephane.plourde@dfo-mpo.gc.ca

Abstract

Initiated in 1991 in support of specific research projects, sampling at the Rimouski station located in the lower St. Lawrence estuary has continued for 18 years with more than 400 sampling sorties. The limited sampling protocol followed during the first years revealed the usefulness of such a monitoring project in describing seasonal and interannual patterns in plankton dynamics in the region. These results led to the long duration of the sampling at this station and eventually to its inclusion in the Atlantic Zone Monitoring Program (AZMP) starting in 2005. In addition to its contribution to the monitoring program, the sampling at the Rimouski station has supported several research activities related to key and emergent topics in biogeochemical oceanography. The maintenance of such a long-term time series has only been possible with the contribution of numerous people through the years.

« Jeffrey Runge avait l'index pointé au centre de la carte marine tout juste au nord de Rimouski. C'est là que l'on ira échantillonner me dit-il. Pour ma part, j'avais le regard dirigé vers l'échelle de la carte. Mon peu d'expérience au large des côtes me disait que j'allais vivre de véritables aventures....»

Pierre Joly 1990

La genèse d'une station de monitorage

Née d'un besoin de récolter du zooplancton pour la réalisation d'expériences en laboratoire durant les premières années de l'existence de l'Institut Maurice-Lamontagne (IML), la station Rimouski a atteint sa majorité en 2008 (18 ans) avec au courant de l'été une 400^{ème} visite d'échantillonnage. La position de la station à 20 km au large de la marina de Rimouski (48°40' N, 68°35' O) a été choisie en regard de la sécurité des sorties en mer (la station est localisée entre les deux voies de navigation commerciale) et de sa profondeur (340 m) assurant ainsi la présence des copépodes dominants du genre *Calanus* (Fig. 1). Bien qu'une vingtaine de sorties aient été

réalisées en 1991 et 1992 afin de décrire le patron saisonnier de la production d'œufs du copépode *Calanus finmarchicus* (Plourde et Runge 1993), l'échantillonnage régulier et continu a réellement débuté en 1993. Divers navires d'opportunité et des petites embarcations ont été mis à contribution durant les deux premières années, mais le *Béluga*, un Boston Whaler en fibre de verre de 25 pieds, deviendra rapidement l'embarcation de prédilection de part sa vitesse, son équipement ainsi que sa grande sécurité pour le travail en mer (Fig. 2). Les premières années, la saison d'échantillonnage débutait



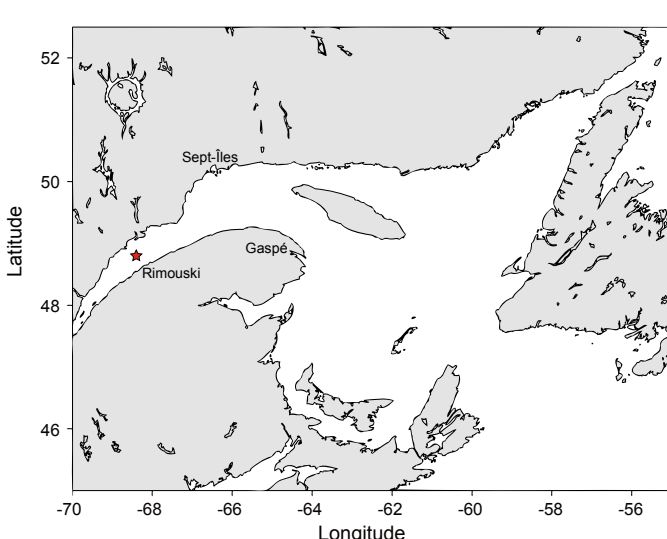
Fig. 2 Le Boston Whaler *Béluga*.

The Boston Whaler, Béluga.

en mai, précédant la période de croissance du phytoplancton, afin de couvrir l'amorce de la floraison du phytoplancton et de la reproduction de *C. finmarchicus*. L'observation de variations interannuelles dans cette dynamique a motivé le leader du projet à l'époque, le Dr. Jeffrey Runge, de poursuivre cette activité sur une base pluriannuelle. De plus, de part sa proximité ainsi que l'utilisation d'une petite embarcation, cette station de monitorage « en devenir » s'avérait relativement peu coûteuse par rapport aux coûts d'opération. Depuis 1993, de 20 à 25 sorties sont réalisées chaque année sous la responsabilité de Pierre Joly (IML). L'échantillonnage débute

Fig. 1 Localisation de la station Rimouski.

Location of the Rimouski station.



dès avril/début mai et se termine le plus tard possible afin de couvrir l'ensemble du cycle saisonnier des espèces de copépodes dominants dans cette région fort dynamique de l'estuaire du Saint-Laurent.

Progression de la station de monitorage

Le protocole d'échantillonnage a rapidement évolué lors des premières années en réponse aux besoins de mieux suivre la dynamique saisonnière et interannuelle du plancton et de l'environnement. En 1991, l'échantillonnage se résumait à : i) un trait de filet de 1 mètre de diamètre et de vide de maille de 333 µm, de 250 m à la surface, pour la récolte des femelles de *C. finmarchicus*; ii) la récolte d'échantillons d'eau avec une bouteille Niskin à trois profondeurs (0, 10 et 20 m) pour la détermination de la biomasse de chlorophylle *a*; et iii) un profil des températures et des salinités sur la colonne d'eau (0–250 m) à partir d'une sonde CTD (Plourde et Runge 1993). Dès 1992, l'échantillonnage du phytoplancton a été porté à huit profondeurs réparties dans la couche 0–50 m, un effort minimal soutenu depuis ce temps. En 1993, l'intérêt de suivre l'abondance de tous les stades de développement (œufs, nauplii et copépodites) de *C. finmarchicus* et des autres copépodes clés du système a motivé l'ajout d'un échantillonnage de la couche de surface (0–50 m) avec un filet de vide de maille de 73 µm en complément du filet de 333 µm. L'analyse des échantillons récoltés avec ce filet de faible vide de maille a permis de mieux décrire la dynamique de *C. finmarchicus* et d'identifier de nouvelles avenues de recherche (voir ci-dessous). À partir de 1995, le Dr. Michel Starr, chercheur principalement intéressé par la dynamique de la production primaire (phytoplancton) et les cycles biogéochimiques, a commencé à s'impliquer activement dans l'échantillonnage et l'analyse des échantillons et des données de la station Rimouski. De plus, à partir de 1999, l'intérêt croissant de M. Starr pour les processus régissant la production primaire et la biomasse de phytoplancton ainsi que son implication dans le Programme de monitorage de la zone Atlantique (PMZA) ont amené l'ajout de mesures d'atténuation de la lumière, de sels nutritifs, de la composition phytoplanctonique et de production primaire. En 2002, la mise à l'eau de la bouée océanographique de surface IML-04 à la station Rimouski a permis de relier les observations récoltées sur une base hebdomadaire à des données en continu et ainsi contribuer à la calibration/validation des dif-

férentes sondes de la bouée. Des problématiques émergentes relatives aux changements climatiques d'origine naturelle ou anthropiques ont amené l'ajout de mesures de la concentration en oxygène (Dr. Denis Gilbert, IML) et du pH (M. Starr, IML) à différentes profondeurs dans la colonne d'eau à partir de 2005, résultant en un protocole d'échantillonnage appliqué depuis (Tableau 1). Récemment, l'accumulation de nouvelles connaissances concernant l'importance de la circulation de type estuarienne en deux couches dans le contrôle du zooplancton dans l'estuaire maritime a amené le Dr. Stéphane Plourde à développer un échantillonnage du zooplancton sur deux strates de profondeur (0–100 m et 100–320 m) depuis 2004. Finalement, l'échantillonnage du zooplancton avec un filet

Tableau 1 Les activités de terrain et les travaux en laboratoire réalisés sur les échantillons récoltés à la station Rimouski.

Field work and laboratory analyses conducted on samples collected at the Rimouski station.

Terrain / Field	Profondeur échantillonnée / Sampling depth (m)	Variables / Variables
Secchi	—	Atténuation de la lumière / Light attenuation
Niskin 5L	0'; 2.5; 5; 10 ^{2,3} ; 15; 20; 25; 35; 50; 100; 200; 320 ^{1,2}	Chl <i>a</i> , concentrations bactériennes et virales, pH, oxygène, composition du phytoplancton, CDOM, sels nutritifs/ <i>Chl a, bacteria and virus concentrations, pH, oxygen, phytoplankton composition, CDOM, nutrients</i>
Sea-Bird 19plus CTD	0-320	Profils in situ : température, salinité, fluorescence, oxygène, pH / <i>In situ profiles: temperature, salinity, fluorescence, oxygen, pH</i>
Filet / Net		
0.5 m Ø, 73 µm, 1:8	0-50	Œufs, nauplii, copépodites / <i>Eggs, nauplii, copepodites</i>
0.75 m Ø, 202 µm, 1:5	0-100; 100-320	Composition du zooplancton / <i>Zooplankton composition</i>
Mesures de laboratoire / Laboratory measurements		
Zooplancton / Zooplankton		Production d'œufs in situ / <i>In situ egg production</i> (<i>Calanus finmarchicus</i> , <i>C. hyperboreus</i> , <i>Metridia longa</i>) Succès d'éclosion / <i>Hatching success</i> (<i>C. finmarchicus</i> , <i>M. longa</i>) Viabilité / <i>Viability</i> (<i>C. finmarchicus</i>) Morphométrie du prosome et de l'urosome, volume lipidique, CHN / <i>Prosome and urosome morphometrics, lipid volume, CHN</i> Taxonomie / <i>Taxonomy</i>
Phytoplancton / Phytoplankton		Caractéristiques optiques et de tailles des cellules (flux cytométrie) / <i>Optical characteristics and cell size (flow cytometry)</i> Viabilité du phytoplancton / <i>Phytoplankton viability</i> Production primaire et bactérienne / <i>Primary and bacterial production</i> Taxonomie / <i>Taxonomy</i>

¹ oxygène/oxygen, ² pH, ³ composition du microzooplancton / *microzooplankton composition*

standard de vide de maille de 202 µm, utilisé dans le cadre du PMZA, a débuté en 2005 suite à l'inclusion officielle des données de zooplancton de la station Rimouski dans les rapports d'état de l'écosystème (Harvey et al. 2005, Bulletin du PMZA). Un effort visant à standardiser les données de zooplancton de la station Rimouski récoltées selon différents protocoles d'échantillonnage depuis 1993–1994 est présentement en cours afin d'éventuellement intégrer les données historiques dans les rapports du PMZA.

La station Rimouski : contribution à la recherche en océanographie biologique à l'IML

La localisation de l'IML sur la rive sud de l'estuaire maritime du Saint-Laurent ainsi que les caractéristiques océanographiques

de cette région supportant une communauté de zooplancton dominée par un mélange d'espèces de copépodes océaniques arctiques et subarctiques typiques des eaux du nord du golfe du Saint-Laurent et du plateau continental du nord-ouest de l'Atlantique font de la station Rimouski un site de choix. L'accessibilité de ce site d'intérêt permet l'échantillonnage et la réalisation d'expériences en laboratoire avec des organismes vivant à une fréquence plus élevée (hebdomadaire) que celle possible au cours des missions sur de grands navires. L'effort soutenu d'échantillonnage à la station Rimouski ne représente qu'une fraction de l'effort investi depuis 18 ans dans l'analyse des échantillons de phytoplancton et de zooplankton, et l'étude de processus en laboratoire tant au niveau de la production primaire, de l'activité bactérienne et virale, et de la dynamique de populations des espèces de copépodes dominantes (production d'œufs, taux d'éclosion, etc.) de l'estuaire du Saint-Laurent.

Dès 1991, la station Rimouski a servi à J. Runge pour les projets de deux étudiants à la maîtrise en science sur l'écologie d'une espèce planctonique dominante du système estuaire et golfe du Saint-Laurent, le copépode *C. finmarchicus*. S. Plourde a décrit la relation directe entre la maturation des gonades chez les femelles de *C. finmarchicus* et la disponibilité de nourriture tant en laboratoire que sur le terrain (station Rimouski), ainsi que la relation fonctionnelle entre le taux de production d'œufs des femelles en relation avec la biomasse phytoplanctonique (Plourde et Runge 1993). Nancy Turriff a quant à elle décrit le processus d'assimilation des toxines d'algues toxiques (ex. *Alexandrium tamarensis*) lors de l'alimentation de *C. finmarchicus* en vue d'évaluer son rôle potentiel dans le transfert des toxines dans le réseau trophique (Turriff et al. 1995).

L'émergence de la problématique de l'effet potentiellement nocif des diatomées sur le taux d'éclosion des œufs de copépodes a amené J. Runge et son équipe à explorer cette question à partir des échantillonnages récoltés à la station Rimouski. Le suivi des taux d'éclosion in situ des œufs de copépodes par P. Joly et l'étude expérimentale de M. Starr sur le rôle de la composition phytoplanctonique sur la fécondité et la viabilité des œufs de *C. finmarchicus* ont résulté en deux publications importantes dans ce domaine de recherche spécifique (Starr et al. 1999, Irigoien et al. 2002).

Parallèlement, S. Plourde a réalisé ses études de doctorat sous la supervision de J. Runge sur la dynamique de population de *C. finmarchicus* et *C. hyperboreus* en grande partie à partir des données récoltées à la station Rimouski de 1991 à 1998. L'analyse en profondeur des patrons saisonniers de la reproduction et de l'abondance de ces deux espèces a permis d'élaborer des hypothèses concernant les facteurs régissant la

dynamique de ces espèces dans la région en relation avec la dynamique physique particulière du système estuaire maritime - golfe du Saint-Laurent, ainsi que dans les changements environnementaux majeurs ayant eu lieu au début des années 1990 (Plourde et al. 2001, 2002, 2003). Ces travaux sont à la base de l'échantillonnage en deux couches de profondeur initié en 2004 à la station Rimouski. Cet échantillonnage divisant la colonne d'eau en deux strates de profondeur vise à différencier les composantes « actives » (strate 0-100 m) et « inactives » (animaux en hibernation) (strate 100-320 m) des espèces de *Calanus* et à étudier les facteurs contrôlant les moments de sortie et d'entrée d'hibernation (lipides, nourriture, température, etc.). De plus, cet échantillonnage fournit des données sur l'axe temporel nécessaires à la validation des modèles couplés biologie-physique de *C. finmarchicus* utilisés pour décrire le rôle de la circulation de type estuarienne en deux couches dans le contrôle de la dynamique de population de cette espèce dans l'estuaire et le golfe du Saint-Laurent. Finalement, les données historiques de la station Rimouski ont été utilisées dans le cadre d'une étude visant à déterminer le moment de sortie et d'entrée en hibernation de *C. finmarchicus* dans différentes régions dans le nord-ouest de l'Atlantique et à explorer les variables environnementales pouvant expliquer ce phénomène (Johnson et al. 2008).

Le suivi de la dynamique de la production et/ou de la biomasse du phytoplancton a permis d'observer d'importantes variations interannuelles dans l'initiation, l'intensité et la durée de la floraison estivale du phytoplancton (Fig. 3) (Starr et al. 2004). Ces variations interannuelles dans la dynamique du phytoplancton peuvent avoir un effet direct dans le contrôle des variations interannuelles de l'intensité de la reproduction de *C. finmarchicus* dans la région (Fig. 4) (Plourde et al. 2001). De plus, la dynamique du phytoplancton pourrait jouer un rôle important sur la production totale de *C. finmarchicus* via des processus densité-dépendant (mortalité des jeunes via cannibalisme ou jeûne) dont l'intensité semble inversement reliée à la biomasse de phytoplancton (disponibilité de nourriture) (Plourde et al. 2009, Plourde et al. ms soumis). Ces études portant sur les processus contrôlant la mortalité/survie et conséquemment le succès de la production de la nouvelle génération de *C. finmarchicus* sont des éléments clés dans l'élaboration de modèles biologiques représentatifs et répondant aux variations environnementales.

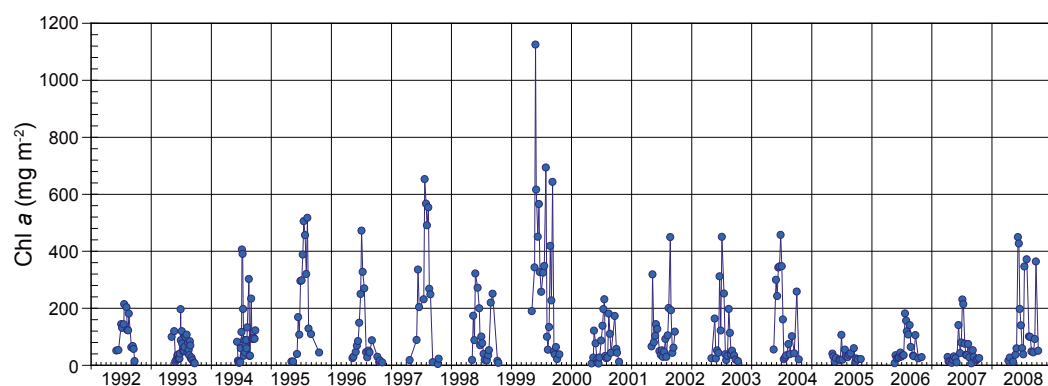


Fig. 3 Biomasse hebdomadaire de chlorophylle *a* (mg m^{-2}) à la station Rimouski de 1992 à 2007.

Weekly chlorophyll a biomass (mg m^{-2}) at the Rimouski station from 1992 to 2007.

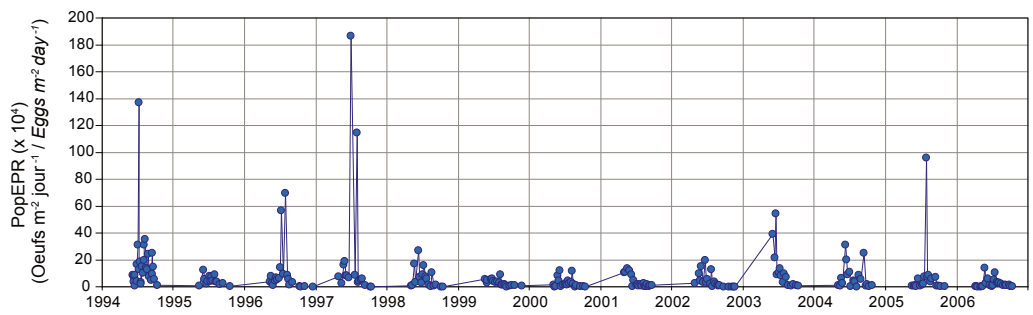


Fig. 4 Taux journalier de la production d'œufs de la population de *Calanus finmarchicus* (PopEPR) à la station Rimouski de 1994 à 2006.

Daily egg production of the *Calanus finmarchicus* population (PopEPR) at the Rimouski station from 1994 to 2006.

L'acquisition hebdomadaire des données de la concentration en oxygène à la station Rimouski a aussi contribué à décrire le phénomène d'hypoxie dans les eaux profondes de l'estuaire du Saint-Laurent (Gilbert et al. 2005). Dans les années 1930, les niveaux d'oxygène à 300 m dans l'estuaire maritime du Saint-Laurent était de 38 % de saturation. Aujourd'hui, les mesures d'oxygène à la station Rimouski sont autour de 20 % avec des observations aussi faibles que 16 %. Les eaux profondes de l'estuaire sont donc sévèrement hypoxiques, présentant un risque pour la santé de l'écosystème. Ce déclin de l'oxygène est attribué à deux facteurs : i) des changements dans le patron de circulation dans l'Atlantique Nord et ii) une augmentation des flux de matières organiques dans les eaux profondes et les sédiments. De plus, les observations récentes de l'équipe de M. Starr à la station Rimouski ont mis en évidence une acidification marquée des eaux profondes de l'estuaire du Saint-Laurent. Cette acidification des eaux de l'estuaire pourrait avoir des effets délétères sur les organismes et notamment ceux possédant des coquilles contenant du carbonate de calcium ou de la calcite (CaCO_3) (foraminifères, échinodermes, mollusques, coraux). L'ajout de mesures d'oxygène et de pH à la station Rimouski permet ainsi de suivre l'évolution de l'hypoxie et du phénomène d'acidification de l'estuaire du Saint-Laurent.

Un important travail visant à optimiser les méthodes d'incubation pour la mesure des taux de production d'œufs et de succès d'éclosion in situ des copépodes a été réalisé dans le cadre des activités de monitorage et de recherche à la station Rimouski. Les résultats de ces expériences ont contribué à l'élaboration de méthodes standards (Runge et Roff 2000). Des données récoltées lors de ces années ont récemment été utilisés afin de comparer le taux de production d'œufs in situ de *C. finmarchicus* et *M. longa* et de quantifier l'importance du cannibalisme des femelles sur leurs œufs durant les incubations en relation avec leur passé alimentaire (biomasse de phytoplancton ambiant lors de la capture à la station) (Fig. 4) (Plourde et Joly 2008). M. Starr et son équipe ont acquis une expertise sur la dynamique de la production primaire, bactérienne et virale, tant au niveau de l'apprentissage et de la mise au point des techniques d'analyses en laboratoire qu'au niveau de la dynamique saisonnière de ces différentes variables, en grande partie en travaillant sur des échantillons récoltés à la station Rimouski. Ces connaissances ont permis le développement de modèles biogéochimiques 3D permettant de mieux comprendre le fonctionnement de l'écosystème du Saint-Laurent (LeFouest et al. 2005).

La station Rimouski : une aventure vécue par une équipe nombreuse

Une sortie à plus de 20 km au large en petite embarcation dans une voie maritime majeure implique une bonne préparation mais surtout une flexibilité d'horaire par rapport aux conditions météorologiques. En de nombreuses occasions, les gens à bord du *Béluga* ont dû affronter les différents impondérables de Dame

nature (ou des prévisions météorologiques), soit de forts coups de vents, le brouillard imprévu, des navires de fort tonnage en dehors de leur voie de navigation habituelle, etc. Bien que parfois stressants, ces évènements ont contribué à ajouter un complément d'aventure à notre travail d'échantillonnage pouvant paraître parfois monotone et répétitif. L'observation de phénomènes physiques particuliers (par exemple clapotis, déplacement de fronts) ainsi que de plusieurs mammifères marins comme des phoques, bélugas, rorquals communs et rorquals bleus sont d'autant d'éléments qui agrémentent le travail d'échantillonnage. Ces derniers sont sans compter la « pause santé » prise dans un silence complet sur une mer d'huile sous un beau soleil de juillet....

Certaines personnes ont particulièrement épaulé le travail mené depuis le début par Pierre Joly. Jeffrey Runge a initié et supporté le travail à cette station durant plusieurs années bien avant que son importance et sa valeur ne soit reconnue dans les années 1990 avec le développement de la vocation monitorage des sciences océanographiques du Ministère des Pêches et des Océans. Durant plusieurs années, Jeffrey a investi des fonds pour l'analyse des échantillons et l'embauche de personnel temporaire pour supporter cette activité sur le terrain et l'analyse des échantillons en laboratoire. Quelques personnes ont particulièrement épaulé Pierre Joly dans cette aventure : Stéphane Plourde durant ses études graduées, Michel Starr toujours fidèle au poste durant quelques années pour se mouiller les pieds à bord du *Béluga*, Eric Dionne, Caroline Lebel et Sandrine Guittard qui ont contribué significativement à l'échantillonnage et à l'analyse des échantillons, Réal Gagnon avec qui Pierre Joly a raffiné et développé l'échantillonnage qui atteint maintenant un haut standard de qualité, Jean-François St-Pierre et Jean-Pierre Allard qui ont su supplé Pierre lors de ses vacances bien méritées, et Caroline Lafleur qui a pris la relève ces dernières années. Le traitement des échantillons en laboratoire sous la responsabilité de Liliane Saint-Amand mérite aussi d'être souligné. Finalement, Sylvie Lessard et Lyse-Bérard Therriault ont analysé les échantillons visant la description de la composition du phytoplancton (de 1997 à aujourd'hui) et Marie-Lyne Dubé et Line McLaughlin ont analysé les échantillons de sels nutritifs (de 1999 à aujourd'hui). À ces personnes importantes s'ajoute une longue liste de gens qui au cours de presque deux décennies ont contribué à l'effort collectif nécessaire à la réalisation de ce travail de longue haleine.

Merci à tous !

Marie-Josée Arseneault, Maryse Bélanger, Sonia Beaulieu, Claire Bertolone, Monica Borobia, Luc Bourassa, Luc Bourgeois, Alice Bui, Gabrielle Chapados, Mélanie Charrette, Lucienne Chénard, Jean-Yves Couture, Claudie Dallaire, François DeMontigny, Aurélie Descroix, Rémi Desmarais, Laure Devine, Patricia Gagnon, Yves Gagnon, Linda Girard, Michel Harvey, Béatrice Huppertz, Chantal Lacoste, Katherine Lafleur, Bernadette Lagacé, Christian Legeault, Martin Lévesque, Frédéric Maps, Alexandra Marion, Liliane Marois, Vickie Mercier, Dominique Morrier, Guylaine Morrier, Geneviève Parent, Étienne Proulx, Marc Ringuette, Jean-Guy Rondeau, François Roy, Isabelle St-Pierre, Gilles Savard, Nathalie Simard, Richard Sirmel, Pierre Sylvestre, Julie Taxil, Nancy Turriff, Pierre Villemure et François Villeneuve.

Références

- Gilbert, D., Sundby, B., Gobeil, C., Mucci, A. et Tremblay, G.-H. 2005. A seventy-two-year record of diminishing deep-water oxygen in the St. Lawrence estuary: the northwest Atlantic connection. Limnol. Oceanogr. 50(5): 1654-1666.
- Harvey, M., St-Pierre, J.-F., Devine, L., Gagné, A., Gagnon, Y. et Beaulieu, M.-F. 2005. Oceanographic conditions in the Estuary and in the Gulf of St. Lawrence during 2004: zooplankton. DFO CSAS Res. Doc. 2005/043, 22 pp.
- Irigoinen, X., Harris, R.P., Verheyen, H.M., Joly, P., Runge, J., Starr, M., Pond, D. et al. 2002. Copepod hatching success in marine ecosystems with high diatom concentrations. Nature 419: 387-389.
- Johnson, C.L., Leising, A.W., Runge, J.A., Head, E.J.H., Pepin, P., Plourde, S. et Durbin, E.G. 2008. Characteristics of *Calanus finmarchicus* dormancy patterns in the Northwest Atlantic. ICES J. Mar. Sci. 65: 339-350.
- LeFouest V., Zakardjian, B., Saucier, F. et Starr, M. 2005. Seasonal versus synoptic variability in planktonic production in a high-latitude marginal sea: the Gulf of St. Lawrence (Canada). J. Geophys. Res. 110, C09012, Doi 10.1029/2004JC002423.
- Plourde, S. et Joly, P. 2008. Comparison of in situ egg production rate in *Calanus finmarchicus* and *Metridia longa*: discriminating between methodological and species-specific effects. Mar. Ecol. Prog. Ser. 363: 165-175.
- Plourde, S. et Runge, J.A. 1993. Reproduction of the planktonic copepod *Calanus finmarchicus* in the lower St. Lawrence Estuary: Relation to the cycle of phytoplankton production and evidence for a *Calanus* pump. Mar. Ecol. Prog. Ser. 102: 217-227.
- Plourde, S., Joly, P., Runge, J.A., Zakardjian, B. et Dodson, J.J. 2001. Life cycle of *Calanus finmarchicus* in the lower St. Lawrence estuary: The imprint of circulation and late timing of the spring phytoplankton bloom. Can. J. Fish. Aquat. Sci. 58: 647-658.
- Plourde, S., Dodson, J.J., Runge, J.A. et Therriault, J.C. 2002. Spatial and temporal variations in copepod community structure in the lower St. Lawrence Estuary, Canada. Mar. Ecol. Prog. Ser. 230: 211-224.
- Plourde, S., Joly, P., Runge, J.A., Dodson, J. et Zakardjian, B. 2003. Life cycle of *Calanus hyperboreus* in the lower St. Lawrence Estuary and its relationship to local environmental conditions. Mar. Ecol. Prog. Ser. 255: 219-233.
- Plourde, S., Maps, F. et Joly, P. 2009. Mortality and survival in early stages control recruitment in *Calanus finmarchicus*. J. Plankton Res. 31: 371-388.
- Runge, J.A. et Roff, J.C. 2000. The measurement of growth and reproductive rates. Dans ICES zooplankton methodology manual. Sous la direction de R. Harris, P. Wiebe, J. Lenz, H.R. Skjoldal et M. Huntley Academic Press, London. pp. 401-451.
- Starr, M., Runge J. et Therriault, J.-C. 1999. Effects of diatom diets on the reproduction of the planktonic copepod *Calanus finmarchicus*. Sarsia 84: 379-389.
- Starr, M., St. Amand, L., Devine, L., Bérard-Therriault, L. et Galbraith, P.S. 2004. State of phytoplankton in the Estuary and Gulf of St. Lawrence during 2003. DFO CSAS Res. Doc. 2004/123, 35 pp.
- Turriff, N., Runge, J.A. et Cembella, A.D. 1995. Toxin accumulation and feeding behaviour of the planktonic copepod *Calanus finmarchicus* exposed to the red-tide dinoflagellate *Alexandrium excavatum*. Mar. Biol. 123: 55-64.

Publications

Primary Publications / Publications primaires

- Harvey, M., P.S. Galbraith and A. Descroix. 2009. Vertical distribution and diel migration of macrozooplankton in the St. Lawrence marine system (Canada) in relation with the cold intermediate layer thermal properties. Prog. Oceanogr. 80: 1-20; doi:10.1016/j.pocean.2008.09.001.
- Head, E., and P. Pepin. 2008. Variations in overwintering depth distributions of *Calanus finmarchicus* in the slope waters of the NW Atlantic continental shelf and the Labrador Sea. J. Northw. Atl. Fish. Sci. 39: 49-69.
- Johnson, C.L., A.W. Leising, J.A. Runge, E.J.H. Head, P. Pepin, S. Plourde and E.G. Durbin. 2008. Characteristics of *Calanus finmarchicus* dormancy patterns in the Northwest Atlantic. ICES J. Mar. Sci. 65: 339-350.
- Li, W.K.W., and W.G. Harrison. 2008. Propagation of an atmospheric climate signal to phytoplankton in a small marine basin. Limnol. Oceanogr. 53(5): 1734-1745.
- Li, W.K.W., M.R. Lewis and W.G. Harrison. 2008. Multiscalarity of the nutrient-chlorophyll relationship in coastal phytoplankton. Estuaries Coasts, doi 10.1007/s12237-008-9119-7.
- Marion, A., M. Harvey, D. Chabot and J.-C. Brêthes. 2008. Feeding ecology and predation impact of the recently established amphipod, *Themisto libellula*, in the St. Lawrence marine system, Canada. Mar. Ecol. Prog. Ser. 373: 53-70.
- Neuheimer, A.B., W.C. Gentleman, P. Pepin and E.J.H. Head. 2009. How to build and use individual-based models (IBM) as hypothesis testing tools. J. Marine Syst. (in press).
- Pepin, P., and E.J.H. Head. 2009. Seasonal variation in the depth-dependent state of stage 5 copepodites of *Calanus finmarchicus* in the waters of the Newfoundland Shelf and the Labrador Sea. Deep-Sea Res. (Part I). doi:10.1016/j.dsr.2009.01.005.

Technical Publications / Publications techniques

NAFO Research Document Series / Séries de Documents de recherche OPANO

Colbourne, E.B., J. Craig, C. Fitzpatrick, D. Senciall, P. Stead and W. Bailey. 2008. An assessment of the physical oceanographic environment on the Newfoundland and Labrador Shelf in NAFO Subareas 2 and 3 during 2007. NAFO SCR Doc. 08/19. Serial No. N5513, 17 pp.

Maillet, G.L., P. Pepin, S. Fraser, T. Shears, G. Redmond, G. Harrison, C. Johnson, E. Head, J. Spy, K. Pauley, H. Maass, M. Kennedy, C. Porter and V. Soukhovtsev. 2008. Biological and chemical oceanographic conditions on the Newfoundland and Labrador

Shelf, Grand Banks, Scotian Shelf, and the Gulf of Maine during 2007. NAFO SCR Doc. 08/12, Serial No. N5504, 16 pp.

Petrie, B., R.G. Pettipas and W.M. Petrie. 2008. Air temperature, sea ice and sea-surface temperature conditions off eastern Canada during 2007. NAFO SCR Doc. 08/14, Serial No. N5506, 15 pp.

Petrie, B., R.G. Pettipas, W.M. Petrie and V.V. Soukhovtsev. 2008. Physical oceanographic conditions on the Scotian Shelf and in the eastern Gulf of Maine (NAFO areas 4V,W,X) during 2007. NAFO SCR Doc. 08/13, Serial No. N5505, 29 pp.

Canadian Science Advisory Secretariat (CSAS) / Secrétariat canadien de consultation scientifique (SCCS)

Research Documents / Documents de recherche

Colbourne, E.B., J. Craig, C. Fitzpatrick, D. Senciall, P. Stead and W. Bailey. 2008. An assessment of the physical oceanographic environment on the Newfoundland and Labrador Shelf during 2007. DFO CSAS Res. Doc. 2008/20, 20 pp.

Colbourne, E.B., and E.F. Murphy. 2008. Physical oceanographic conditions in NAFO Division 3P during 2007 - potential influences on the distribution and abundance of Atlantic cod (*Gadus morhua*). DFO CSAS Res. Doc. 2008/027, 26 pp.

Galbraith, P.S., D. Gilbert, R.G. Pettipas, J. Chassé, C. Lafleur, B. Pettigrew, P. Larouche and L. Devine. 2008. Physical oceanographic conditions in the Gulf of St. Lawrence in 2007. DFO CSAS Res. Doc. 2008/001, 59 pp.

Harrison, G., C. Johnson, E. Head, K. Pauley, H. Maass, M. Kennedy, C. Porter and V. Soukhovtsev. 2008. Optical, chemical and biological oceanographic conditions in the Maritimes regions in 2007. DFO CSAS Res. Doc. 2008/044, 66 pp.

Harvey, M., and L. Devine. 2008. Oceanographic conditions in the Estuary and the Gulf of St. Lawrence during 2007: zooplankton. DFO CSAS Res. Doc. 2008/037, 35 pp.

Pepin, P., G.L. Maillet, S. Fraser, T. Shears and G. Redmond. 2008. Biological and chemical oceanographic conditions on the Newfoundland Shelf during 2007. DFO CSAS Res. Doc. 2008/034, 61 pp.

Petrie, B., R.G. Pettipas, W.M. Petrie. 2008. An overview of meteorological, sea ice and sea-surface temperature conditions off eastern Canada during 2007. DFO CSAS Res. Doc. 2008/016, 42 pp.

Petrie, B., R.G. Pettipas, W.M. Petrie and V.V. Soukhovtsev. 2008. Physical oceanographic conditions on the Scotian Shelf and in the Gulf of Maine during 2007. CSAS Res. Doc. 2008/017, 47 pp.

Science Advisory Reports / Rapports d'avis scientifiques

(All advisory reports are available in English and French / Tous les rapports d'avis sont disponibles en français et en anglais)

DFO (Colbourne, E.B.). 2008. 2007 state of the ocean: physical oceanographic conditions in the Newfoundland and Labrador Region. DFO CSAS Sci. Advis. Rep. 2008/017, 11 pp.

DFO (Galbraith, P.S.). 2008. State of the ocean 2007: physical oceanographic conditions in the Gulf of St. Lawrence. DFO CSAS Sci. Advis. Rep. 2008/016, 19 pp.

DFO (Pepin, P.). 2008. 2007 state of the ocean: chemical and biological oceanographic conditions in the Newfoundland and Labrador Region. DFO CSAS Sci. Advis. Rep. 2007/038, 8 pp.

DFO (Petrie, B.). 2008. State of the ocean 2007: physical oceanographic conditions on the Scotian Shelf, Bay of Fundy and Gulf of Maine. DFO CSAS Sci. Advis. Rep. 2008/025, 10 pp.

Others / Autres

Colbourne, E.B., M. Stein, M. Ribergaard, R. Hendry, B. Petrie, G. Maillet, G. Harrison and M. Taylor. 2008. The 2007 NAFO annual ocean climate status summary for the Northwest Atlantic. On line at <http://www.nafo.int/science/frames/ecosystem.html>.

Devine, L., and C. Lafleur. 2008. Quality control of bottle data at Institut Maurice-Lamontagne. ICES CM 2008/R:27.

Head, E., K. Azetsu-Scott, G. Harrison, R. Hendry, W.K.W. Li, I. Yashayaev and P. Yeats. 2008. Changes in environmental conditions and the population dynamics of *Calanus finmarchicus* in the Labrador Sea (1990-2006). ICES CM 2008/Q:05.

Li, W.K.W. 2008. A latitudinal gradient in the prokaryote to eukaryote ratio in marine microbes. ICES CM 2008/A:02.